

*Report on the Hydrocarbon Exploration and Seismicity
in Emilia Region*

INTERNATIONAL COMMISSION ON HYDROCARBON EXPLORATION AND
SEISMICITY IN THE EMILIA REGION

Appendices

Appendix A. Biographies of Commissioners

The Commission comprises six scientists from four countries with experience in hydrocarbon exploration and seismicity. This section provides a short biographical sketch of each Commissioner.

Peter Styles, chair of the Commission, is Professor of Applied and Environmental Geophysics at the Keele University and has been Head of the School of Earth Sciences and Geography and Director of the Research Institute for Environment, Physical Sciences and Mathematics. He is a Fellow of the Geological Society, a Chartered Geologist and is also a Fellow of the Royal Astronomical Society, a Fellow of the Institute of Materials, Minerals and Mining, and a Member of the American Geophysical Union and the European Association of Geoscientists and Engineers. He served as a Board Member of the British Geological Survey for 6 years and as Chairman of the BGS University Collaboration Advisory Committee (UCAC). He was appointed to Chair the DEFRA/DTI Criteria Proposals Group (CPG) Sub-Surface Exclusion Criteria for Geological Disposal of Radioactive Waste (MRWS) which reported to Government in May 2007. He was a member of the Royal Society Committee on Non-Proliferation of Nuclear Weapons and has been a member the Geosphere Characterisation Panel of the Nuclear Decommissioning Authority. He is a Past-President of the Geological Society of London, the oldest national Geological Society in the World, founded in 1807 and was President of the British Association for the Advancement of Science (Geology Section) for 2007 and was listed for the first time in Whos Who in 2008. He is Editor-in-Chief of Geoscientist. He is currently conducting a global lecture programme as the first Distinguished Visiting Lecturer in Environmental Geophysics for the European Association of Geoscientists and Engineers (EAGE) for the near Surface Division and has been invited to be Distinguished Visiting lecturer by the American Society of Exploration Geophysicists on Microgravity. He was joint author of the 2012 DECC report on Induced Seismicity and Shale Gas Drilling in Lancashire and has given some 50 lectures and interviews on this subject over the past 2 years in 7 countries to date.

Paolo Gasparini, secretary of the Commission, is Professor Emeritus of Geophysics at the University of Napoli Federico II and Chief Executive Officer of the AMRA (Analisi e Monitoraggio del Rischio Ambientale) Scarl, an applied research institutions held by the University of Napoli Federico II and having as additional partners four public universities and three national research centres. As Chief Executive Officer of AMRA he has promoted and overseen several national, European and international projects on all the aspects of environmental risks, including earthquake risk. In his capacity of scientific advisor for the environment of the European Commissioner (2005-2008) he has promoted EC activities on real time earthquake risk mitigation, early warning methods and multi risk assessment. His main research interest relevant to the aims of the commission is the experience on origin of tectonic earthquakes, the use of Bayesian methods for real time risk evaluation of eruptions and other natural events. He is principal investigator of the European FP7 project REAKT (strategies and tools for Real Time EArthquake RiSk ReducTion) and he is in the Steering Committee of SAFER, the European project dedicated to earthquake early warning. He has been consultant of several oil

companies for the environmental impacts of geophysical surveys for oil and he was also consultant of several companies for the exploitation of geothermal potential as source of energy. He is the author of more than 120 publications, in the latest years more and more concentrated on earthquakes, and of about ten books and editor of special issues of international journals. Gasparini received his degrees from the University of Napoli. He was visiting professor/ Researcher at Rice University, Houston, Texas, at the Lawrence Radiation Laboratory at Berkeley, at the National Research Council of Norway, at the University of Sao Paulo, Brazil. He has been Director of the Mt. Vesuvius Volcanological Observatory since 1970 till 1983, President of the International Association of Volcanology and Chemistry of the Earth's Interior (IAVCEI) since 1991 to 1995, Director of the Italian Civil Protection Panel that formulated the earthquake research plan (GNDT) in 1995 and of the Protezione Civile- INGV National Group of Volcanology. He was member of the Civil Protection Commissione Grandi Rischi in the nineties. He was secretary of the International ICHEF (International Commission of Earthquake Forecasting) Commission. He has been awarded the Gold medal of the Italian Republic for culture.

Ernest Huenges is head of the section "Reservoir Technologies" and the "International Geothermal Research Centre" at the Helmholtz-Centre Potsdam GFZ German Research Centre for Geosciences. Since September 2012 he chairs the European Energy Research Alliance (EERA) Joint Programme Geothermal Energy. Ernst Huenges received his qualification as physicist and process engineer at the universities of Bonn and Düsseldorf. His other stations touched several research institutes in Berlin, Windischeschenbach, Aachen, and Hannover. His numerous scientific papers refer to Earth's transport processes including thermal, hydraulic, and mechanical aspects. In the recent years he has focussed on the utilization of underground resources. He is chair of an interdisciplinary working group of engineers and geoscientists and head of the petrophysical laboratories at the GFZ. He has been involved in a number of scientific deep drilling projects and geothermal projects. He and his co-workers develop stimulation techniques to enhance the fluid productivity of reservoirs (Enhanced Geothermal Systems) and to guarantee a long-term extraction of geothermal energy. The underground laboratory in Groß Schönebeck was developed to a lighthouse project in European geothermal research. The multidisciplinary working group binds basic and applied research focusing on new technologies for an economical exploration and utilization of geothermal energy for power supply as well as heating and/or cooling. His book "Geothermal Energy Systems" edited in 2010 has received a considerable resonance in the geothermal community. Ernst Huenges is spokesman of the research topic "Geothermal Technologies" within the Helmholtz association with working groups in Potsdam, Karlsruhe, and Leipzig. He is contributing author of the IPCC-special report on renewable energies.

Paolo Scandone is Retired Professor of Structural Geology at University of Pisa where he still participates to didactic activities by teaching Seismic Interpretation of Tectonic Structures in the MS course of Exploration and Applied Geophysics and tutoring graduate students in their MS thesis work. Scandone received his degrees from the University of Naples in 1961 and completed his education studying theoretical tectonics in Zurich, ETH and studying kinematics and structural balance

in Basel. With regard to the goals of the ICHESE Commission, his principal contributions are concerned with petroleum geology, structural geology and seismotectonics. He has been consultant of several oil companies for regional structure definition by seismic-line interpretation and integration of surface and subsurface geological information. He has been also consultant of public administrations for the identification and characterization of seismogenic tectonic structures. Paolo Scandone was leader of the Sub-Project "*Structural Model of Italy*" in the Geodynamics Project of the Italian National Research Council; leader of the Research Line "*Seismotectonics*" and of the Research Line "*Seismic Zoning and Seismic Code*" in the National Group for Defence against Earthquakes; leader of the Sub-Project "*CROP 04-Southern Apennines*" in the Italian CROP ("CROsta Profonda", i.e. "Deep Crust") Project. He was also member of the Civil Protection Commissione Grandi Rischi, from which presented his resignation in 1996. Scandone is the author of about 200 publications. In 2008 he has been awarded the Premio Linco for Geology, Palaeontology and Mineralogy; since 2001 is member of Accademia dei Lincei.

Stanislaw Lasocki is a Full Professor, the Head of Department of Seismology and Physics of the Earth's Interior in the Institute of Geophysics, Polish Academy of Sciences in Warsaw and the President of Scientific Council of the Institute. Graduated initially as a physicist, since 1975 he has been involved in geophysics with a particular interest in induced seismology. His main research interest relevant to the aims of the commission is the application of statistical methods to analyzing natural as well as anthropogenic seismicity, to identifying common statistical properties of anthropogenic seismic processes differing them from tectonic seismic processes, to assessing time dependent seismic hazard due to induced seismicity and to managing this hazard. He has authored or co-authored well over 100 research papers and has taken part as an advisor and instructor in various projects for mining industry in Poland and also in South Africa and the United States. As a consultant of UNESCO he ran a strong motion monitoring trainings and advised strong motion observation in Libya. He also conducted courses on induced seismicity in Poland and in Vietnam. Since 2007 Professor Lasocki is chairing the Triggered and Induced Seismicity (TAIS) Working Group of the International Association of Seismology and Physics of the Earth Interior (IASPEI). As a result he and his colleagues launched in 2010 Teamwork for Hazard Assessment of Induced Seismicity (THAIS), a world initiative on the assessment of seismic hazard due to anthropogenic seismicity. The initiative has been welcomed with interest by many induced seismicity research groups from all over the world. It also received an official support from IASPEI. Also since 2010 Professor Lasocki has been deeply involved in integrating European infrastructure of induced seismicity in the framework of European Plate Observing System (EPOS) integration project, the major infrastructural long-term Earth science project in Europe. He is an initiator and a co-chair of Working Group 10: "Infrastructure for Georesources" of EPOS, which is integrating European research infrastructure for studies of seismic processes due to human operations.

Franco Terlizzese is General Director for Mineral and Energetic Resource at the Ministry of Economic Development from 2009. He graduated as an engineer in Rome in 1979 with a master degree in Engineering, specialized in Environmental

Impact Assessment and Management. Before, from 2007 to 2009, he was Director of the National Mining Office for Hydrocarbon and Georesources - UNMIG at the Ministry of Economic Development - Directorate General for Energy and Mineral Resources. He currently holds position as Chairman of the Commission Hydrocarbons and Mineral resources (the National Commission for the safety of mining operations). From 2000 he is the Italian representative at Offshore Oil & Gas Environment Forum and also a member of the Technical Committee of UNI (Ente Nazionale Italiano di Unificazione). In 1980 he began his career in the Public Administration as inspector for mines and quarries at the Ministry of Industry - Directorate General of Mines - Mining District of Carrara. Between 1981 and 1992 he held the position of Technical Responsible for development programs and drilling activities at the Ministry of Industry – UNMIG. In this position he carried out the investigation on the mining disaster of the Val di Stava, whose results have led to the actual Italian technical framework on mining tailings ponds. Between 1993 and 2007 he held the position of Chief Engineer (technical manager) at the Ministry of Productive Activities - Directorate General for Energy and Mineral Resources - National Mining Office for Hydrocarbon and Georesources - UNMIG, performing controls, testing and pre-qualification of plants of hydrocarbon exploration. He has held relevant positions as President and member of ministerial committees for mines and plants in Italy and abroad and as Technical consultant in legal proceedings relating to environmental disasters, workplace safety and labor issues, in hydrocarbons exploration and production. On behalf of the Ministry, from 2012 he sits on the Board of Directors of Acquirente Unico S.p.A., a subsidiary company of the Gestore dei Servizi Energetici GSE S.p.A.

Appendix B. Induced and Triggered Seismicity

A. Introduction

Earthquakes almost always occur when the forces acting to generate movement (shear stress) along a pre-existing fracture exceed the frictional forces (normal stress) acting to resist that movement. This is known in geomechanics as Mode II failure (implying of course that there is a Mode I failure of which more shortly) When that fracture/fault moves it radiates energy into the surrounding rock in a complex way as a combination of wave types depending on where the fracture is located with respect to a free surface and other geological discontinuities. The principal energy is transported away by a sequence of wave trains of which the first but not the largest is a compressional wave (P-Wave) where the direction of cyclic deformation is parallel to the direction of transport, followed by waves which produced shear deformations perpendicular to the direction of propagation, called not surprisingly shear waves (S-Wave). If a free surface is relatively close to the failure then strong deformations can occur and propagate at and below that surface as Rayleigh (vertically polarised) and Love (horizontally polarised) wave trains (**Figure B.1**). The S, Rayleigh and Love are slower than the P waves and the two latter have frequency dependent velocities (dispersion). It is, of course, true that initially those lines of weakness must form somehow in order to then act as failure surfaces but there is a school of thought based on the observation of anisotropic velocity relationships of shear waves that small fractures occur universally through rock and that the process of large scale fracturing is essentially a re-organisation and coalescing of those microfractures. Once localised, movements tend to occur close to or on pre-existing surface as this is energetically favourable and we see very large displacements of many kilometres on major faults systems which are confined to remarkably limited zones of deformation. It appears that the actual displacement in any given event is really not as large as is commonly anticipated and even the very largest of earthquakes will have net displacements which may only amount to a few metres, However, the length of the rupture can be very large and it is this which is the critical parameter in many cases (**Figure B.2**). You need long faults to produce large earthquakes.

Faults will fail under an applied stress system if the balance of forces is such that shearing, (τ) can overcome friction, σ_n and will continue until that is no longer the case but often leaving the system in a quasi-critical state where a minor perturbation can initiate failure. This is often described geometrically by the Mohr Circle construction (**Figure B.3**) which shows the conditions necessary for failure to occur under a system of stresses resolved in to three orthogonal components, which can be described as principal stresses [$\sigma_1, \sigma_2, \sigma_3$], as [$S_{h_{max}}, S_{h_{min}}$ and S_v] stresses or resolved into the direction of a particular planar surface such as a fault. Once failure has occurred frictional sliding can take place at stresses lower than required to initiate primary failure. It should also be noted that rocks are much stronger under compression than they are under tension.

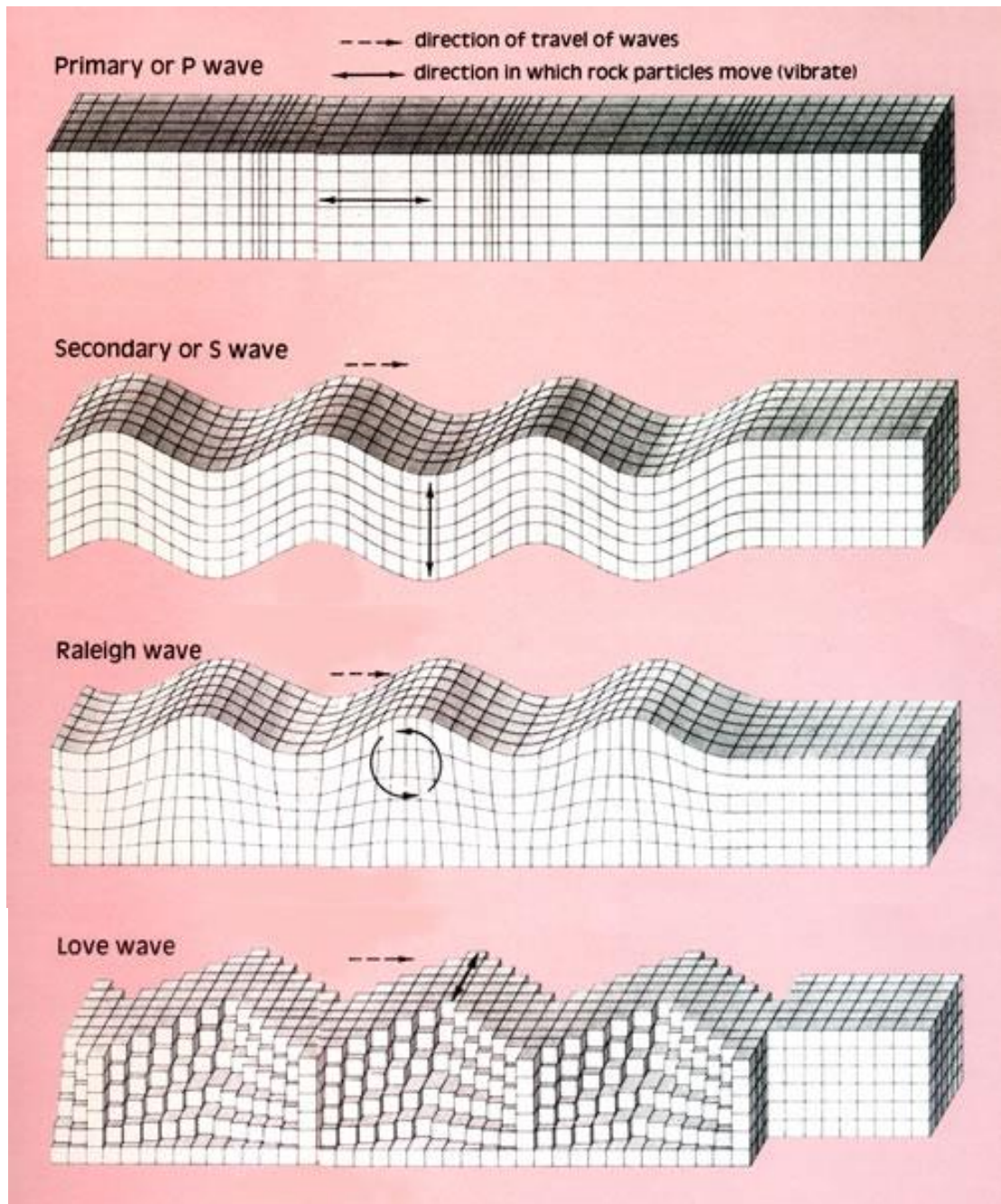


Figure B.1 Seismic wave types

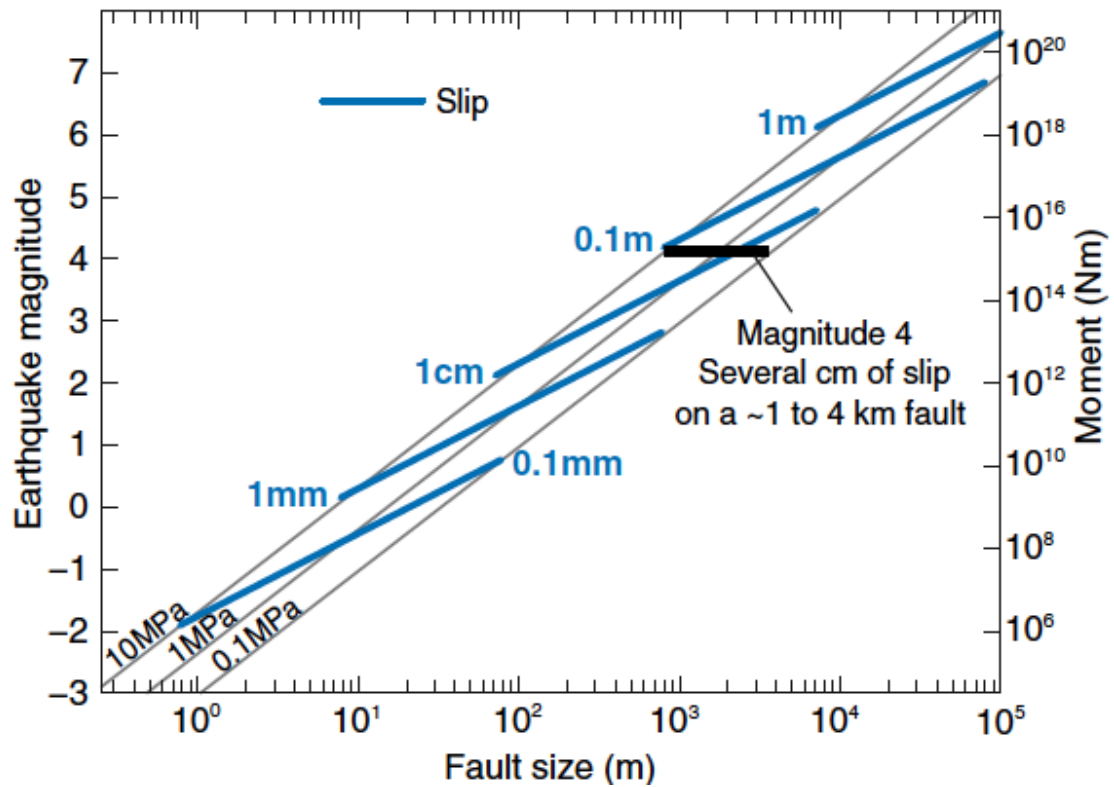


Figure B.2 Earthquake magnitude against fault length and the relationship to stress drop and displacement (after Zoback 2012)

A simplified mechanism of seismic event generation can be deduced from the Coulomb failure criterion, which states that in order to have slip along a fault plane the shear stress in the direction of slip, τ , must equal or exceed the frictional strength of the fault. The formation of a fault involves an additional shear resistance due to cohesion, c , and then the failure criterion becomes:

$$|\tau| = \mu(\sigma_n - p) + c$$

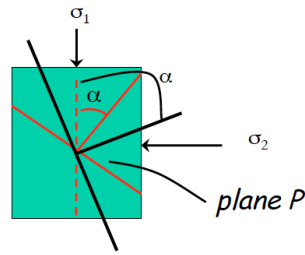
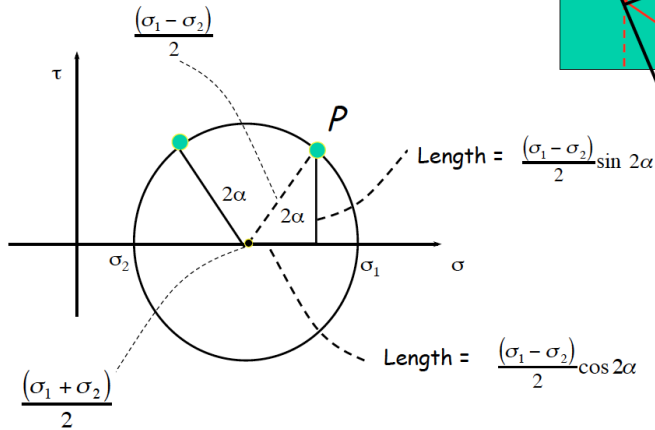
- τ : the shear stress in the direction of slip,
- σ_n : is the compressive stress, normal to the fault plane,
- p : is the fluid pore pressure,
- μ : is the coefficient of friction and
- c : this is the cohesion or 'strength of the fault'.

a.

$$\sigma = \frac{(\sigma_1 + \sigma_2)}{2} + \frac{(\sigma_1 - \sigma_2)}{2} \cos 2\alpha$$

$$\tau = \frac{\sigma_1 - \sigma_2}{2} \sin(2\alpha)$$

Mohr Circle.



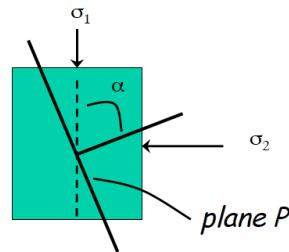
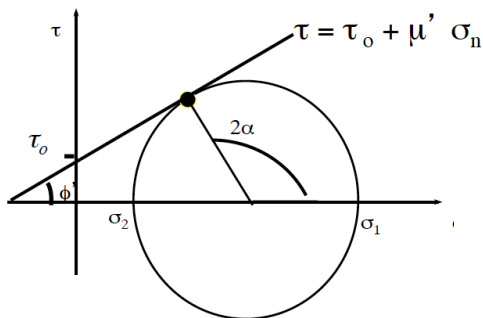
b.

$$\sigma = \frac{(\sigma_1 + \sigma_2)}{2} + \frac{(\sigma_1 - \sigma_2)}{2} \cos 2\alpha$$

$$\tau = \frac{\sigma_1 - \sigma_2}{2} \sin(2\alpha)$$

Mohr Circle.

Coulomb Failure Criterion



The Coulomb and Frictional failure criteria may be considered together, on a Mohr diagram

This shows that pre-existing planes of weakness, of orientations from ϕ_1 to ϕ_2 , will fail by frictional slip prior to a new fracture forming at orientation ϕ_3 .

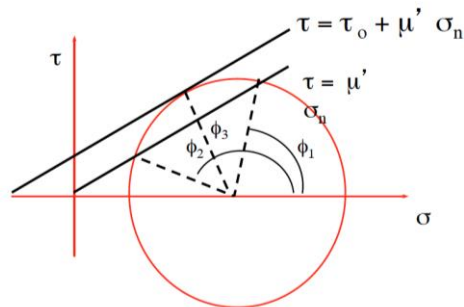


Figure B.3

- a geometric relationship between the principal stresses as resolved onto a plane P (σ_3 is into the plane of the figure)
- b Mohr's Failure criterion for a system of stresses described by $[\sigma_1, \sigma_2, \sigma_3]$

(amended after http://www3.geosc.psu.edu/courses/Geosc508/508L2_20130903_online.pdf)

The Coulomb criterion indicates that a fault can be brought towards failure either by increasing the shear stress in the direction of future rupture or by increasing the fluid pore pressure or both. Based on these possible elastic – poroelastic mechanisms McGarr and Simpson (1997) and McGarr et al. (2002) summarized scenarios of the generation of induced seismicity associated with different technologies. In their view MIS (Mining Induced Seismicity) is mostly due to possible simultaneous decrease of the normal stress and increase of the shear stress. An impoundment of surface reservoirs, leading to RIS (Reservoir Induced Seismicity), elevates the pore pressure, and can also increase the shear stress. A volume contraction caused by conventional withdrawal of hydrocarbons gives rise to a decrease of the pore pressure but also decreases the normal stress, and in some circumstances increases the shear stress. A pore pressure increase is mostly responsible for injection induced seismicity accompanying secondary oil and gas recovery, hydraulic fracturing for shale gas production, waste water disposal wells, geothermal energy production and underground storage of fluids and gases. It should be noted that while the indicated causative factors are important, often the main, they are not however the only ones involved in generating the particular kinds of seismicity and the actual driving mechanisms of induced seismicity are mixtures of different impacts.

It is also possible to create failure in rock by creating a wedge shaped tear where the rock is subjected to a volume change and a crack tip propagates away from a zone of disturbance which is often associated with an injection of a fluid into a previously undisturbed (but not unstressed) rock. This is known as Mode I or tensile failure and is often observed in volcanic, geothermal and hydraulically stimulated hydrocarbon fields, which we will discuss in more detail later.

1. Source Mechanisms

The source mechanism describes the physical movement of the rock during failure. The formation of the generated seismic waves is controlled by the dynamics of the fracturing event. Sufficient records of the event allow the fracture dynamics to be determined.

The two most common descriptions of a source mechanism are the double couple mechanism, and the moment tensor source (Bullen and Bolt, 1985). The double couple mechanism is regarded as the best representation of slip on a fault plane. It describes a pure shear failure with no volume change. Two opposing force couples with no net torque represent this mathematically. The double couple mechanism is fully described by three parameters: the strike and dip of the fault plane, and the rake of the direction of slip on that fault plane.

The moment tensor source is a more general description of the source mechanism that includes volume change. It represents crack motions as nine equivalent forces, of which six are independent (Gibowicz, 1993). As a result, the moment tensor is much more complex to calculate than the double-couple mechanism, and requires more data for its determination.

B. Anthropogenically Influenced Seismicity

In areas, which are geologically active, such as zones of active rifting or active thrusting in the forelands of mountain belts, it is very likely that the crustal and cover rocks are in a critically stressed state. **The Appenines and their foreland basins are such an area.** In such areas minor perturbations to an already precariously balanced stress system can initiate fault movements with associated, sometimes large, earthquakes. The important distinction made by McGarr and Simpson (1997) and McGarr et al. (2002) is between induced and triggered events. For induced seismicity human activity accounts for either most of the stress change or most of the energy associated with the earthquakes. In triggered seismicity human activity accounts for only a small fraction of the stress change and of the energy associated with the earthquakes, whereas tectonic loading plays the primary role.

It is conceptually possible to divide these earthquakes into a number of different categories but it should be appreciated that the boundaries between these are diffuse:

1. **Natural Earthquakes**, which have occurred and would have occurred, due to naturally existing stress systems where the seismogenic stress has exceeded the resisting frictional stress and the region is seismogenically 'ripe'.

2. **Anthropogenic Earthquakes, where human activity has played some part in bringing the stress system to failure:**

a. **Triggered Earthquakes** where a minor, anthropogenically generated perturbation (we will discuss these later) has occurred which has been sufficient to move the stress state from quasi-critically stable to unstable but where the event would have eventually occurred anyway although probably at some significantly later time. That is, we have advanced the earthquake clock but also in doing so simultaneously reduced the probable eventual magnitude. In this case the additional perturbing stress is often very small indeed in comparison with the pre-existing stress system. These are likely to be relatively common because the perturbation does not need to be large. The necessary condition for the occurrence of seismicity is a tectonically prestressed fault near (where 'near' can be many kilometres away depending on the duration and type of the stimulus) the human operations altering the stress field. Under (un!) favourable circumstances such stress changes can eventually cause the loaded fault to fail. Importantly, since technological operations only act to activate the tectonic stress release process, the magnitudes of such earthquakes can be high, and of the same range as those of natural earthquakes, depending on the amount of elastic strain accumulated on the fault due to tectonic loading.

b. **Induced Earthquakes** where an external anthropogenic stress is sufficiently large as to produce a seismic event in a region, which was not necessarily in a stress-state which would have led to an earthquake in the reasonably foreseeable (in a geological sense!) future. This not so easy to do and it probably requires some major change in rock conditions such as the removal of support by mining in either deep hard -rock mining (Gold/Nickel etc) or shallower soft-rock (coal/evaporite etc) with the depth related to the intrinsic strength of the host rocks. The perturbation is therefore much larger in comparison to the naturally occurring stresses. Earthquakes produced by fracking procedures and Enhanced Geothermal Systems fall in this category.

1. How do we tell the difference between natural and triggered/induced seismicity?

It is clear that there are many, many possible mechanisms which can bring about the minor stress changes which are necessary to trigger seismic events during anthropogenic activities. The magnitude of these man-made events can be large and is controlled by the ambient stress field, the magnitude and the duration of the perturbation and the dimensions of the faults which are available to be stimulated. Some of the physical mechanisms are illustrated in Dahm et al 2010 sums up the situation very well:

“Human operations, such as mining, hydrocarbon production, fluid withdrawal or injection, drilling, hydro-fracturing and reservoir impoundments, can positively and negatively impact tectonic stresses, pore pressure, fluid migration and strain in the sub-surface. Earthquakes occurring in spatial and temporal proximity to such operations are immediately under suspicion to be triggered or induced. The discrimination between natural, triggered, and induced earthquakes is a difficult task, and clear rules and scientific methods are not well established or commonly accepted”.

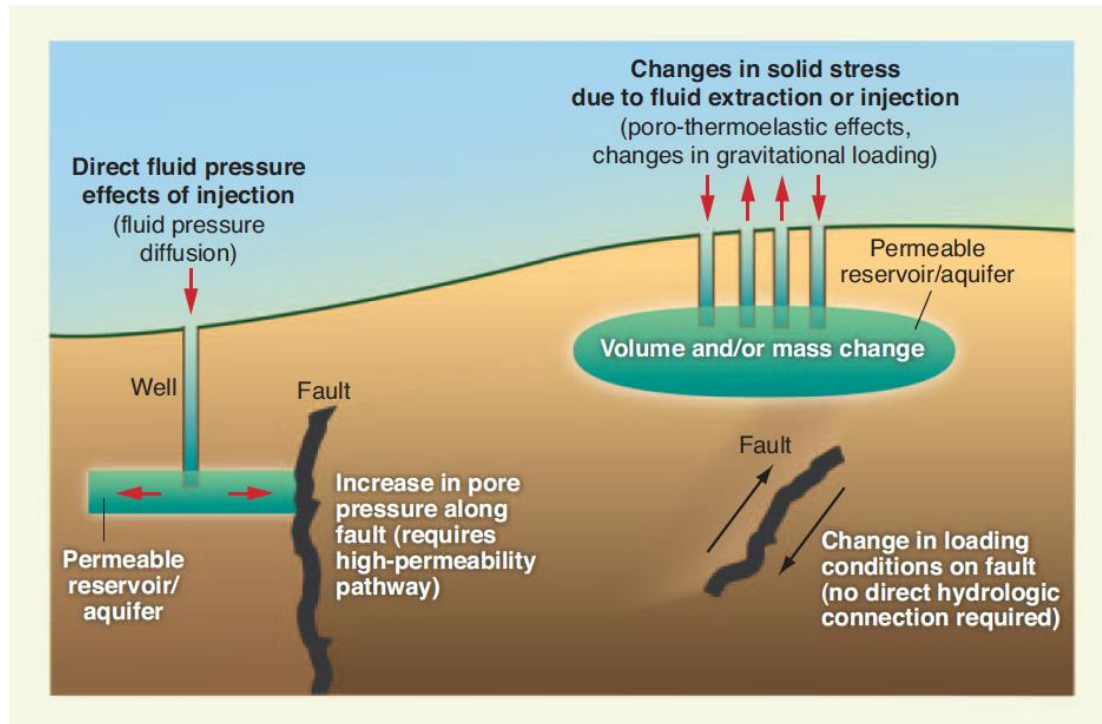


Figure B.4 Potential causative mechanisms for triggered/induced seismicity from Ellsworth (2013)

There are seven discriminatory criteria which are often applied (modified after Davis and Frohlich 1993). These are:

1. Are these events the first known earthquakes of this character in the region?
2. Is there a clear correlation between injection/abstraction and seismicity?
3. Are epicentres near wells (within 5 km)?
4. Do some earthquakes occur at or near injection/abstraction depths?
5. If not, can known geologic structures channel flow to sites of earthquakes?
6. Are changes in fluid pressures at well bottoms sufficient to generate seismicity?
7. Are changes in fluid pressures at hypocentral distances sufficient to generate seismicity?

These can be useful in many cases to improve the confidence that any particular event or set of events is induced/triggered and this was the case for the 2011 Hydraulic Stimulation events (Fracking) detected in Blackpool Lancashire (Green et al 2012). More recent studies show, however, that these criteria are not appropriate in all cases. When there are many activities occurring in a region which is itself seismically active then these criteria cannot be simply applied and it is necessary to look very carefully at spatial and temporal relationships between seismicity and operational parameters associated with pre-existing faults either mapped on the surface or from seismic investigations and also statistical parameters of the seismic events themselves.

The threshold epicentral distance of 5 km used by Frohlich and Davis now seems to be too short compared to observed cases (e.g. Ellsworth 2013). Sometimes the depth of induced events correlates well with the injection depth, however at other

times the hypocentral depth can significantly exceed the injection interval (e.g. Keranen et al., 2013). Violation of the criteria of Davis and Frohlich (1993) seems to occur particularly often for triggered earthquakes. Keranen et al. (2013) report an 18 yr. long lag between the start of fluid injection and the occurrence of Oklahoma, US earthquake sequence from 2011. The lag inferred for the Romashkino Oil Field, the biggest oil field in Russia, was 28 yr. (from 1954 to 1982, Turuntaev, 2012). Induced seismicity may continue even long after termination of injection operations. The induced, and specifically the triggered, seismic response to injections is complex and variable among cases and its correlation with technological parameters is far from being fully known (e.g. Brodsky and Lajoie, 2013; van der Elst et al., 2013).

Of course it is not always so easy to see which of these situations has arisen and in order to assess this we need to look at a range of scenarios, which have been observed in recent years around the world from a variety of different regions.

2. Induced Seismicity around the world

Because of the occurrence of a large number of recent seismic events which have a prima facie relationship to anthropogenic activities, there have recently been a number of excellent reviews in the last four years of induced seismicity

Hitzman et al to the Committee on Induced Seismicity Potential in Energy Technologies of National Academy of Sciences (2013), Suckale (2009) for Hydrocarbon Fields, Ellsworth (2013) on deep high volume waste water related seismicity and Evans et al. (2012) and Gruenthal (2013) for induced seismicity related to geothermal projects and other types of induced seismic events in Central Europe and Davies et al 2013 for hydraulic fracturing activities in relation to other activities.

It is not useful to attempt to summarise this vast volume of literature and this review will simply draw attention to some of the most significant conclusions and especially those which may be relevant to the seismicity observed in Northern Italy in 2012.

Possible causes of Induced and Triggered Seismicity fall into two main categories:

- Removal of physical support, e.g. Mining where stress change is comparable to ambient stress. Maximum Magnitudes range as high as 5.5 MI and related to the physical strength of the rock, which is failing. This is also the case for later phases of oil and gas extraction where significant volumes of fluids have been removed so that hydraulic support from pore fluids is lacking, and subsidence and compaction processes come into play.
- Hydrological Changes to include extraction or Injection of water/Gas/Oil which is probably triggered, as the stress changes are small compared to the ambient stress. The magnitudes here also depend on the rock strength but also on the total volume of injected (and presumably extracted fluid). It has been acknowledged that although injections inducing or triggering earthquakes are only small fractions of all underground injection cases they can pose a serious risk in particular when injections are performed in naturally active regions (also e.g. Zoback, 2012; Ellsworth, 2013)

Working Group 10 “Infrastructure for Georesources” of European Plate Observing System (EPOS) project has defined five induced/triggered seismicity categories related to the inducing technologies (e.g. Lasocki et al., 2013a; Lasocki, 2013a). In Davies et al (2013) there were compiled 190 possible examples of induced earthquakes occurring since 1929 with magnitudes equal or greater than 1.0 with a maximum of 7.9. The possible causes and observed magnitude ranges are:

- **Mining (1.6 - 5.6);**
Mining-induced seismicity, MIS. The seismicity induced or triggered by withdrawal of minerals either by underground mining or by open-pit mining and quarrying. This is the oldest known kind of induced seismicity. The first chronicled mining seismic event, a

rockburst, occurred in Derbyshire, England in 1738. The strongest MIS earthquake, of M5.6, occurred in a potash mine in Volkershausen, Germany in 1989. Deep gold mining in South Africa induces seismic earthquakes, occasionally exceeding magnitude 5.0 (e.g. M5.3 earthquake in a gold mine in Klerksdorp region in RSA in 2005, Durrheim, 2010), whereas the copper-ore mining and the coal mining in Poland are accompanied by seismic activity with 1-2 events $M > 4.0$ yearly. More recent comprehensive reviews of MIS can be found in Gibowicz and Lasocki (2001) and Gibowicz (2009).

- **Hydrocarbon Extraction and Oil and gas field depletion (1.0 - 7.3);**

Comprehensive reviews of IEIS are provided in Suckale, 2009 and Committee on Induced Seismicity Potential in Energy Technologies (2013) Injection/Extraction Induced Seismicity (IEIS). In this category the seismicity induced or triggered by conventional as well as unconventional (shale gas, heavy oil) oil and gas exploitation, and the seismicity accompanying underground storage of liquids and gases are grouped. Maximum magnitudes of IEIS vary over a wide range depending on the inducing technology. The largest earthquakes, up to M6+, have been associated with conventional hydrocarbon production (e.g. M6.1 Kettleman North, USA, M = 6.0 Barsa-Gelmes-Wishka oilfield .Turkmenistan). In addition conventional oil and gas production, which quite often takes places in tectonically active regions, may have a triggering effect for some strong, sometimes catastrophic earthquakes.

- **Water injection for secondary oil recovery (1.9 - 5.1);**

- **Reservoir impoundment (2.0 - 7.9);**

Reservoir-induced seismicity, RIS, is triggered by the impoundment of surface reservoirs of liquids. It is usually connected with hydroelectric power plants and high dams. RIS is responsible for the most tragic indubitable induced earthquake, the Koyna event M6.5 in 1967, which took some 200 lives, caused more than 1500 injuries and left thousands of people homeless. Events exceeding magnitude 6.0 are not infrequent for this category, e.g. M6.3 Kremasta, Greece, M6.2 Kariba, Zambia/Zimbabwe, M6.1 Xinfengjiang, China. (Gupta 2002).

- **High volume waste water disposal (2.0 - 5.3);**

Discussed in detail later

- **Academic research boreholes testing for induced seismicity (2.8 - 3.1);**

- **Evaporite solution mining (1.0 - 5.2);**

- **Geothermal operations (1.0 - 4.6);**

Discussed in detail later

- **Hydraulic fracturing of low-permeability sedimentary rocks (1.0 – 3.8);**

Most seismic events induced by hydrofracturing for shale gas exploitation are below magnitude 3.0 and in most in fact below zero (Green et al 2012) and are not discussed further here.

- **Cases in Debate (CiD);**

These are strong and often catastrophic earthquakes, whose origin, whether a purely tectonic or tectonic triggered by a technological activity has not been resolved yet. In these cases the triggering influence of human actions cannot be proved but cannot be excluded either. The best known CiD are the M7.9 Wenchuan (China) earthquake from 12/05/2008, whose occurrence might be connected with the impoundment of Zipingpu reservoir (Shemin Ge et al., 2009; Chen Yong 2009), those connected with conventional hydrocarbon production: M6.7 Coalinga, USA, 2/05/1983 (McGarr, 1991), the sequence in Gazli (Uzbekistan) region: M7.3, 8/04/1976; M7.0, 17/05/1976; M5.7, 4/06/1978; M7.0, 19/03/1984 (Eyidoğan et al. 1985; Simpson and Leith 1985), and the recent (2011) Lorca, Spain M5.1 case, which might be triggered by long-lasting water pumping to irrigate (Avouac 2012; González et al. 2012). The most famous CiD is perhaps the Coalinga earthquake sequence of 1983 shown in **Figure B.5** and **Figure B.6**.

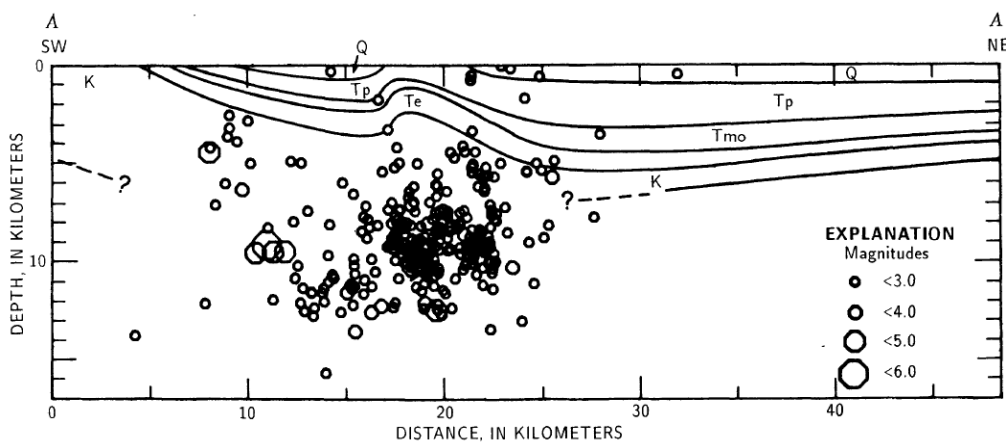


Figure B.5 Southwest-northeast geologic cross section through the Coalinga area, showing locations of the main shock and M>3 aftershocks for May-July 1983. (Segall P. and Yerkes, R.F., USGS)

On 2 May 1983, a magnitude 6.7 M_L occurred approximately 35 km northeast of the San Andreas Fault and about 12 km northeast of the town of Coalinga, California, near two major oil fields, Coalinga Eastside and Coalinga East Extension¹ in a previously aseismic (by Californian standards) region. There was considerable damage to the area including to underground wells, which were sheared. This led to speculation about a relationship between oil extraction and the seismicity. Segall (1985) calculated the poroelastic stress change as a consequence of fluid extraction to be 0.01–0.03 MPa which at the time was thought to be a negligible amount in

¹ Coalinga: giant oil field discovered in 1890, cumulative production more than 912,000 million barrels, 1,646 producing wells (data from California Department of Conservation, 2006).

comparison with the eventual main event although current thinking would not necessarily agree.

The U.S. Geological Survey concluded that the earthquake was associated with a blind fault located on the structural boundary between the Coastal Ranges and the San Joaquin Valley (Figure 3). Two additional major events occurred in the vicinity of Coalinga at Kettleman North Dome² 1985 and at Whittier Narrows in 1987 directly beneath major oil fields and McGarr (1991) pointed out the similarity between the three events and postulated some mechanisms for their occurrence in terms of crustal unloading.

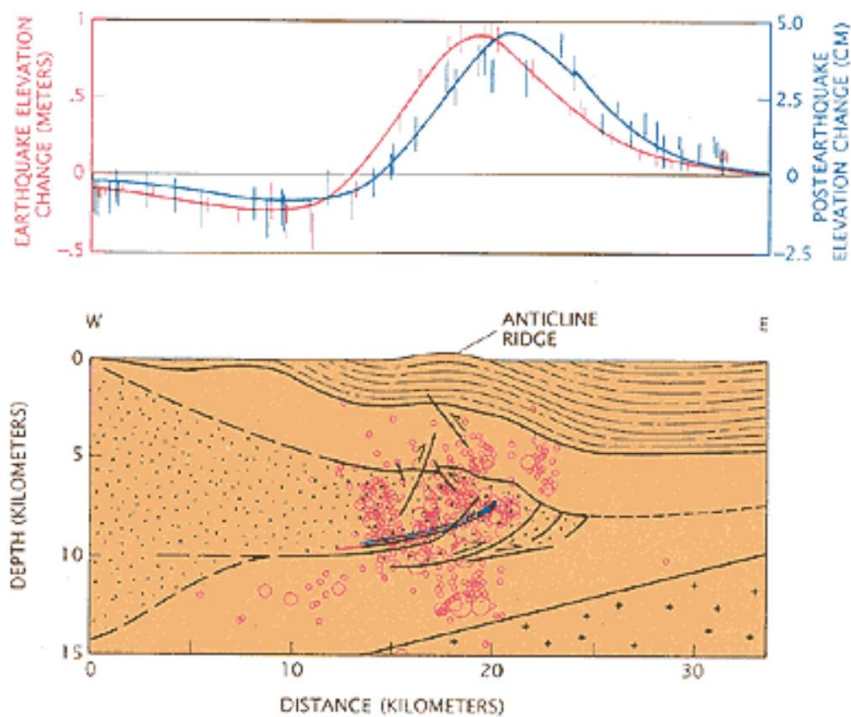


Figure B.6 Subsurface structures beneath the anticlinal fold and elevation changes over the Wilmington reservoir (From Stein and Yeats, 1989)

However a further CID and one of the oldest suggestions of hydrocarbon related seismicity is local to Northern Italy in the Caviaga³ region (Figure 7) where oil and gas are in roll-over anticlines within the blind thrusts beneath the Po Plain.

- Two earthquakes of magnitudes M 5.4 & M 4.5 were recorded on May 15th & 16th 1951 with a hypocentral depth at 5 km area in the Lodigiano, northern Italy region.

² Kettleman North Dome: Giant oil field discovered in 1928. is one among the major oil-producing areas of the world; cumulative production more than 458,000 million barrels, 40 producing wells (California Department of Conservation, oil and gas Statistics, Annual report, 2006).

³ Caviaga: giant gas field cumulative production more than 13,000 MSm³ (2013 data). About 700 MSm³ were been produced from 1944 to 1951.

- These earthquakes were studied by Caloi et al. (1956) who was able to calculate directions of the first arrivals from paper-recorded data from twenty seismological stations.
- Caloi argued that there was a possible correlation between seismic events and hydrocarbon activities.

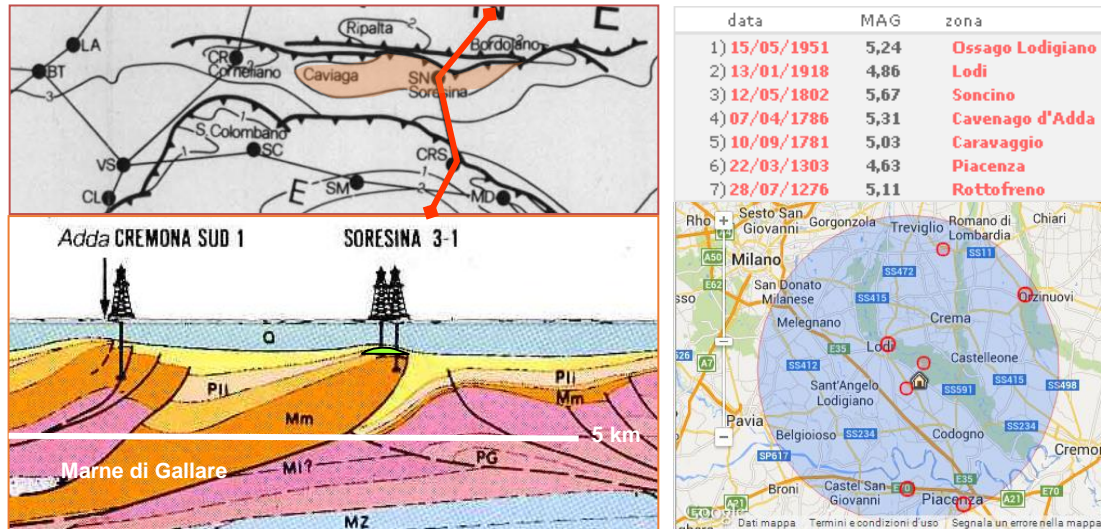


Figure B.7 Structural cross-section, location of oil and gas fields of the Caviaga region, Northern Italy and historical and recent seismicity (Caloi et al., 1956)

In fact in many compilations of induced seismicity, Caviaga IS listed as an accepted case of anthropogenic induced seismicity.

A recent CiD is from Sichuan, China where an earthquake of M_w 7.9 occurred in May 2008 with the epicentre near to a large new dam at Wenchuan and it has been suggested that the loading or even fluid percolation acted as a trigger. However the fault rupture in this event was almost 250 km long, with a large proportion of energy being released far from the influence of the reservoir pore-pressure changes but nevertheless the initial failed patch might have very well have propagated all along the fault.

Although at present it is not possible to discriminate unequivocally between man-made and natural tectonic earthquakes, some characteristics of seismic processes have already been identified, which can speak for or against possible connections between seismicity and human technological activity.

In most of these cases the intensity and potential damage are slight for magnitudes as high as 4.5 M_L as can be seen from **Figure B.8**. However once we reach magnitudes exceeding 5 M_L the potential for damage is considerable particularly for historic and vernacular architecture.

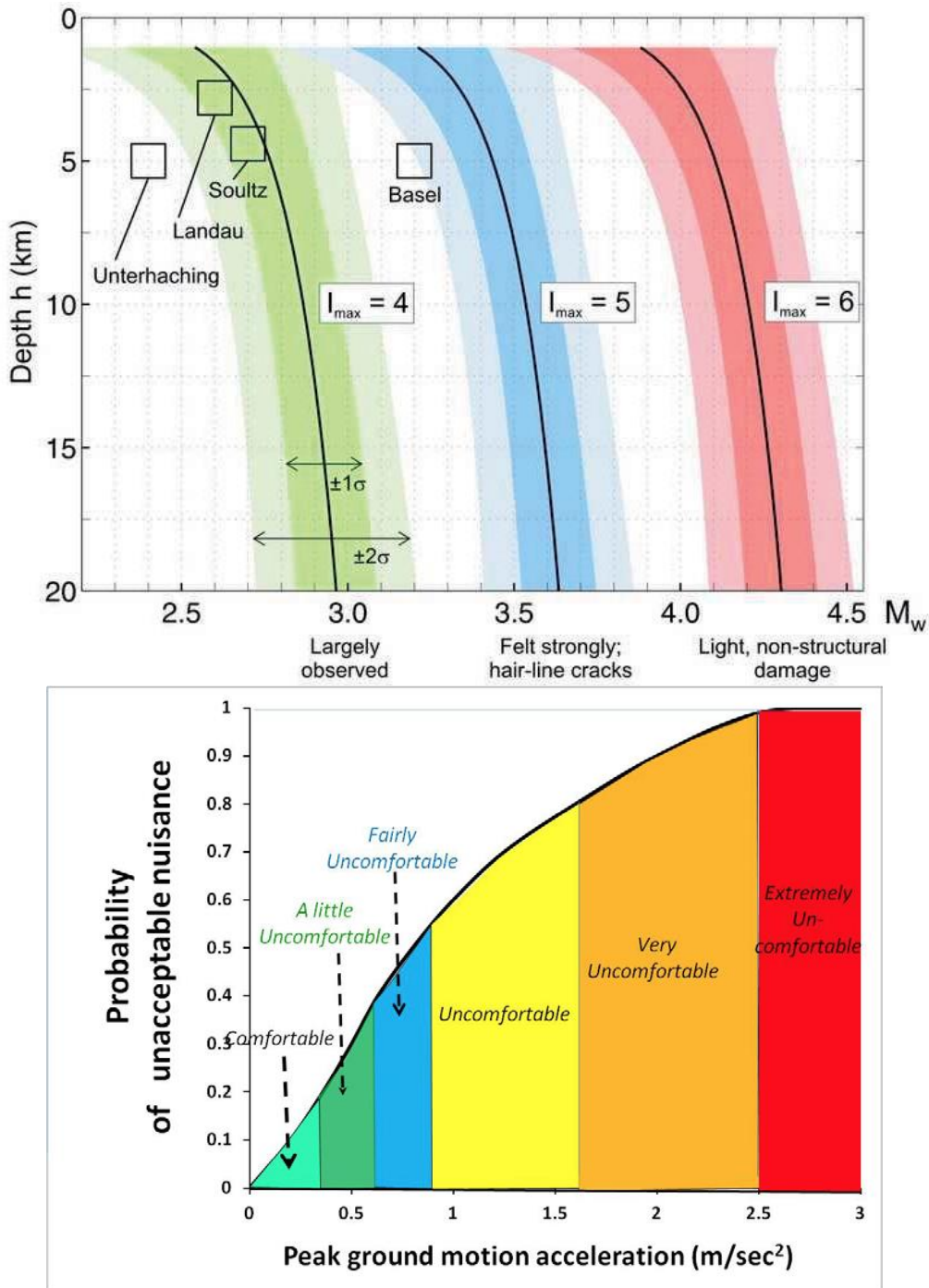


Figure B.8 Intensity and damage potential fields for a range of depths and magnitudes (from Gruenthal 2013)

While mining induced seismicity is very important in many parts of the world and has produced some very large events it is not directly of relevance to the Ferrara seismicity and will not be discussed further here, of more importance are those seismicity types which are related to the range of activities which have taken place in the Po basin which are mostly related to fluid injection and abstraction activities. **Figure B.9** shows the global distribution of induced/triggered seismicity and the maximum magnitudes observed and **Figure B.9** breaks this down further into a frequency plot.

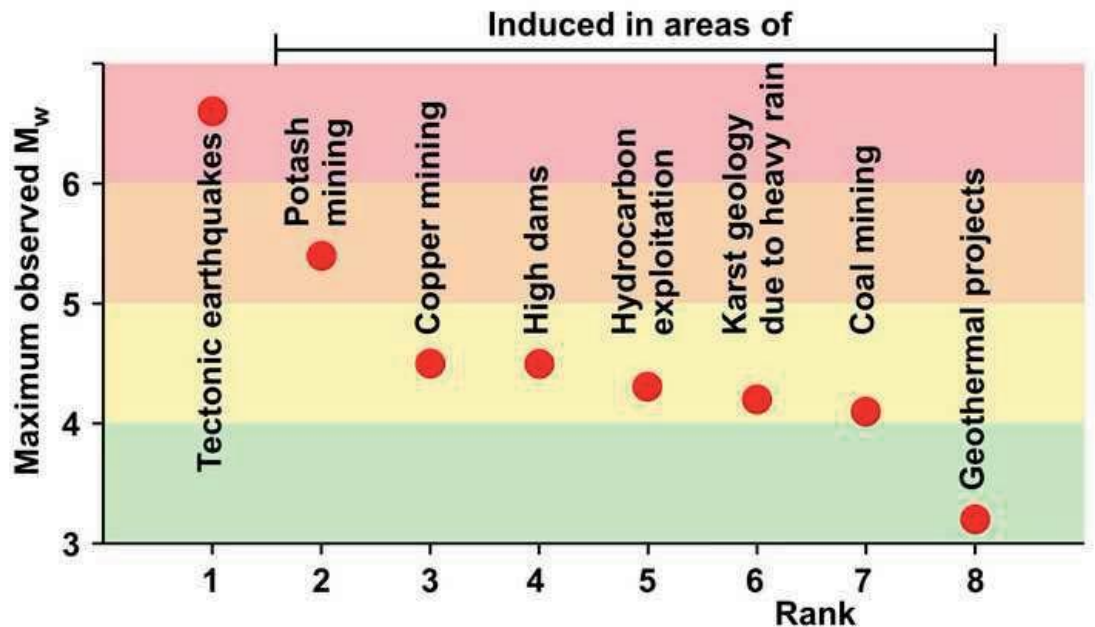
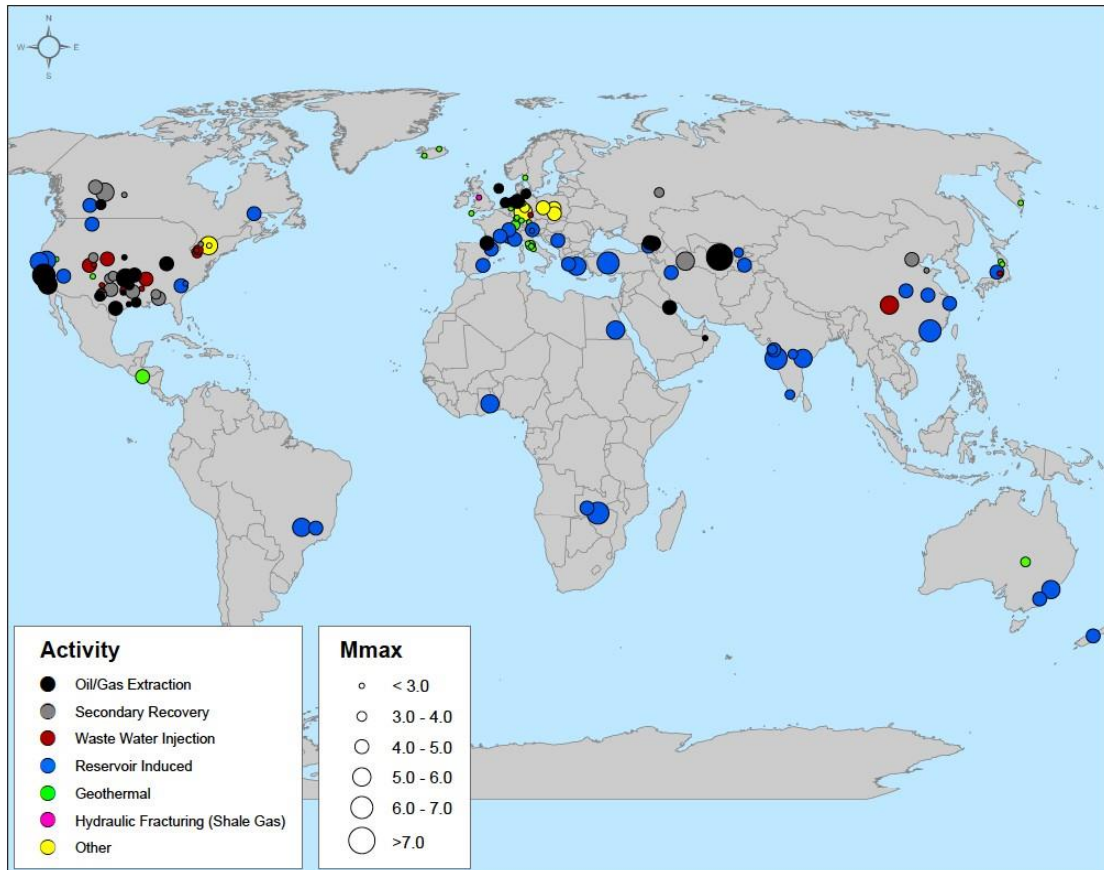


Figure B.9 (top) **Figure B.10** (bottom) Worldwide locations of seismicity by or likely related to human activities, with the maximum magnitude induced at each site and by type of activity, after Hitzman et al (2013) and Gruenthal et al (2013)

Figure B.11 from Davies et al (2013) is a histogram of induced seismicity type and **Figure B.12** specifically show the geothermally and CO₂ injection related incidents which have occurred in Europe.

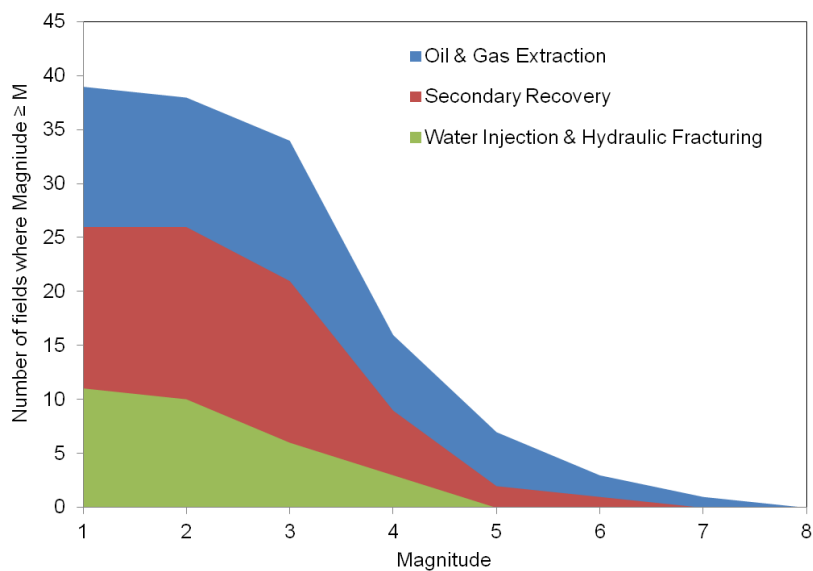
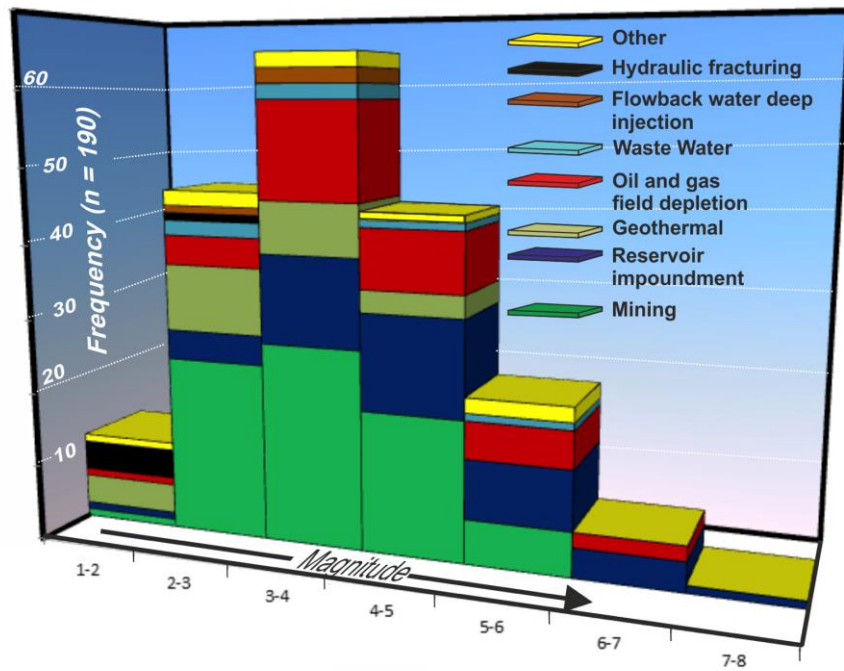


Figure B.11 Graph of frequency versus magnitude for published examples of induced seismicity for mining, reservoir impoundment, geothermal, oil and gas field depletion, secondary oil recovery, research, solution mining, shale gas flowback water disposal, and hydraulic fracturing for shale gas. From Davies et al. (2013) and Hitzman et al (2013)

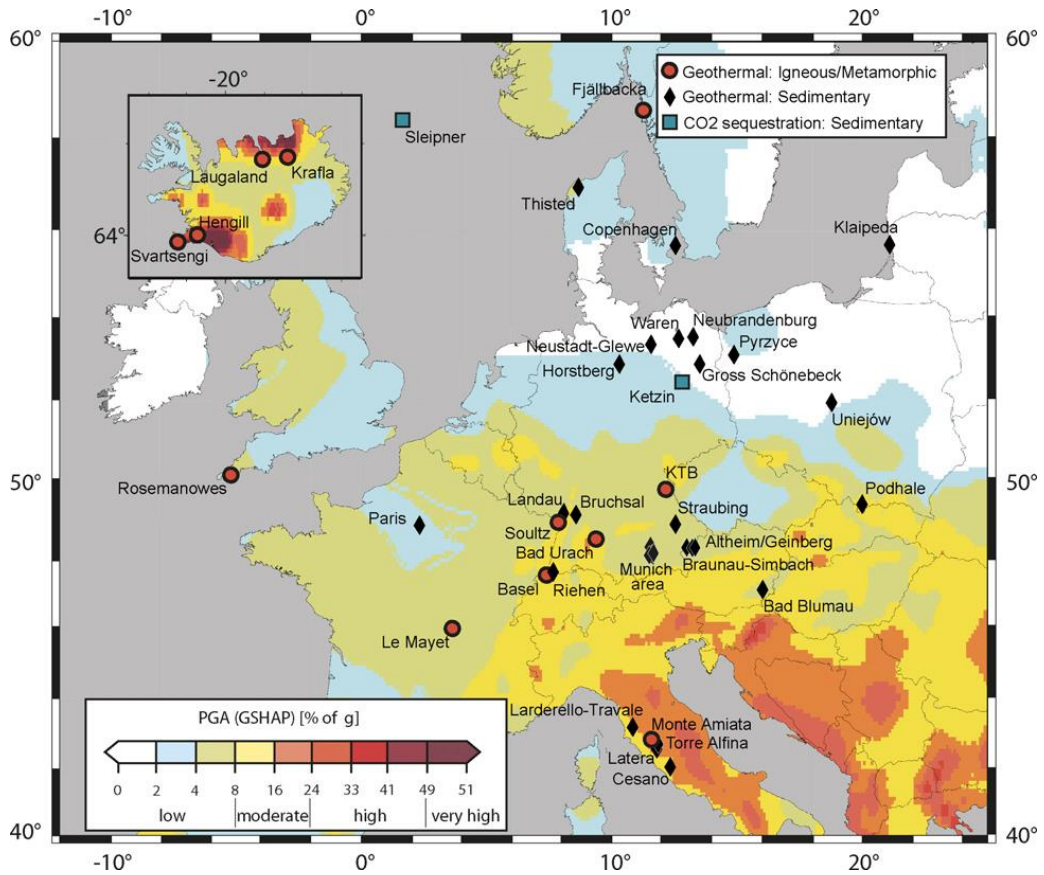


Figure B.12 Location of geothermal injection sites from Evans et al. (2012). The background is taken from the global seismic hazard map of the Global Seismic Hazard Assessment Program (GSHAP) <http://www.seismo.ethz.ch/static/GSHAP>.

The colour scale denotes the GSHAP index of local seismic hazard from natural earthquakes defined in terms of the peak ground acceleration (PGA) in %g on stiff soil that has a 10% probability of being exceeded in 50 years (equivalent to a recurrence period of 475 years).

3. Statistical Relationships and scaling laws

It has been observed over a long period of time (many decades) and over a huge range of magnitudes and tectonic scenarios that there is a scaling law that relates the number of earthquakes and their frequency of occurrence and this is known as the Gutenberg-Richter Law. It is, of course, intuitive that there will be a lot of small earthquakes, a reasonable number of medium sized ones and fewer and fewer large ones but it seems that there is an inbuilt mathematical power – law relationship in that when we plot the Logarithm of the number of events exceeding a certain magnitude against that magnitude we get a straight line above some minimum level where we are probably not seeing all of the actual events (**Figure B.13**).

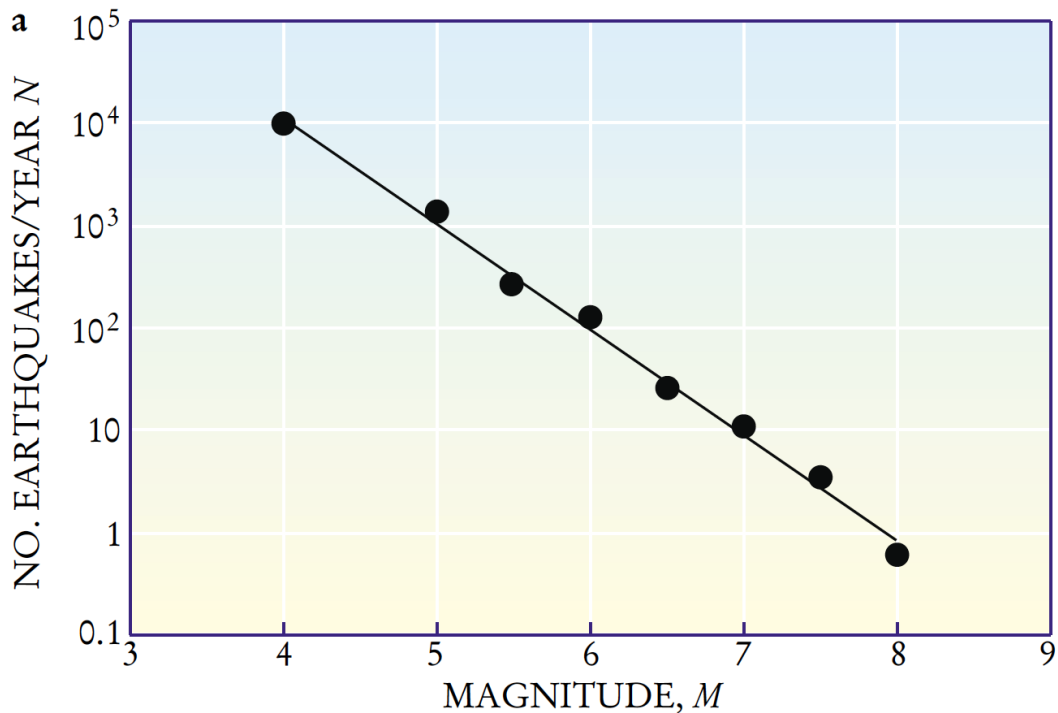


Figure B.13 Gutenberg Richter plot for global earthquakes (From Kanamori and Brodsky, 2001)

The slope of this line is known as the b-value and while it is globally about -1, it varies in way, which is thought in some senses to be diagnostic of the type and source mechanism of the set of earthquakes.

This relationship is shown in **Figure B.14**: where cluster of seismic events is called an Earthquake swarm. In the Reno case b is about -0.836.

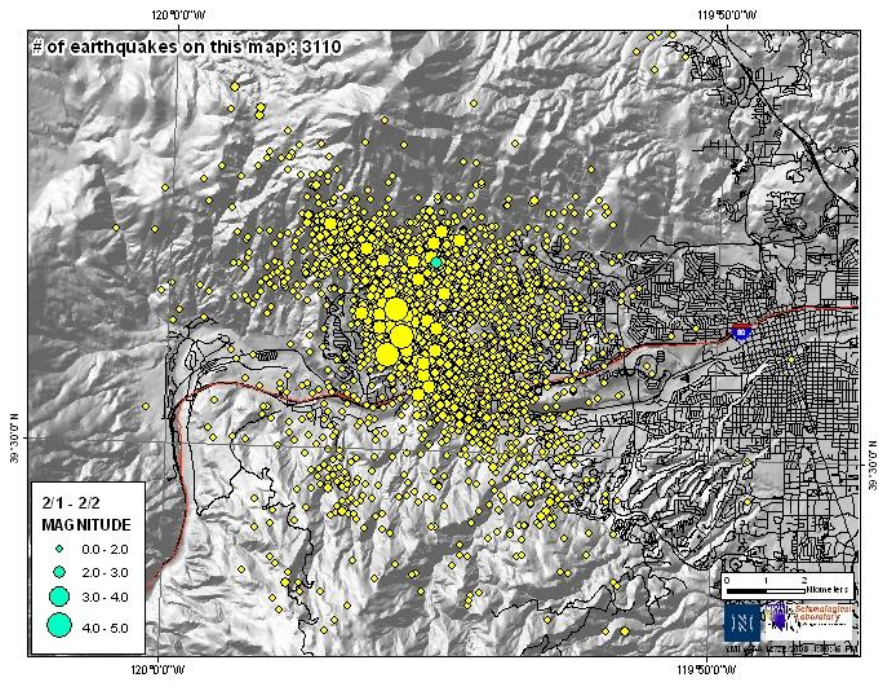
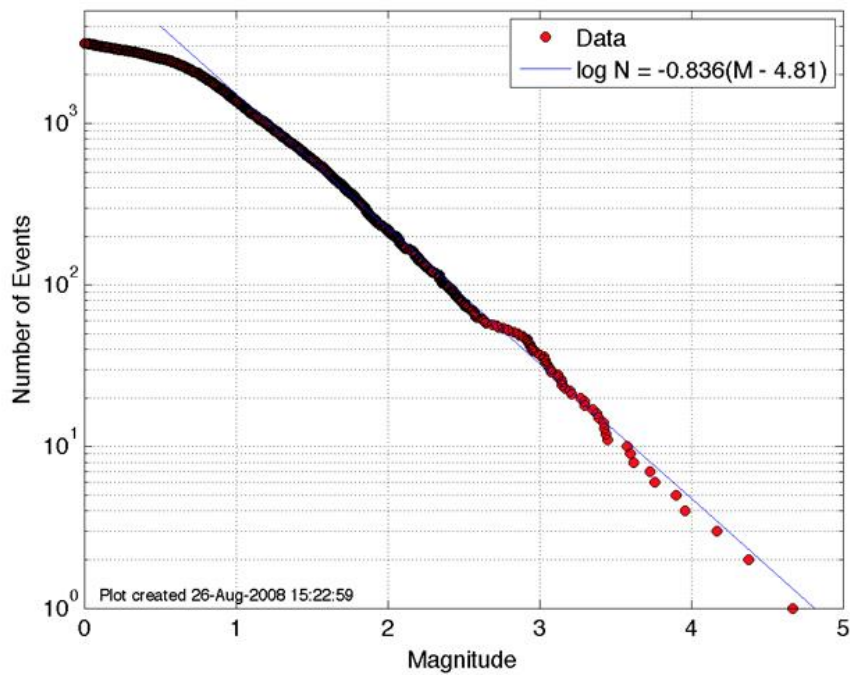


Figure B.14 2008 Mogul-Somerset Earthquake Sequence; West Reno, Nevada (From Nevada Seismological Observatory)

An earthquake nucleating anywhere, at any time, will randomly grow to a magnitude $\geq M$ according to the distribution

$$\log(N) = a - bM,$$

Which implies that the probability that any nucleating earthquake will grow to magnitude $\geq M$ is

$$P(M) = 10^{-b(M - M_{\min})}$$

N = number of eqs $\geq M$, a is earthquake rate, b = constant (1.0), M_{\min} = minimum earthquake magnitude.

C. Fluid Injection and Abstraction Related Seismicity

It has been known since the 1960s that earthquakes can be induced by fluid injection when military waste fluid was injected into a 3671 m deep borehole at the Rocky Mountain Arsenal, Colorado (Hsieh, 1981). This induced the so-called ‘Denver earthquakes’. They ranged up to M 5.3, caused extensive damage in nearby towns, and as a result, use of the well was discontinued in 1966. Reviews of activity often focus on selected mechanisms although there are notable exceptions (National Academy of Sciences, 2013). Artificially injecting fluids into the Earth’s crust induces earthquakes (e.g. Green et al., 2012). **Figure B.15** show a simple mechanism which represents this.

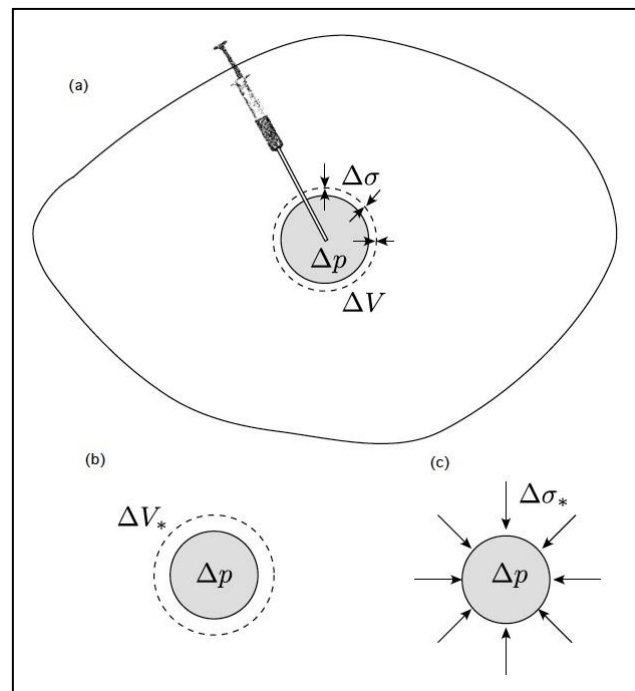


Figure B.15 Injection of fluid inside a porous elastic sphere within a large impermeable elastic body induces a pore pressure increase inside the sphere as well as a stress perturbation inside and outside the sphere (after Hitzman et al 2013)

1. Hydrocarbon Extraction Related Seismicity

Hydrocarbon extraction activities sometimes occur in regions which are naturally seismically active due to tectonic processes which have possibly created the structures and conditions in which oil and gas can be found and the extraction activities and the seismicity are not seen or considered to be related. Whether this is a valid assumption may be questioned in some cases but for the time being it is considered that this is true for the majority of cases. However, there are a number of authoritative reports which list a number of well-examined cases where hydrocarbon extraction has been

associated (it may not be possible to use the word proven) with sometime large and damaging earthquakes. The recent IEA Report: Induced Seismicity and its implications for CO₂ storage risk, Report 9/2013 is one such publication and **Figure B.16** identifies those areas.



Figure B.16 Sites where Hydrocarbon extraction is firmly considered to be related to hydrocarbon activity (from IEA Report: Induced Seismicity and its implications for CO₂ storage risk, Report 9/2013)

Ottermoller et al (2005) in a presentation on Ekofisk Seismic event Of May 7, 2001 from The North Sea also list a number of events which overlap but do not exactly coincide with the IEA map.

The most relevant cases are discussed below.

Rangely Colorado USA

Situated within the Rangely anticline the Rangely oil field has produced oil and gas since 1945 to the present day from the Carboniferous (Pennsylvanian) and Permian Weber sandstone, a low-permeability sandstone lying at 1700 metres with a thickness of 350 metres. In order to enhance permeability and increase declining pressure to sustain production, water flooding was implemented from 1957 to 1986 followed by gas injection. These procedures induced a number of relatively small earthquakes (M_L 3+) and experiments were undertaken which showed that seismicity could be triggered and then controlled by the rate of water injection. Such simple clear and reproducible relationships have been harder to repeat or discern in other parts of the world.

Gazli , Uzbekistan

The Gazli Field (**Figure B.17**) has been actively producing oil since 1962 (average rate of 20 billion m³/y) and in 1976 (twice), and 1984 large earthquakes of 6.8, 7.3 and 7.2 ML were experienced in the region with extensive local damage, one fatality and more than 100 people injured. The producing horizons are of Cretaceous

age and again water injection was trialled to attempt to halt rapidly declining production levels.

Surface subsidence was noted in these cases, which was correlable with production rates. This is a relatively aseismic area and in fact these are the largest events recorded anywhere in central Asia. They do lie close to a major Fault, the Bukhara-Ghissar structure but the mechanisms do not show stress direction which appear to align with this feature. There is no clear consensus as to the exact mechanism if these were in fact triggered events but they are clearly a cause for concern. Activity is continuing with a sizeable event in 2006.

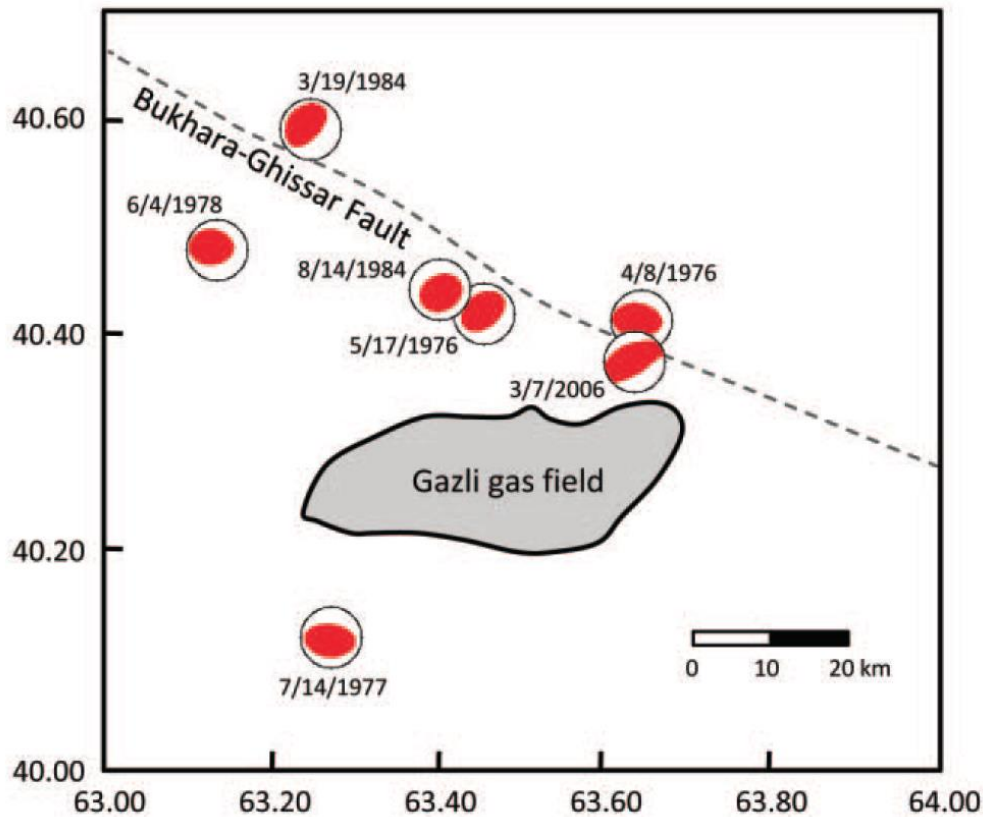


Figure B.17 The extremely large and enigmatic events, which occurred, close to the Gazli Gas field with a maximum magnitude of 7.3 M_L (after Suckale 2009)

Romashkino, FSU

The Romashkino field (**Figure B.18**) which has been operational from 1948 until the present day (total production more than 15 billion barrels), is the largest in the Volga Basin with a dimension of c 100 km by 70 km and with oil extraction from Devonian sandstone sequences at about 1800 metres depth. Again, water flooding was implemented to enhance production from the relatively low permeability reservoir formations, commencing in 1954 with very large volumes injected, in fact exceeding the total extracted volume and pressures up to 25 MPa (c 250 bar) from initial values of 18 MPa.

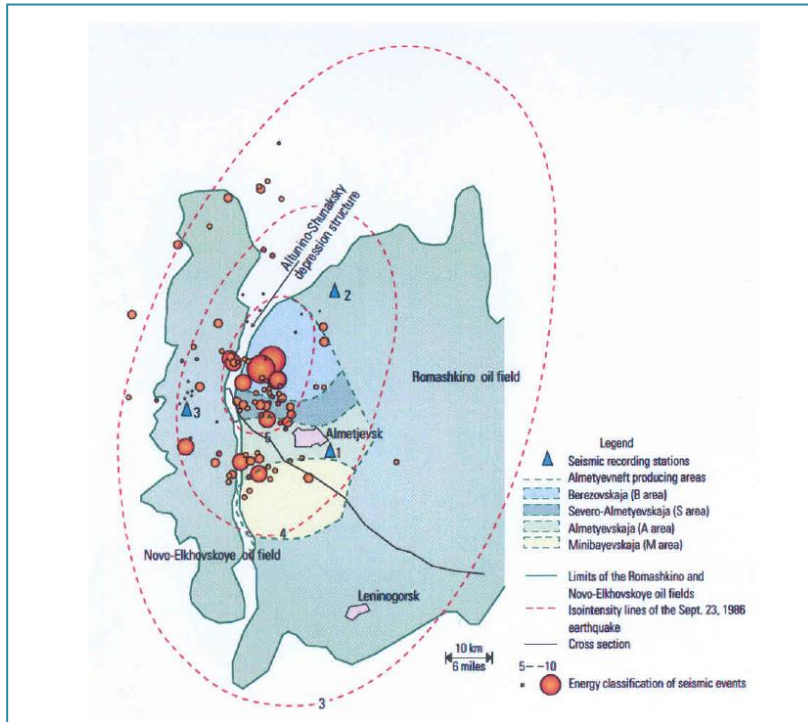


Figure B.18 Seismicity in the Romashkino Oil field region and associated geological structures (from Adushkin et al 2000)

Moderate seismicity with magnitudes of up to 4 ML was experienced throughout the 80's and 90's and almost 400 events were detected on a local network installed in 1985. A clear relationship between the fluid balance (excess or deficit) between extracted oil and injected water and seismicity rates can be demonstrated here as shown in the **Figure B.19** again from Adushkin (2000).

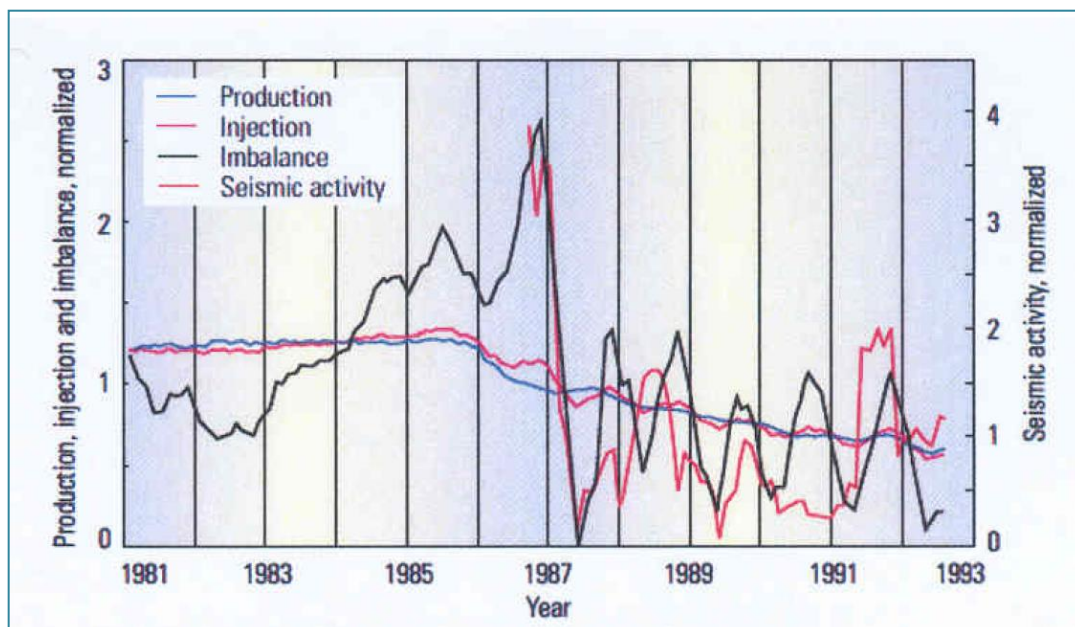


Figure B.19 Relationship between operational parameters and seismicity with a clear correlation between fluid imbalance and the rates of seismic activity at Romashkino Oilfield. (From Adushkin et al 2000)

Wilmington, California, USA

The Wilmington oil field is the largest in California and in total more than 2.5 Billion barrels of oil have been extracted over an 80 years period since 1932 from relatively deep turbiditic reservoirs, which extend down to 3200 metres. This enormous extracted volume has led to significant subsidence of greater than 9 metres with horizontal displacements of almost 4 metres in some places with extensive surface damage (**Figure B.20**). The years 1947,1949,1951,1954, 1955 and 1961 saw a sequence of moderate size, shallow (0.5 km) earthquakes in the Wilmington area with magnitudes ranging from 2.4 to 3.3 M_L although it is very likely that there were many others of much lower magnitudes. In this case water injection to replace extracted volume successfully mitigated both the subsidence and the seismicity.

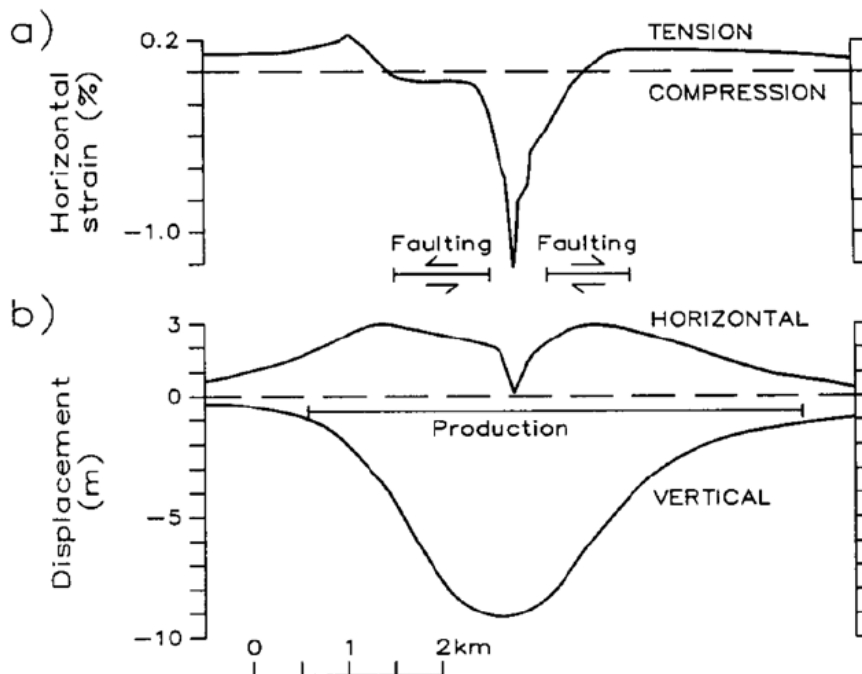


Figure B.20 Surface displacements in the Wilmington region associated with oil extraction (from (Yerkes and Castle 1970))

This led Segall to develop his theory of induced seismicity associated with surface subsidence and associated flexural stresses, which was successfully applied to the Lacq and other fields (**Figure B.21**).

Chanpura R. (2001) carried out an extensive set of models of the effects which depletion would have on pre-existing faults depending on their geometric relationship to the extracted zone and the orientation of the extraction. The set of his final conclusions are shown in **Figure B.22** where it is clear that for various parameters it is faults below the extracted zone which are destabilised.

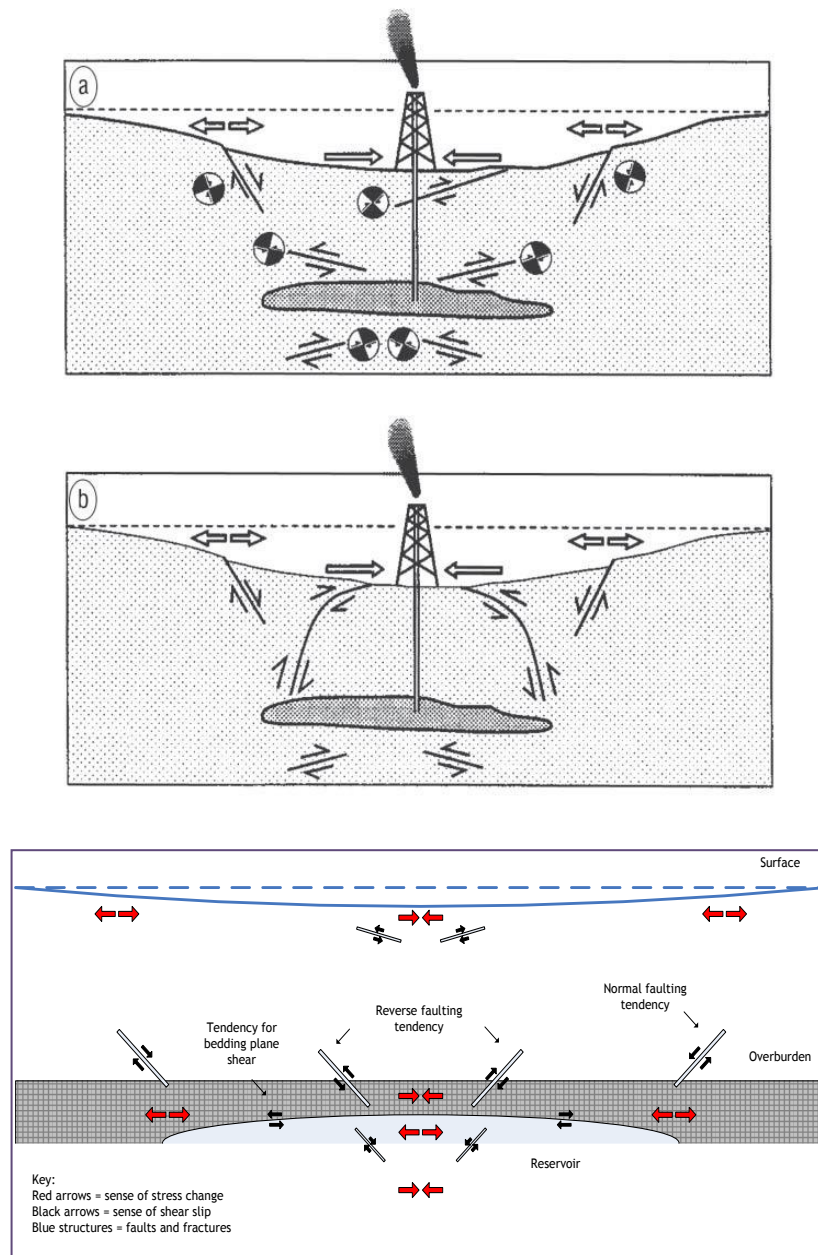
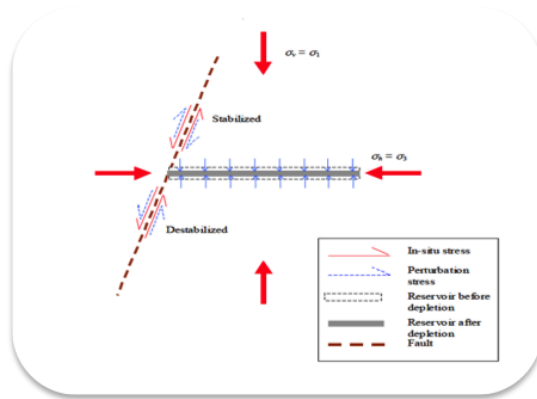
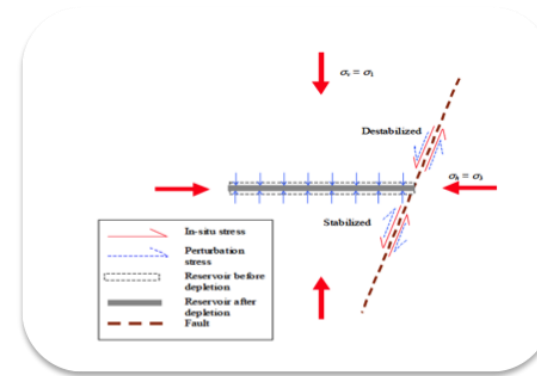


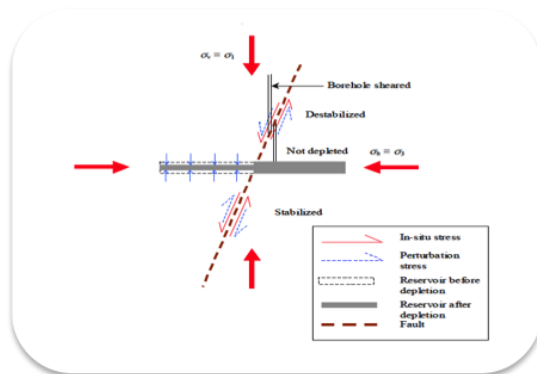
Figure B.21 Segall (1989) model for deformation and seismicity associated with water/Oil extraction



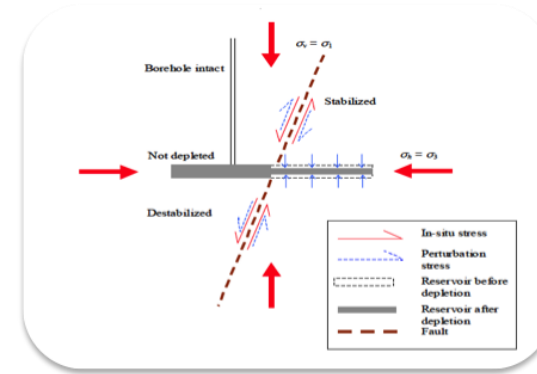
Schematics of instability of left end fault when the reservoir is depleted



Schematics of instability of right end fault when the reservoir is depleted



Schematics of instability of crossing fault when the reservoir is depleted from left to right



Schematics of instability of crossing fault when the reservoir is depleted from right to left

Figure B.22 Changes in Stress Conditions on faults as a consequence of hydrocarbon extraction and reservoir depletion

Groningen Netherlands

More recently there has been significant seismicity (c 900 events up to 3.5 M_L) in the North of Holland, which is clearly related to the long-term depletion of the Groningen Gas Field, and this is shown in **Figure B.23**.

The Groningen field is the largest gas field in Europe and the tenth largest in the world. It covers an area of 900 Km^2 . Gas already recovered: about 1,700 billion m^3 ; gas still recoverable: about 1,100 billion m^3 ; original reservoir pressure: about 350 bar; number of wells drilled: about 300 in 29 production cluster.

The reservoir is situated in the sandstones of the Upper-Rotliegend (lower Permian) at varying depths ranging from about 3,150 to 2,600 meters. The induced seismicity was observed at around this depth. The first event occurred in 1991, 28 years after the gas production started. From 1991 to 2003, 179 events with magnitudes in the range $-0.2 \leq M \leq 3.0$ was identified. (Van Eck et al., 2006).

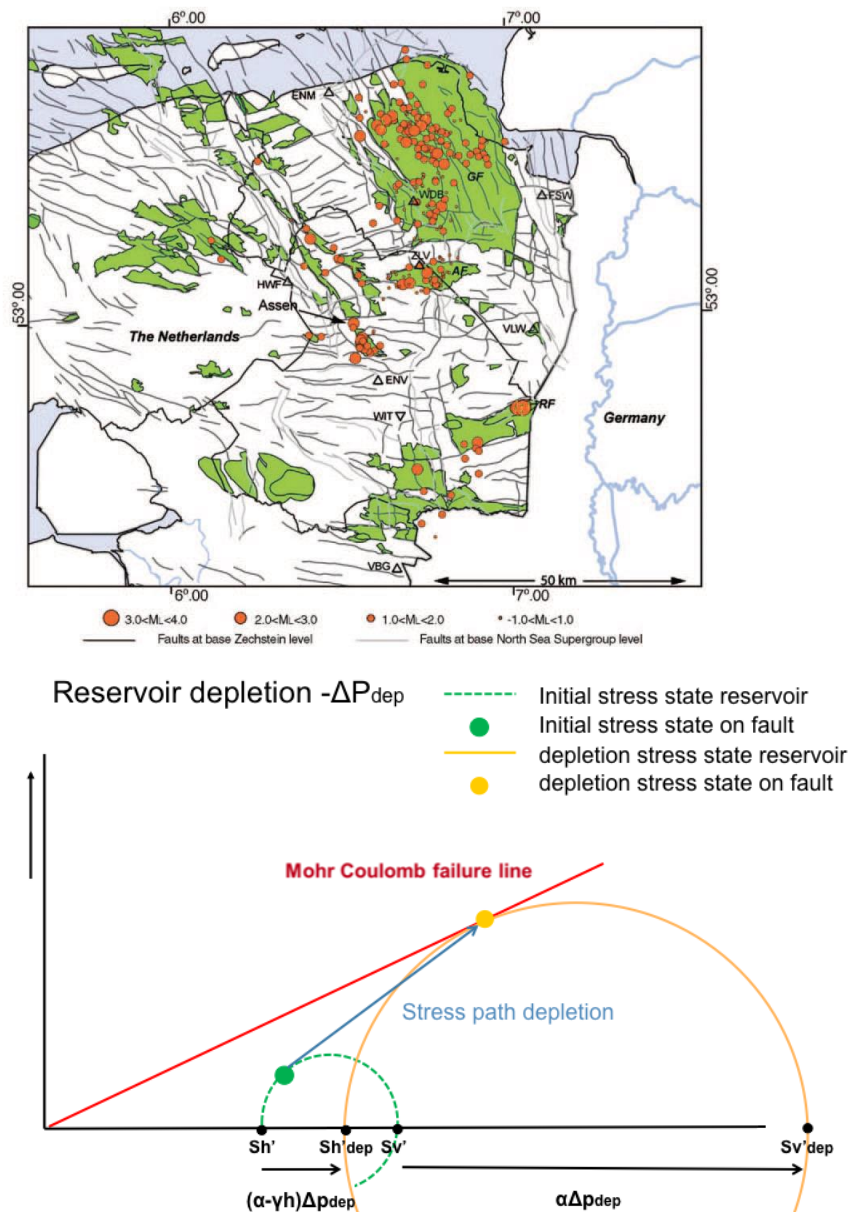


Figure B.23 Recent seismicity in the northern Netherlands over the Groningen Gas Field and the stress changes associated with reservoir depletion and changes in the stability leading to failure according to Mohr-Coulomb theory (Dost, 2013)

A physical causative mechanism for natural fluid-driven swarms as well as for induced seismicity is pore pressure diffusion (Shapiro and Dinske, 2009). Increases in pore fluid pressure act to reduce fault strength, bringing pre-existing fractures closer to failure according to the Mohr–Coulomb failure criterion. The initiation of fluid injection in a region leads to substantial increases in pore fluid pressure, which build up over time and diffuse outward for significant distances and for significant times from a well. The amount and magnitude of seismicity induced therefore depends on the ambient tectonic stress, as well as local geological and hydraulic conditions. Thus, induced seismicity can continue even after injection has ceased, as was the case at the Rocky Mountain Arsenal where three ~ 4:5 earthquakes occurred the year after waste fluid injection ceased (Healy et al., 1968; Hsieh and Bredehoeft, 1981). Fluid injection not only perturbs stress by changing the poro-elastic condition (Scholz, 1990, Segall 1992) and creates new fractures, but it also potentially introduces pressurised fluids into pre-existing fault zones, causing slip to occur earlier than it would otherwise have done naturally by reducing the effective normal stress and moving the failure closer to the Mohr-Coulomb criterion. This was first observed in the LACQ gas field in the Aquitaine Basin ⁴ (Segall, 1985, 1992) (**Figure B.26**).

The stress perturbation attenuates rapidly away from the sphere, over a distance of about twice the sphere radius. The stress induced inside the sphere is elastic stress diffusion.

Pore pressure and stress perturbation associated with fluid injection increases the risk of slip along a fault within the zone of influence. Just as injection can trigger seismicity abstraction can also do so by the same mechanisms of poro-compressive when fluid is injected but tensile for fluid withdrawal As fluid is extracted, declining pore pressures cause the permeable reservoir rocks to contract, which stresses the neighbouring crust. In the case of fluid withdrawal, the region at risk is generally outside the reservoir. The geomechanical interpretation of these is shown in **Figure B.24**.

⁴ The Lacq gas field in France is one of the best-documented cases of seismicity induced by extraction of fluid (Grasso and Wittlinger 1990, Segall et al. 1994). The reservoir was highly over pressured when production started in 1957, with a pressure of about 660 bars at depth of 3.7 kilometres below sea level. The first felt earthquake took place in 1969, at a time when pressure had decreased by about 300 bars. By 1983, the pressure had dropped by 500 bars (10 Mm³ of water were injected). 800 seismic events with magnitude un to M 4.2 had been recorded. The epicentres of 95% of the well-located events and all of the M>3 events were within the boundaries of the gas field. The subsidence reaching a maximum of 60 mm in 1989. The gas volume already recovered is over 246,000 MSm³ (source: Total).

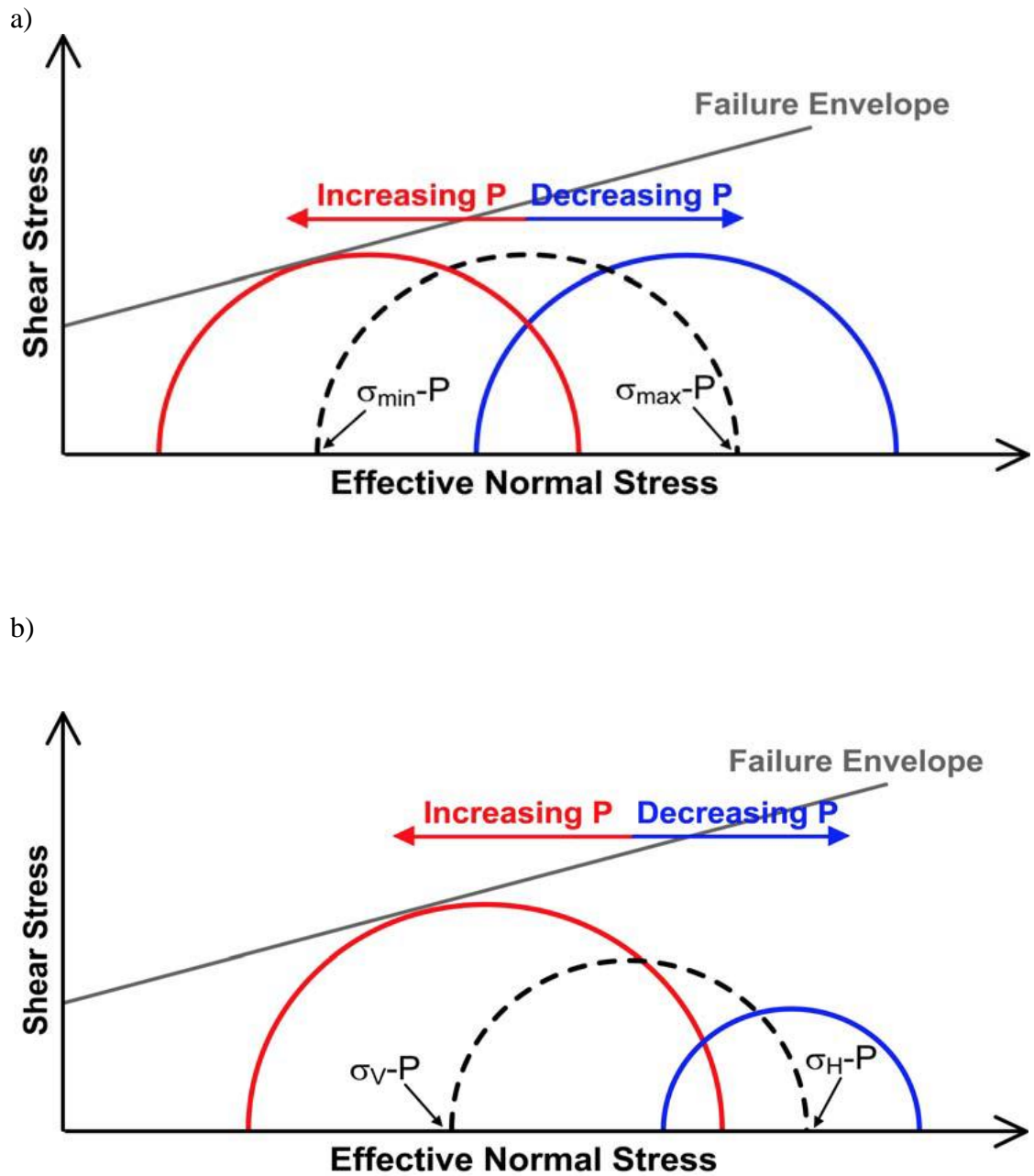


Figure B.24 Increasing pore pressure counteracts the normal stress leading to increased probability of failure. For an initial state of stress (dashed line) the effective differential stress is reduced for increasing pore pressure (red line). Decreasing P has the contrary effect (blue line).; **b)** The effect of pore pressure increase (red line) and decrease (blue line) on an initial effective state of stress (dashed line) **in a thrust faulting regime**, assuming that the vertical stress is not affected by pore pressure change, from Altmann (2010)

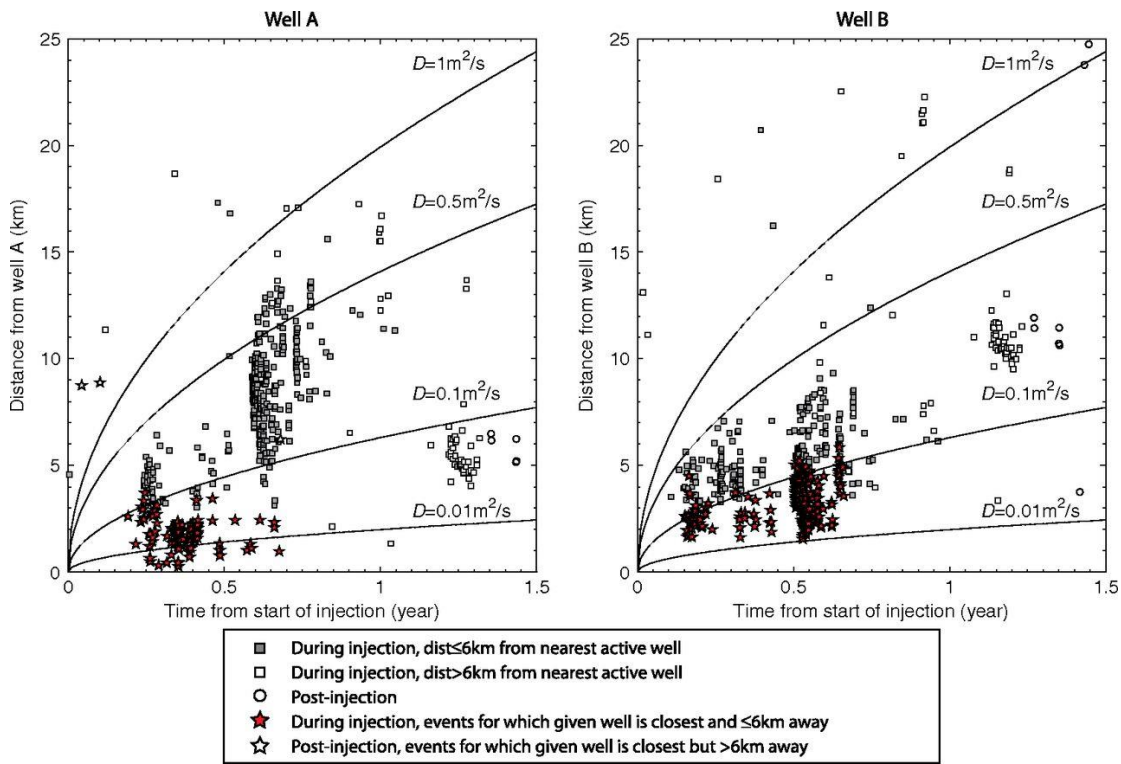


Figure B.25 Pore pressure diffusion modelling for two waste-water injection wells in Arkansas where seismic events occurred at distances of 25 km within two years of injection commencing. Black lines are pore pressure diffusion curves for different values of hydraulic diffusivity D . Seismicity from 2009 to 2012 are plotted by distance and time from start of injection at the given well. From Llenos et al (2013).

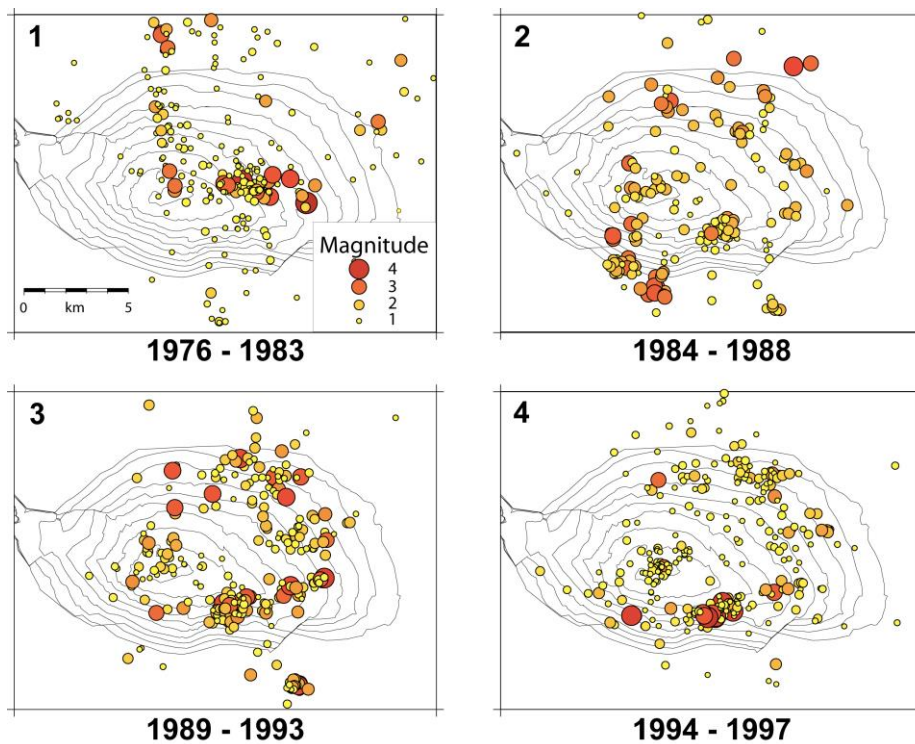


Figure B.26 Seismicity in the Lacq Gas field in the Aquitaine Basin in France from 1976 through 1997

3. Excessive Groundwater Extraction

González et al (2012) in *Nature Geoscience*, suggest that stress induced by extreme groundwater extraction to irrigate (since the 1960s, natural groundwater levels in the region had reduced by 250 metres probably triggered the M_w 5.1 earthquake that occurred in Lorca, southeast Spain, on 11 May 2011 (**Figure B.27**) with nine fatalities and considerable devastation for such a relatively small event, principally because the focus was relatively shallow at about 2-4 km depth.

Isostatic unloading and the associated elastic response of the crust and lithosphere is well known as a cause of seismicity. The Betic Cordillera is one of the most seismically active areas in the Iberian Peninsula reflecting the neotectonics and it is not unexpected that the removal of 250 metres of groundwater since 1960 together with many centimetres of subsidence caused by compaction are sufficient to act as the minor perturbation (the straw which breaks the camel's back) for a stress system which was probably near to failure.

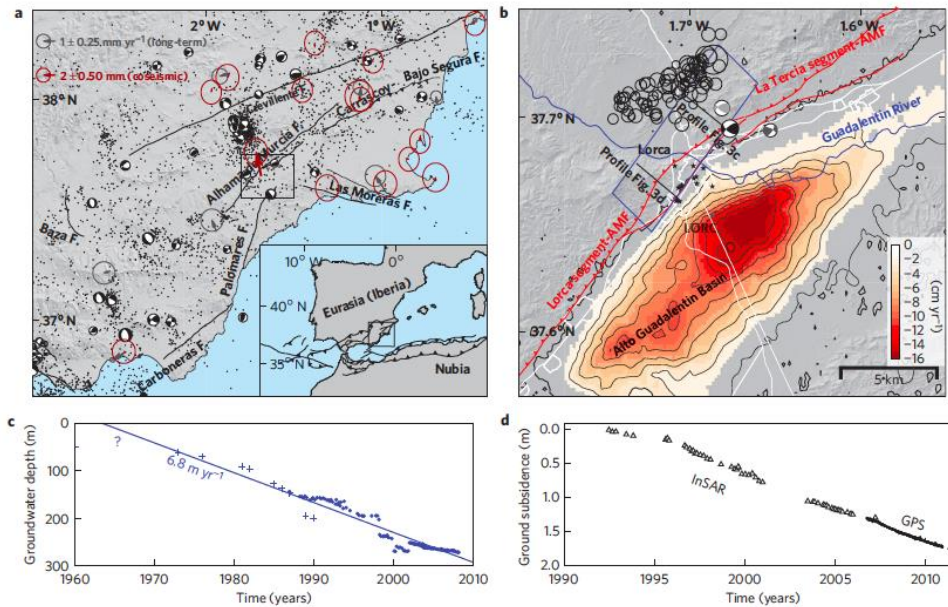


Figure B.27 Kinematics and Seismicity of Southern Spain together with induced seismicity and net subsidence contours (Gonzalez 2012)

4. Gas Storage and CCS

A new phase of what appears to be induced seismicity has been reported from offshore Spain associated with Gas Storage in the Castor offshore field.

23 earthquakes were recorded between October 2nd and 3rd 2013, with magnitudes between 1.7 and 4.2 M_L . On September 26 an earthquake with magnitude 3.6 M_L was felt and the activities at the gas field were stopped (**Figure B.28**)

Oil was extracted from this field between 1973-1989 and gas started being injected last September. (http://elpais.com/elpais/2013/10/03/media/1380808588_671803.html).

Additionally a new study by Wei Gan and Cliff Frohlich at The University of Texas at Austin, Institute for Geophysics, correlates a series of small earthquakes near Snyder, Texas between 2006 and 2011 with the underground injection of large volumes of gas, primarily carbon dioxide (CO₂) which is relevant to Carbon Sequestration, the process of capturing and storing CO₂ underground (**Figure B.29**).

Although the study suggests that underground injection of gas triggered the Snyder earthquakes, it also points out that similar rates of injections have not triggered comparable quakes in other fields which implies that local geology and probably the presence of faulting may be a significant factor.

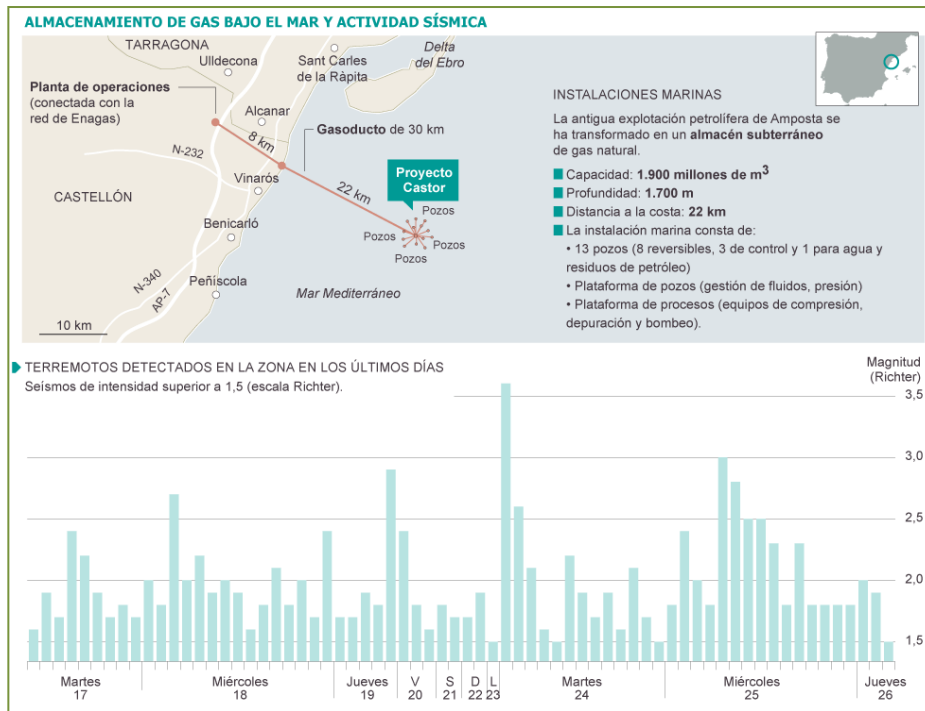


Figure B.28 Induced seismicity reported from offshore Spain and associated geographically with the Castor offshore gas storage project (available at http://inducedseismicity.files.wordpress.com/2013/10/1380225246_145513_1380232164_sumario_grande4.png)

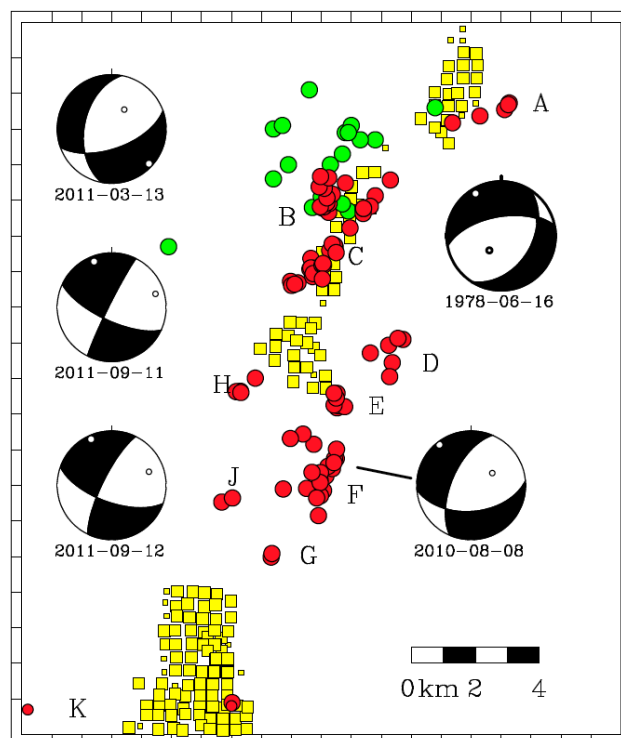


Figure B.29 Recent seismicity recorded in the Cogdell area of Texas. Red Circles are seismic events with focal mechanisms and the yellow squares are gas injection wells active since 2004

5. Induced Seismicity of Geothermal Reservoirs

Examples of seismicity generated by geothermal extraction and water re-injection are numerous and only a small relevant selection are described here. A good recent overview is given by Bromley and is available at:

<http://iea-gia.org/wp-content/uploads/2012/10/Bromley-Induced-Seismicity-International-Taupo-June-2012.pdf>

However, there are some classic papers and Majer et al (2007) is perhaps the best known. There are many examples of mainly low-level seismicity globally as shown in **Figure B.30** and **Figure B.31**. Immense numbers of seismic events mostly of small magnitude are generated during geothermal activities as shown in **Figure B.32** of the intense clouds of relatively low-magnitude seismic activity observed at the Soultz facility in France.

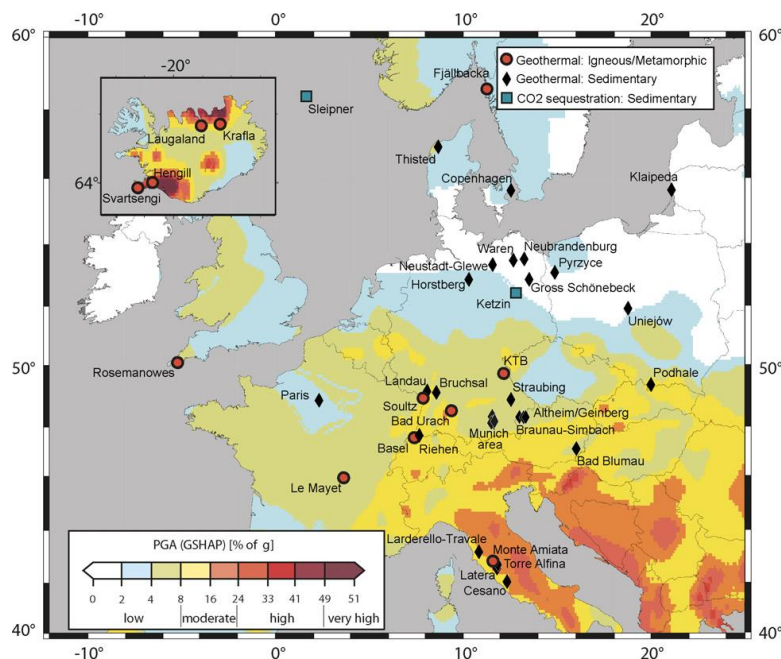


Figure B.30 Location of European geothermal injection sites from Evans et al. 2012

The Geysers field in California is particularly active. Water has been reinjected and seismicity has occurred both above and below the geothermal reservoir. **Figure B.33** shows the relationships between steam and water injection and seismic activity with the activity in a single 24 hour period shown in **Figure B.34**

However, High-pressure hydraulic fracturing in Engineered Geothermal Systems (EGS) has caused seismic events that are large enough to be felt and have caused some considerable public alarm with associated very large total insurance claims in Basel Switzerland from only a 3.4 M_L event. The correlation between activity and well-head pressure and injection rate for Basel are shown in **Figure B.35**.

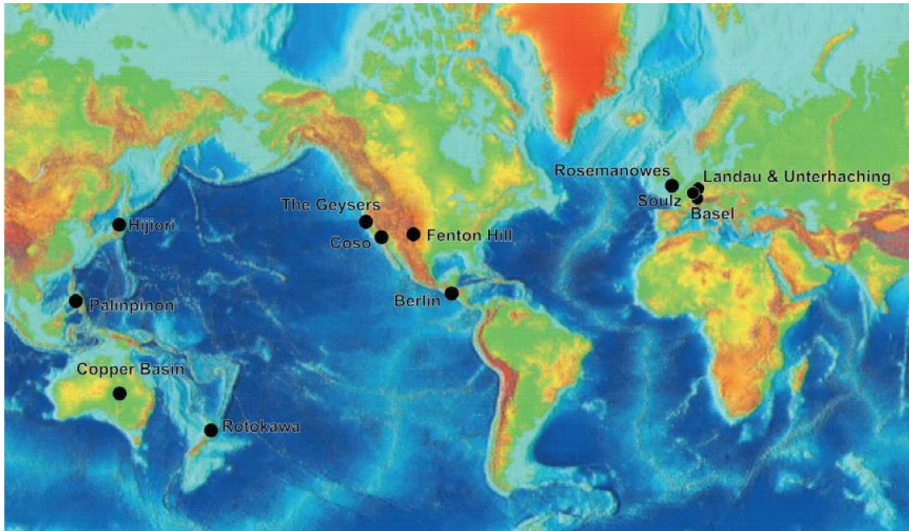


Figure B.31 Some important examples of geothermal related seismic activity

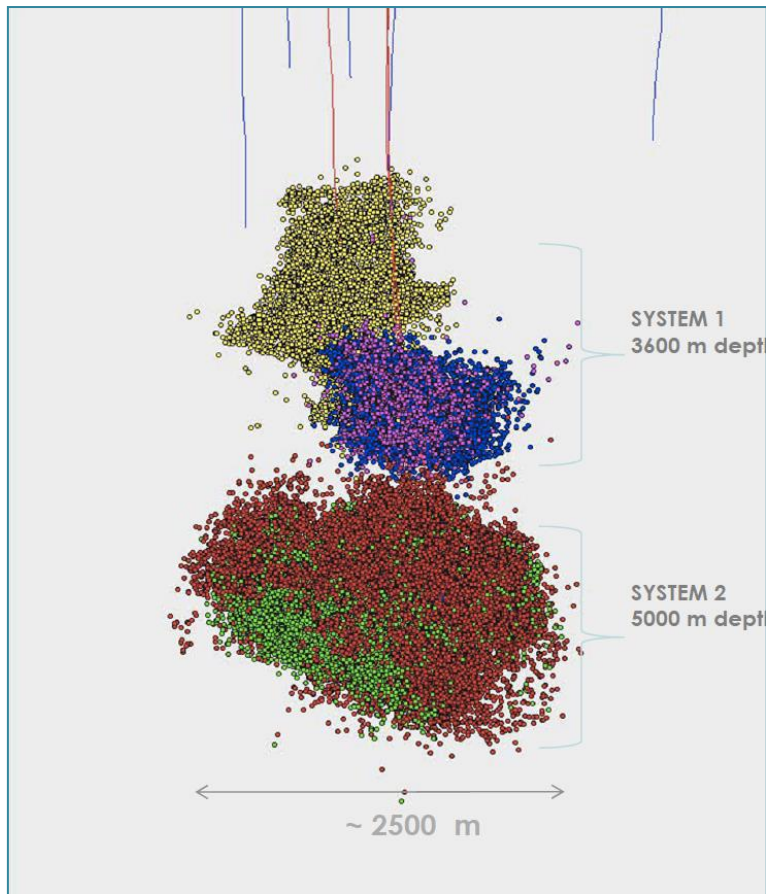


Figure B.32 Seismicity observed at Souz-sous Foret during a 10 year period from 1993 to 2003 from Baria EGS

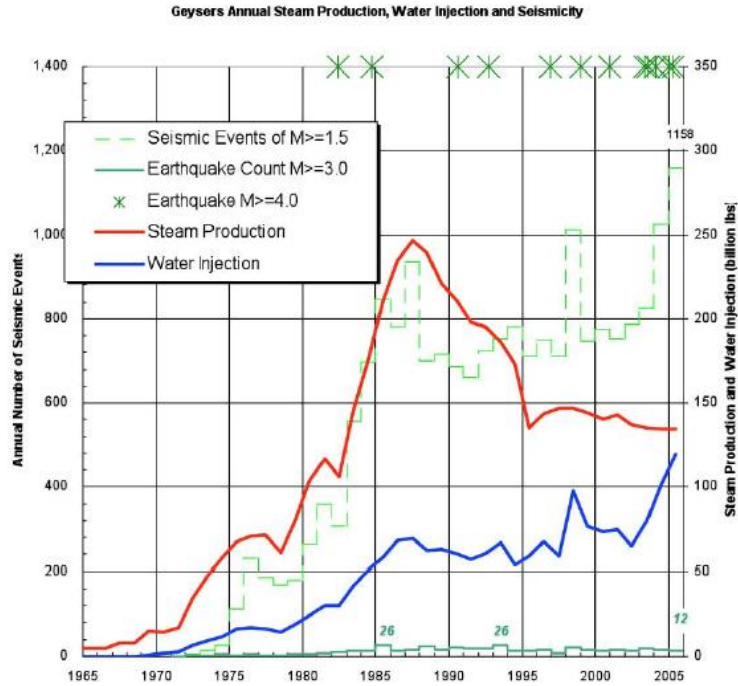


Figure B.33 Operational parameters and seismicity at the Geysers Field California

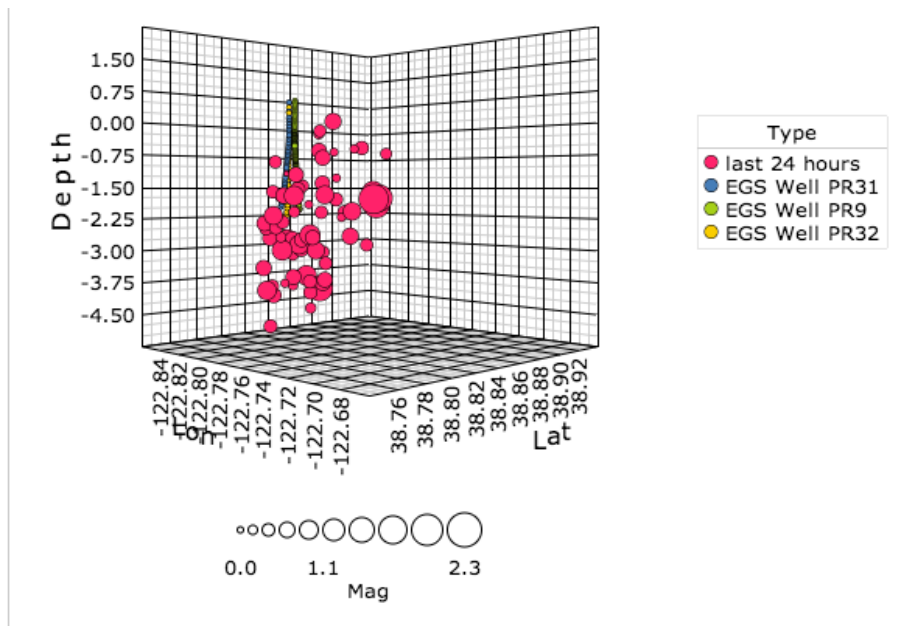


Figure B.34 Geysers activity in a single 24 hour period

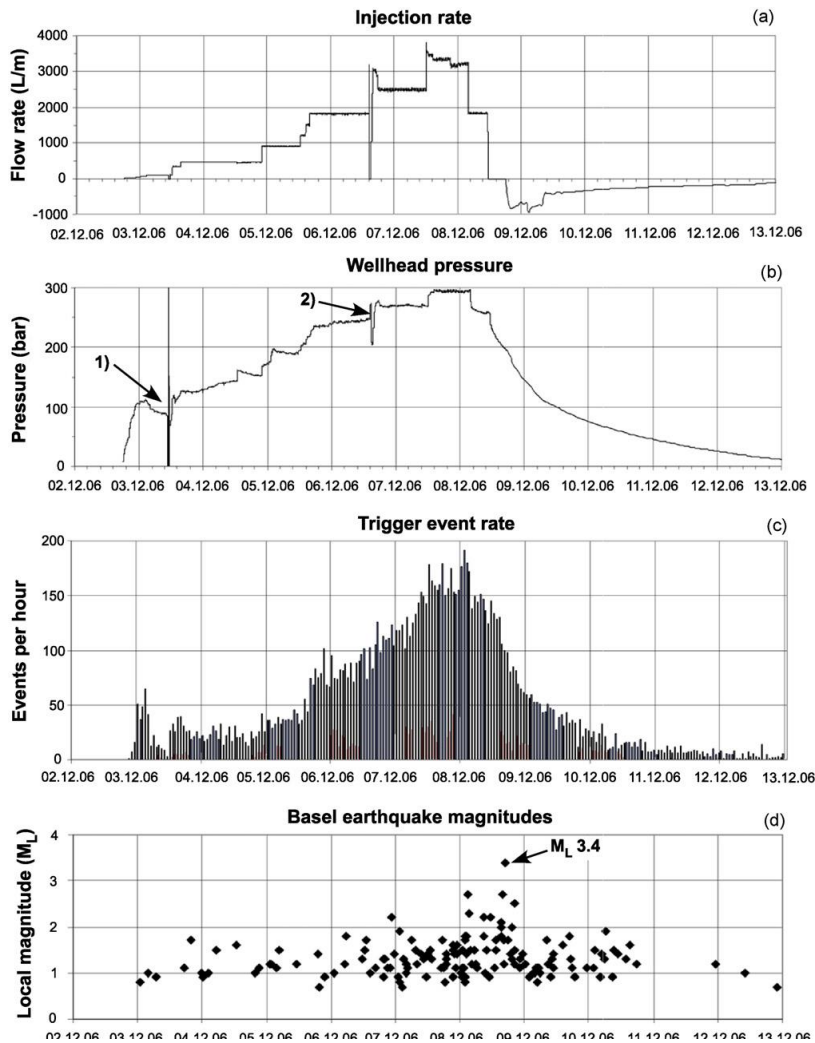


Figure B.35 Data on the hydraulic stimulation of well Basel-1. History of (a) injection rates, (b) wellhead pressures, (c) trigger event rate and (d) Basel earthquake magnitude as determined by Swiss Seismological Survey (SED). From Haring et al., (2008)

The causes of geothermal seismicity have been vigorously debated as they appear to be more complex than those associated just with fluid changes almost certainly because of thermo-geomechanical effects and the range of suggested mechanisms are given below:

- Increased pore pressure (effective stress changes)
- Thermal stress
- Volume change (subsidence, inflation)
- Chemical alteration of slip surfaces
- Stress diffusion
- Production (extraction) induced
- Injection related

It is likely that all of these may play some part but an important recent paper by Brodsky and Lajoie (2013) has shown that for the Salton Sea Geothermal Field the most important parameter appears to be net fluid balance i.e. the difference between extraction and re-injection.

However, High-pressure hydraulic fracturing in Engineered Geothermal Systems (EGS) has caused seismic events that are large enough to be felt and have caused some considerable public alarm with associated very large total insurance claims in Basel Switzerland from only a 3.4 M_L event. The correlation between activity and well-head pressure and injection rate for Basel are shown in **Figure B.35**.

Salton Sea (California) seismicity is shown in **Figure B.36** and **Figure B.37**

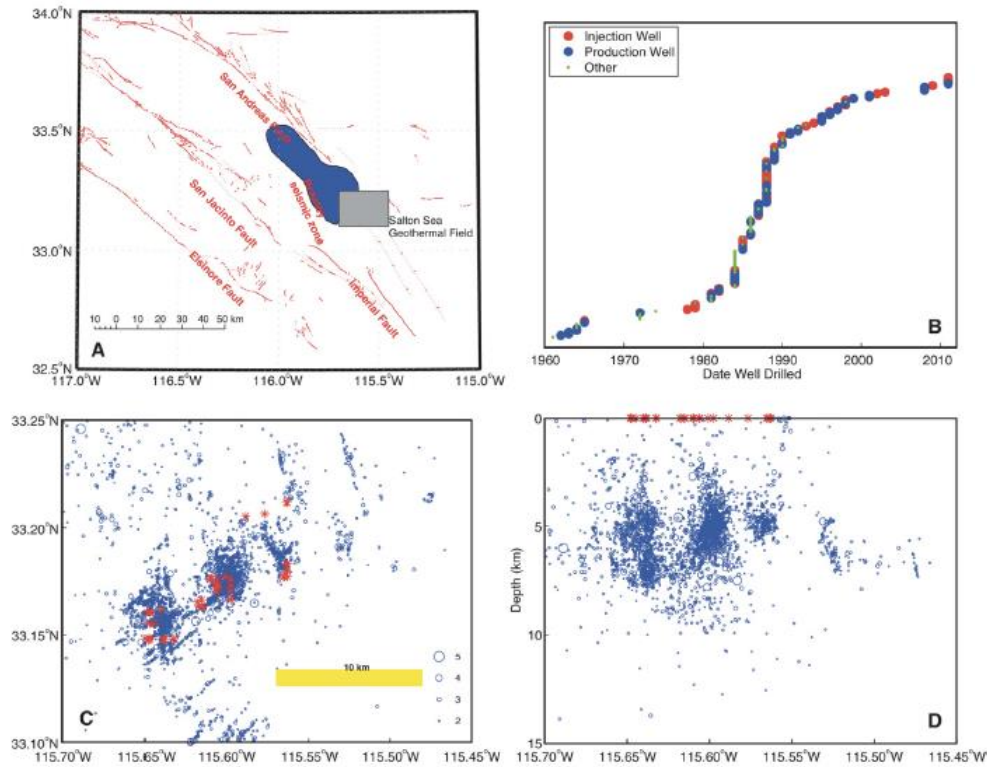


Figure B.36 Earthquake and geothermal facility locations and activity. (A) Regional map with faults and location of the Salton Sea Geothermal Field. (B) Drill year of the wells 1960-2012. (C) Earthquakes (blue circles) and injection wells (red stars) in map view. (D) E-W cross-sectional view

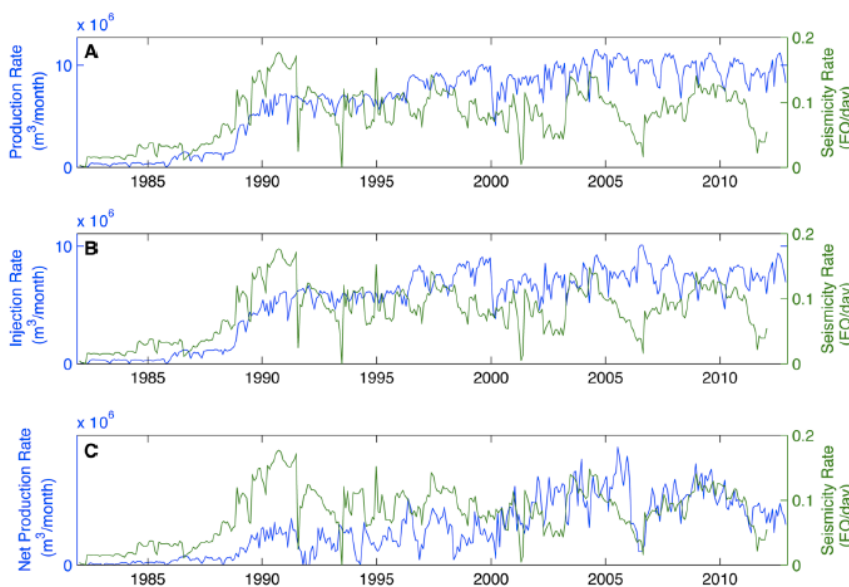


Figure B.37 Background seismicity rate (μ) compared to fluid volumes at the Salton Sea Geothermal Field. The seismicity the right hand axis, green curve and the operational rate (left axis, blue curve) is (A) Production rate, (B) Injection rate and (C) Net Production rate. From Brodsky (2013)

6. Waste fluid disposal

During extraction of conventional oil and gas and as flow-back after hydraulic stimulation, a great deal of water (and other fluid components and solutes) are generated and in many case these have been re-injected back into the ground at sites close to extraction wells to minimise transport and treatment costs. Since 2000 a significant increase in observed seismicity of moderate ($3M_L$) to disturbing ($5.7M_L$) earthquakes have been observed in the mid-USA as shown in **Figure B.38** from Ellsworth (2013) and the relationship between this and the large volumes of long-term produced water injection have come under immense scrutiny. The author pointed out that the clear increase from 2005 coincides with the rapid increase of shale gas wells and associated increased deep waste-water injection. In fact, between 2005 and 2012, the shale gas industry in US grew by 45% each year.

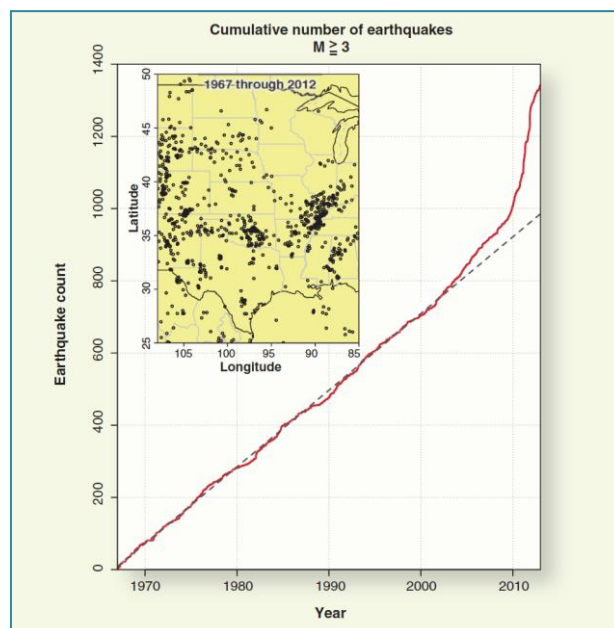


Figure B.38 Growth in the number of mid-continental earthquakes in the last decade (from Ellsworth 2013)

Moment exceeds predictions based on volume injected (McGarr 1976) by several orders of magnitude and therefore needs significant tectonic stress release.

This a potential case of fluid injection into isolated compartments resulting in seismicity **delayed by nearly 20 yr from the initiation of injection**, and by 5 yr following the most substantial increase in wellhead pressure.

Three significant earthquakes with magnitudes of 5.0, 5.7, and 5.0 (**Figure B.39**) occurred near Prague, Oklahoma, United States (on 5th, 6, and 8 November 2011) ~180 km from the nearest known Quaternary-active fault. Earthquakes with magnitudes greater than 5 are not common in the United States but have increased in frequency 11-fold between 2008 and 2011, compared to 1976–2007 (Keranen et al 2013).

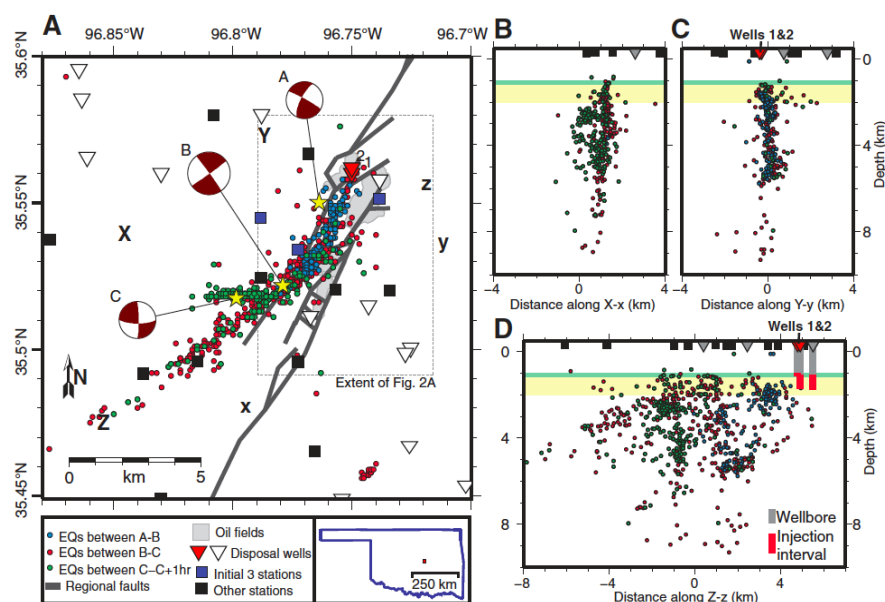


Figure B.39 Seismic centroid moment tensor mechanisms, seismic Stations, active disposal wells, and oil fields in Prague Central Oklahoma, United States. Wells 1 and 2 inject near aftershocks of events . B–D: Cross sections of seismicity projected from within 4 km of plane of each section. From Keranen et al (2013)

Usually, induced seismicity occurs fairly soon after the start of injection; seismicity began within months of injection commencing at the Rocky Mountain Arsenal⁵ (Healy et al., 1968), in Arkansas (Horton, 2012), and Dallas–Fort Worth (Texas) airport (Frohlich et al., 2011). However, at Prague, Oklahoma, the first significant earthquake (M_w 4.1, in 2010) did not occur until 17 years after injection commenced which has considerable significance in the context of pore-pressure diffusion processes.

Continuing injection over 18 years into subsurface compartments in the Wilzetta field may have refilled a compartment, eventually reducing the effective stress along reservoir bounding faults triggering the 2010–2011 earthquakes. Injection has continued and earthquakes with magnitudes ≥ 3.0 continue to occur.

The first event (A) of M_w 5.0, seems to have been induced by increased fluid pressure, exceeding the largest earthquake of 4.8 M_L previously known to be induced by injected fluid. Aftershocks of event A appear to deepen away from the well and may propagate into basement rocks. It is clear that injection at a relatively shallow level can have consequences for stress changes at significant depths probably into the basement.

Keranen et al (2013) consider that while the second event event B, which is much larger at M_w 5.7, and event C may also be due to injection but it is also possible that they have been triggered by Coulomb stress transfer as the fault geometries are consistent with triggering by stress transfer (Cochran et al., 2012) if the faults were close to failure, supporting the view that favorably oriented faults are critically stressed and so small- to moderate-sized injection-induced events may result in release of additional tectonic stress. The scalar moment released in this sequence exceeds predictions based on the volume of injected fluid (McGarr, 1976) by several orders of magnitude, implying that there has been the release of substantial tectonic stress. The 2011 Prague, Oklahoma, earthquakes necessitate reconsideration of the maximum possible size of injection-induced earthquakes, and of the

⁵ A deep well was drilled in 1961 to dispose of contaminated waste water from the production of chemical warfare.

time scale considered diagnostic of induced seismicity. This point is emphasized here as this may well have relevance for the Ferrara situation.

In Paradox Valley, to decrease the salinity from the Dolores River, brine has been extracted from nine shallow wells along river and, after treating, it has been injected into the ground in the Paradox basin, 4.3-4.8 km below the surface (total injected volume: 4 Mm³) since 1991. Between 1985 and June 1996, only three tectonic earthquakes were detected within 15 km of the well and 12 within 35 km. Subsequently, hundreds of earthquakes below M_L 3 were induced during injection tests conducted between 1991 and 1995. High injection pressure (70 MPa) was required and induced earthquakes were not unexpected. The activated zone expanded, with earthquakes occurring as far away as 8 km from the injection point within a year to beyond 12 km several years later. As a precaution shutdowns of 20 days occurred to attempt to allow the fluid pressure to equilibrate, and preclude larger events; however, a M 4.3 event was induced in May 2000.

The Paradox Valley seismicity also illustrates how long-term, high-volume injection leads to the continued expansion of the seismically activated region and the triggering of large-magnitude events many kilometres from the injection well more than 15 years after commencement of injection (**Figure B.40**).

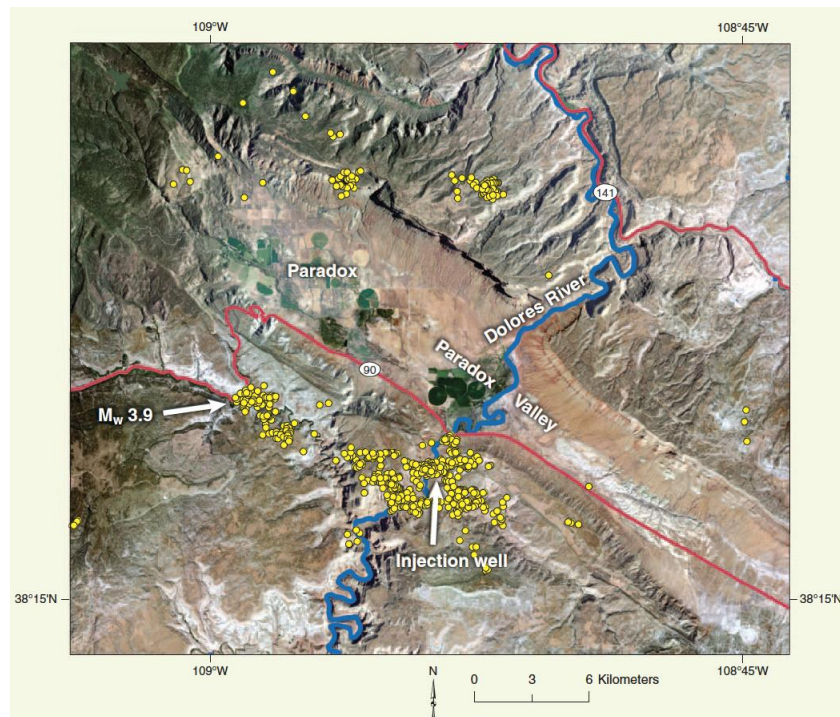


Figure B.40 Seismicity associated with injection in the Paradox Basin Utah, USA

A striking number of medium sized earthquakes have been recently reported from the mid USA and have been well characterised because of the Transportable Array (**Figure B.41**).

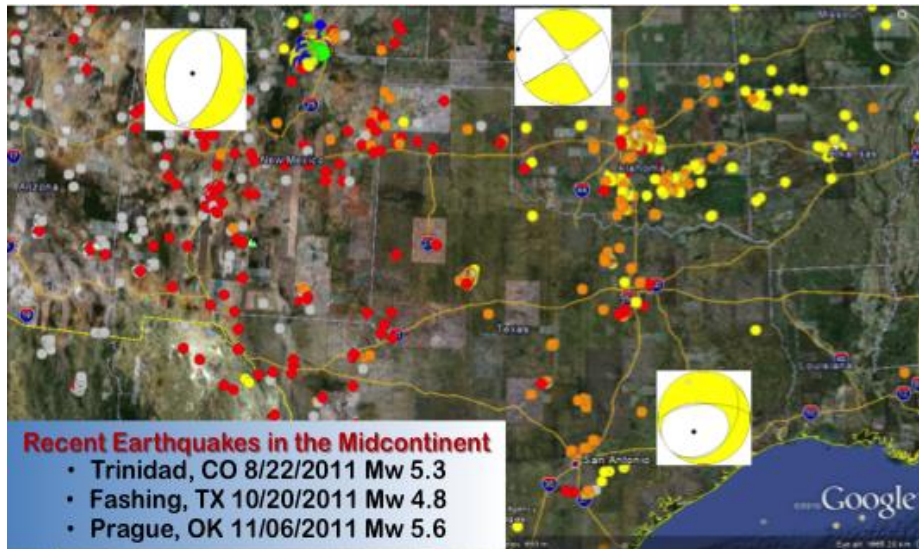


Figure B.41 A compilation of seismic events from the midcontinental USA compiled by McGarr (2013 pers comm)

McGarr (2013) plots the maximum magnitude (from the USA **Figure B.42**) and maximum seismic moment (global **Figure B.43**) for against total injected fluid volume and there appears to be a reasonable correlation with both increasing and approaching the theoretical maximum of $G\Delta V$.

McGarr considers the Painesville, Ohio, (POH) earthquake of January 1986 (Nicholson et al., 1988), in some detail. Although the distance between the two high-volume injection wells and the Painesville earthquakes at 12 km is relatively large, there is some precedence for earthquakes being induced at comparable distances from injection wells. Most of the Guy, Arkansas, earthquakes were located in the basement at distances ranging up to between 10 and 15 km from the two injection wells implicated in this sequence (Horton, 2012).

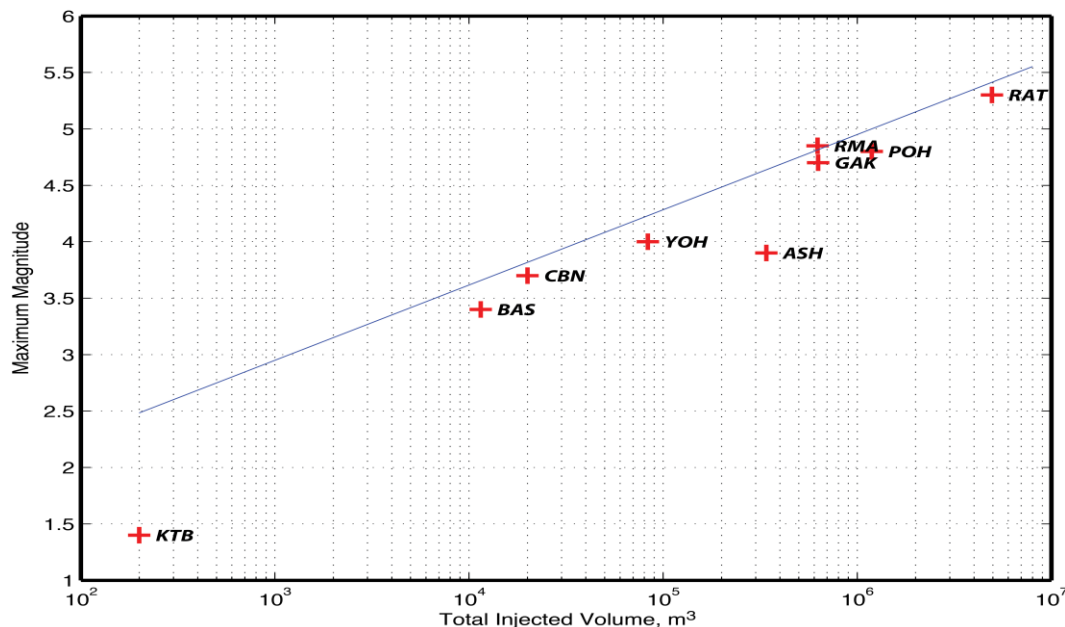


Figure B.42 Maximum Magnitude plotted against total injected volume for a number of injection sites, (Table B.1)

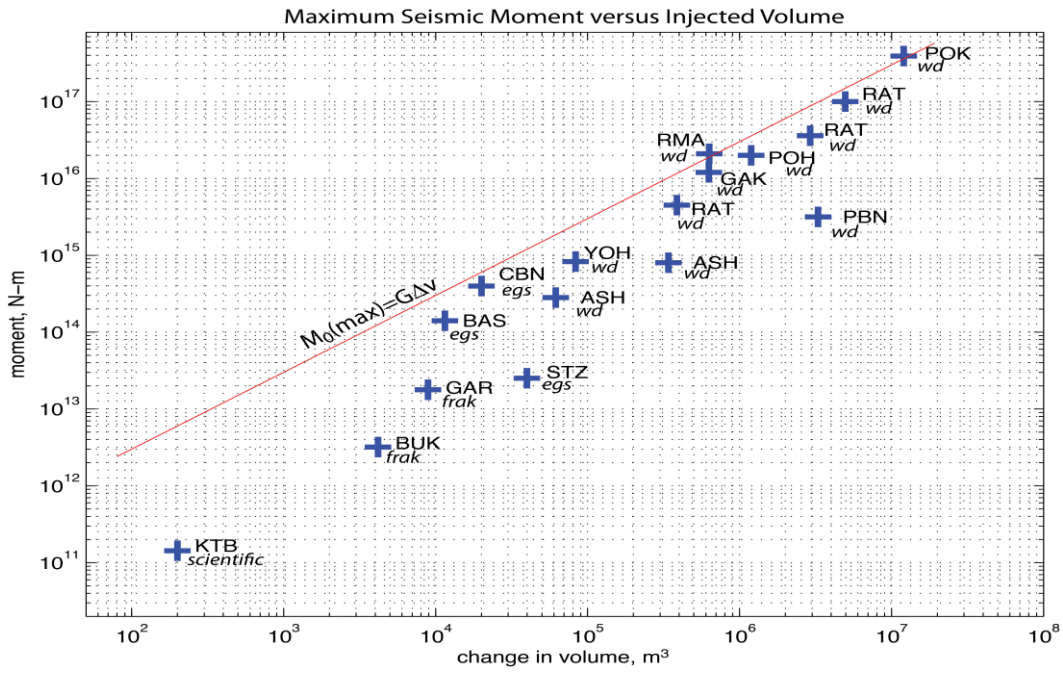


Figure B.43 Maximum Seismic Moment plotted against total injected volume for a number of injection sites, wd=water disposal and frack is hydraulic stimulation (**Table B.1**)

Table B.1 Maximum seismic moment $M_0(\text{max})$ and total injected volumes ΔV (McGarr, 2013 pers comm)

Event	$M_0(\text{max}), \text{Nm}$	$\Delta V, \text{m}^3$	Type*	M	Location
KTB ¹	1.43e11	200	scientific	1.4	Eastern Bavaria, Germany
BUK ²	3.2e12	4.17e3	frak	2.3	Bowland shale, UK
GAR ³	3.5e13	1.75e4	frak	3.0	Garvin County, OK
STZ ⁴	2.51e13	3.98e4	egs	2.9	Soultz, France
DFW ⁵	8.9e13	2.82e5	wd	3.3	Dallas-Fort Worth Airport, TX
BAS ⁴	1.41e14	1.15e4	egs	3.4	Basel, Switzerland
ASH ⁶	2.82e14	6.17e4	wd	3.6	Ashtabula, OH, July, 1987
CBN ⁴	3.98e14	2.0e4	egs	3.7	Cooper Basin, Australia
ASH ⁶	8.0e14	3.4e5	wd	3.9	Ashtabula, OH, January 2001
YOH ⁷	8.3e14	8.34e4	wd	4.0	Youngstown, OH
PBN ⁸	3.16e15	3.287e6	wd	4.3	Paradox Valley, CO
RAT1 ⁹	4.5e15	4.26e5	wd	4.4	Raton Basin, CO, September 2001
GAK ¹⁰	1.2e16	6.29e5	wd	4.7	Guy, AR
POH ¹¹	2.0e16	1.19e6	wd	4.8	Painesville, OH
RMA ¹²	2.1e16	6.25e5	wd	4.85	Denver, CO
TTX ¹³	2.21e16	9.91e5	wd	4.8	Timpson, TX
RAT2 ¹⁴	1.0e17	7.84e6	wd	5.3	Raton Basin, CO, August 2011
POK ¹⁵	3.92e17	1.20e7	wd	5.7	Prague, OK

*frak – hydraulic fracturing; egs – Enhanced Geothermal System; wd – wastewater disposal. ¹Zoback and Harjes (1997); ²de Pater, C. J. and S. Baisch (2011); ³Holland (2013); ⁴Majer, E. L., et al. (2007); ⁵Frohlich et al. (2011); ⁶Seeber et al. (2004), Nicholson and Wesson (1990); ⁷Kim (2013); ⁸Ake et al. (2005); ⁹Meremonte et al. (2002); ¹⁰Horton (2012); ¹¹Nicholson et al. (1988); ¹²Herrmann et al. (1981), Hsieh and Bredehoeft (1981); ¹³Frohlich et al. (2014); ¹⁴Rubinstein et al., manuscript in preparation; ¹⁵Keranen et al. (2013).

Rongchang and Huangchei Gas fields, Chongqing, China

In many of the cases described here the injection of waste water is carried out into deeper formations or even into basement rocks where larger magnitude events might be expected but even injection into the same reservoir from which oil and gas is being extracted can cause seismicity. A very good example of this comes from the Huangchei and Rongchang gas

fields⁶ Chongqing, Sichuan basin⁷, China which is reported by Lei et al (2008) and Lei et al (2013).

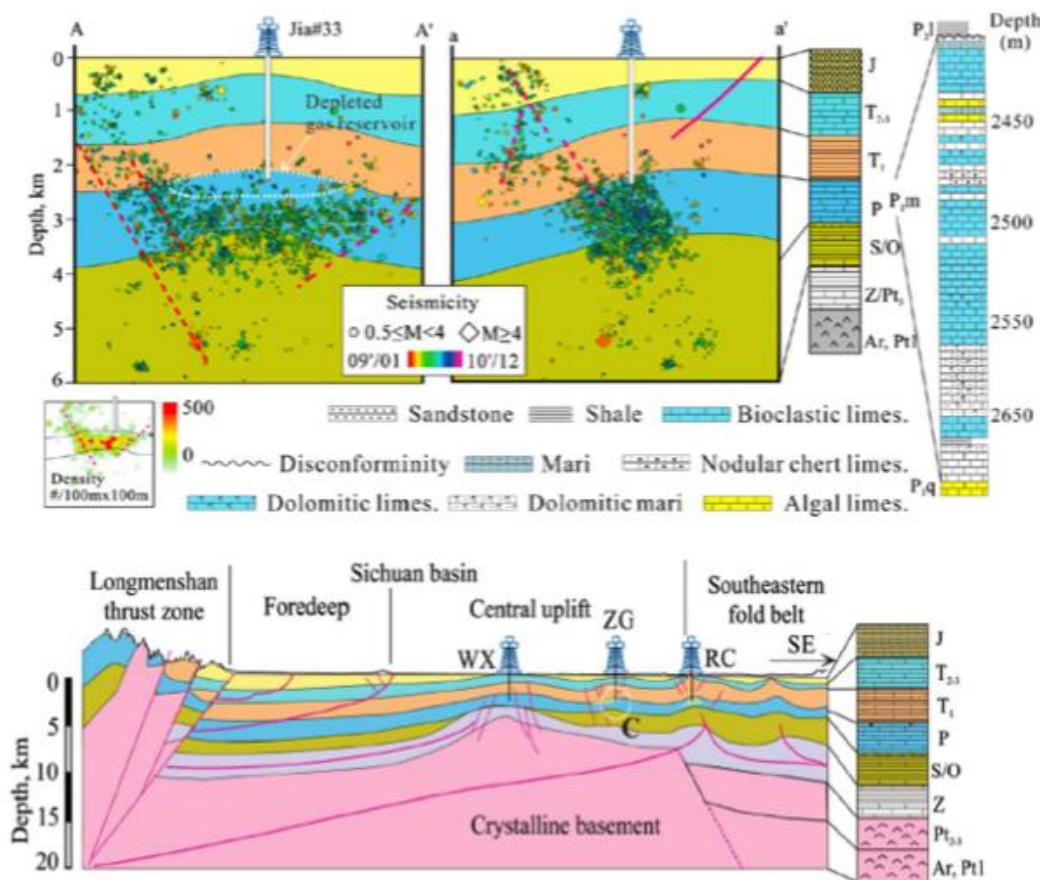


Figure B.44 Geological Cross Section across a thrust zone and its associated foreland basin (lower) and seismicity generated on the thrusts around the anticline where oil and gas have been extracted from a limestone reservoir subsequent to injection of some 120,000 m³ of waste-water at 6 MPa. After Lei et al (2013)

Seismicity began to be observed at a gas reservoir in the relatively stable Sichuan Basin, China, after injection of over 120,000 m³ waste water into the depleted Permian limestone reservoir at depths between 2.45 to 2.55 km, at a wellhead pressure of up to 6.2 MPa from 9 January 2009 to July 2011.

More than 7000 surface-recorded earthquakes, up to 4.4 ML occurred with 2 M4+, 20 M3+, and more than 100 M2+ events located at depths ranging from 2.5 to 4 km, within the Permian limestone and lying in a zone of 6 km by 2 km with a NNW trend, centred on the

⁶ **Huangchei field:** since 2007 a production well was used for the injection of unwanted water that was collected through pipelines from nearby production wells. The injection rate was <300 m³/day up until April 2008, and then increased to about 500 m³/day toward the end of 2008. During this period, fluid was placed into the well under gravity flow. Since 2009, pumping under high pressure was required for injection (up to 6.2 MPa).

Rongchang field: unwanted water has been injected since 1988. The major injection well was not a gas production well (Luo-4); the water injection rate was 683 l/min. The pumping pressure was variable, with a maximum value of 2.9 MPa. The average monthly injection volume in 1988 was about 2,000 m³, increasing to about 10,000 m³ in 1990. In the following years, the average monthly injection volume varied between 6,000 and 15,000 m³. A total of more than 1Mm³ of water had been pumped into the formations.

⁷ The Sichuan Basin is a major petroleum producer with an annual production of over 120 x 10⁸ m³ in recent years. The southeast Sichuan Basin (where is located Rongchang gas fields) is a major area of gas reservoirs that has a production history of over than 30 years. In addition to gas reservoirs, this area is also known for the production of mine salt by pumping water from salt formations.

injection well⁸. Lei et al (2013) consider that the induced earthquakes were due to lowering of the effective normal stress on critically-loaded, pre-existing, blind faults. It appears that despite the injection being into the extracted zone this did not appear to balance out the fluid effects and significant and prolonged activity occurred from within the faulted reservoir.

D. Mechanisms of Fluid Injection and Abstraction Related Seismicity

It has been known since the 1960s that earthquakes can be induced by fluid injection when military waste fluid was injected into a 3671 m deep borehole at the Rocky Mountain Arsenal, Colorado (Hsieh, 1981). This induced the so-called ‘Denver earthquakes’. They ranged up to ML 5.3, caused extensive damage in nearby towns, and as a result, use of the well was discontinued in 1966. Reviews of activity often focus on selected mechanisms although there are notable exceptions (National Academy of Sciences, 2013). Artificially injecting fluids into the Earth’s crust induces earthquakes (e.g. Green et al., 2012). Indeed this can have effects at even the smallest scales as Hainzl et al (2006) showed that very tiny pressure variations associated with precipitation can trigger earthquakes to a depth of a few kilometres. Observations of isolated swarm-type seismicity below the densely monitored Mt. Hochstaufen, SE Germany, revealed strong correlation between recorded seismicity and spatiotemporal pore pressure changes due to diffusing rain water in good agreement with the response of faults described by the rate-state friction laws. Similar results have been observed in Switzerland (**Figure B.45**).

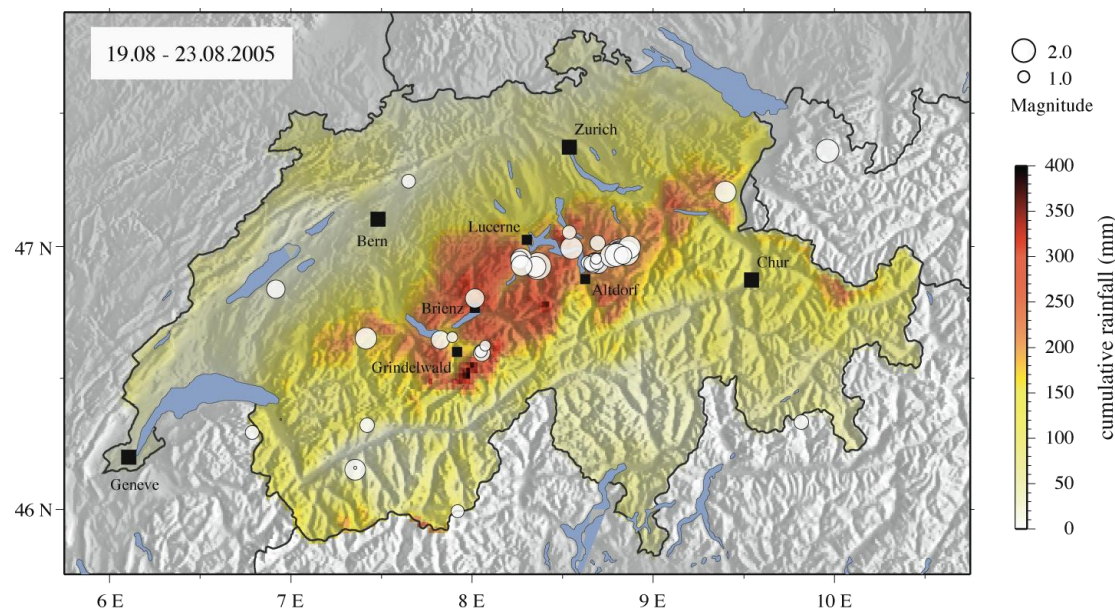


Figure B.45 Rain-triggered shallow seismicity in Switzerland in August 2005 (Husen et al. 2007)

If pore fluid is present then the induced pore pressure change is the pressure change times the Skempton’s coefficient B .

Skempton’s B coefficient is an important characteristic of a porous medium that describes the relationship between pore pressure and changes in the mean stress under undrained conditions. (B) is defined to be the ratio of the induced pore pressure to the change in applied

⁸ In general, the seismic activity in Zigong is thought to be associated with either the production of salt water, natural gas, or water injection. The timing and location of recent seismic activity (2009-2010) are strongly statistically correlated with fluid injections and the seismic activity falls into the category of induced earthquakes.

stress for undrained conditions - that is, no fluid is allowed to move into or out of the control volume:

$$B = - \left. \frac{\partial p}{\partial \sigma} \right|_{\xi=0} = R/H = \beta_p/S_\sigma$$

The negative sign is included in the definition because the sign convention for stress means that an increase in compressive stress inducing a pore pressure increase implies a decrease in σ for the undrained condition, when no fluid is exchanged with the control volume.

Skempton's coefficient must lie between zero and one and is a measure of how the applied stress is distributed between the skeletal framework and the fluid.

It tends toward one for saturated soils because the fluid supports the load. It tends toward zero for gas-filled pores in soils and for saturated consolidated rocks because the framework supports the load.

A physical causative mechanism for natural fluid-driven swarms as well as for induced seismicity is pore pressure diffusion (Shapiro and Dinske 2009). Increases in pore fluid pressure act to reduce fault strength, bringing pre-existing fractures closer to failure according to the Mohr–Coulomb failure criterion. The initiation of fluid injection in a region leads to substantial increases in pore fluid pressure, which build up over time and diffuse outward for significant distances and for significant times from a well. The amount and magnitude of seismicity induced therefore depends on the ambient tectonic stress, as well as local geological and hydraulic conditions. Thus, induced seismicity can continue even after injection has ceased, as was the case at the Rocky Mountain Arsenal where three ~ 4:5 earthquakes occurred the year after waste fluid injection stopped (Healy et al., 1968; Hsieh and Bredehoeft, 1981). Fluid injection not only perturbs stress by changing the poro-elastic condition (Scholz, 1990, Segall 1992) and creates new fractures, but it also potentially introduces pressurised fluids into pre-existing fault zones, causing slip to occur earlier than it would otherwise have done naturally by reducing the effective normal stress and moving the failure closer to the Mohr-Coulomb criterion.

Nicol (2011), somewhat even before McGarr, drew the conclusion that the expected maximum magnitude is related to the total injected /extracted volume but in some cases where significant tectonic stress is present even larger events than are suggested by this relationship can be stimulated (**Figure B.46**). He also comments on the depth to which stimulation of activity can take place with special emphasis on zones where interaction with large tectonic features may occur.

*“The depths of induced seismicity and injection are generally on average, slightly deeper than the reservoir interval. These deeper events may in some cases be induced by loading or unloading of the sub-reservoir rock volume by fluid injection or extraction, respectively. These conclusions apply equally to the largest earthquakes, which are randomly distributed within the depth range of seismicity for each site. **Large magnitude earthquakes produced up to 10 km beneath large-scale hydrocarbon extraction sites (volumes >120 million m³) are a notable exception to the above conclusions. The greater focal depths for some extraction-related earthquakes have been interpreted to be a direct reflection of the fact that extraction of large volumes of fluids has the potential to induce crustal -scale deformation and seismicity”.***

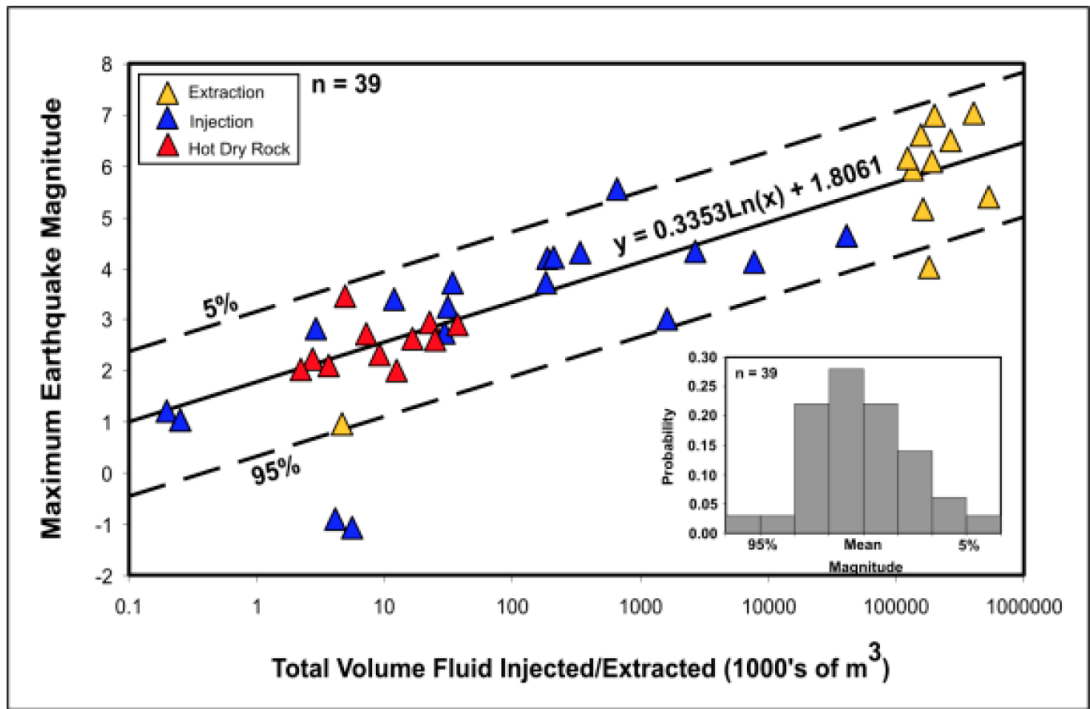


Figure B.46 Maximum magnitude and its relationship to total injected volume

He also plots the maximum expected radius of simulation from an injection zone and this is shown in **Figure B.47** and it is clear that this can easily exceed 20km for large injected volumes where critically stressed faults of appropriate orientation exist. **Figure B.48** shows the expected time of occurrence as a function of the total operational time and it clear that near events occur rapidly but distant events may have onset times of many years.

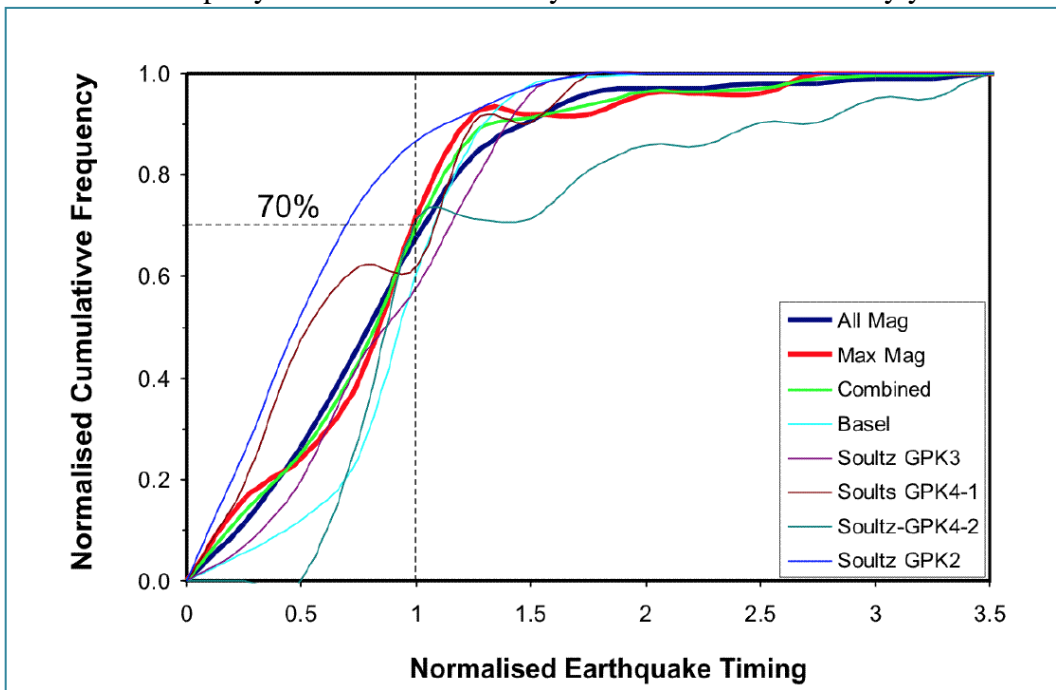


Figure B.47 Maximum radius of induced seismicity from the injection well plotted against the volume of fluid injected (from IEA 9/2013 after Nicol 2011)

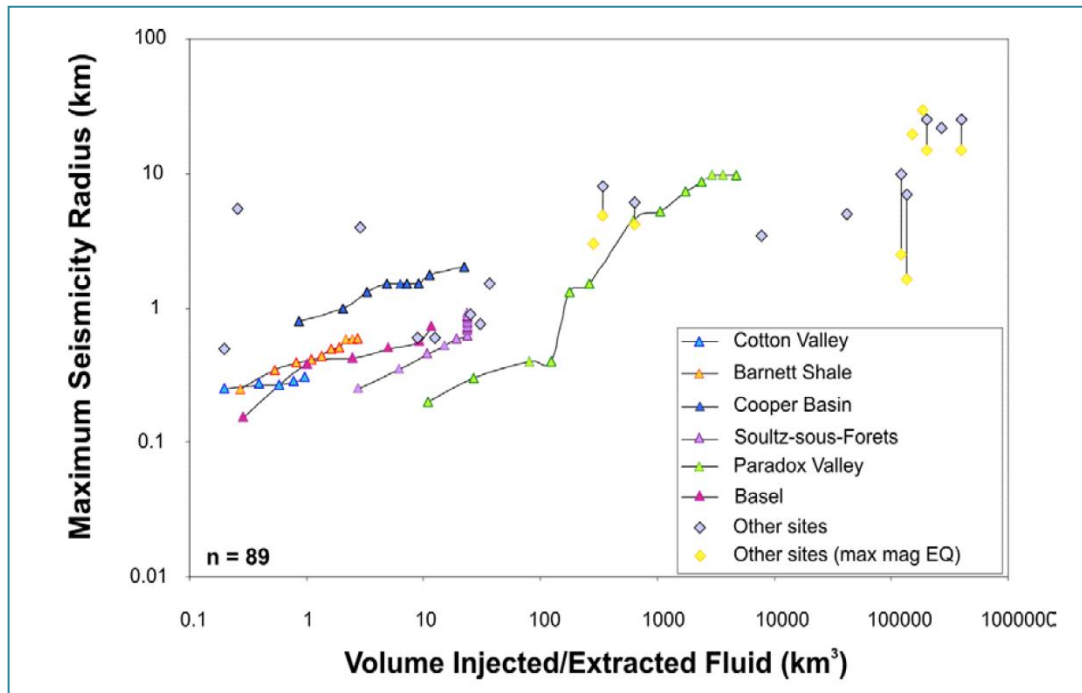


Figure B.48 Timing of induced earthquakes relative to the onset (0) and completion (1) of injection/extraction. (from IEA 9/2013 after Nicol 2011)

1. Stress Transfer

Whenever an earthquake happens it produces local (and distant) stress changes of two types:

- **Static**

These are permanent changes, which occur because stress has been redistributed and can lead to sufficient stress change that adjacent faults become unstable and fail with additional seismicity. The effects depend on the orientation of both the failing fault and the receiving fault and can be calculated. A stress change of c 0.01 MPa is considered **sufficient to act as trigger to another seismic event.**

- **Dynamic**

These are transient effects which occur because waves carrying energy from the first seismic event travel away from the source and produce a short duration cyclic loading which can in some circumstances produced a large enough stress change to trigger an earthquake. It has been suggested by Van de Elst that even distant teleseisms from giant earthquakes may be influential in some circumstances. Again it depends on the geometry and stress state of the receiving faults.

This is shown in cartoon form in **Figure B.49** from <http://www.eos.ubc.ca/courses/eosc256>.

Figure B.50 shows the consequence of stress changes on two instances of blind thrusts, which are the dominant reservoir structures in the Po Basin. If the thrust cuts the surface the stress becomes reduced but if the fault is ‘blind’ i.e. it doesn’t reach the surface, the stress is increased.

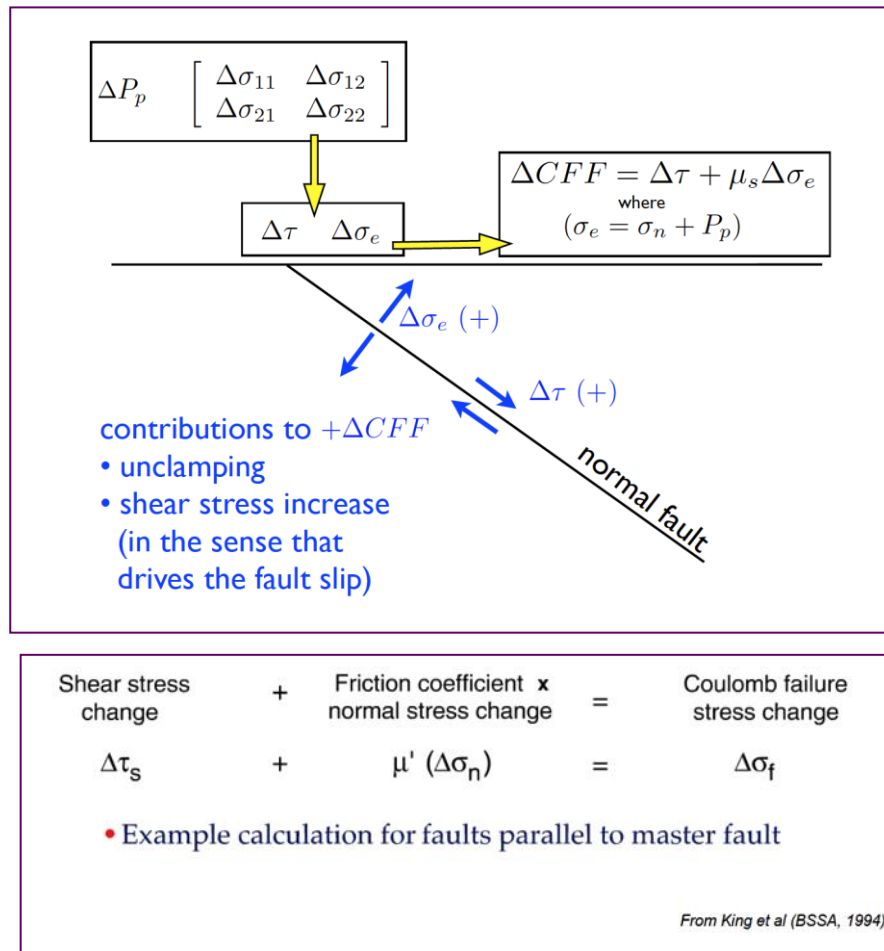


Figure B.49 Stress changes on a fault of particular geometry which consist of two parts:

- A change in normal stress which will either reduce or increase the frictional force depending on the polarity of the change
- A change in shear stress which will either expedite or inhibit fault movement depending on the polarity of the change

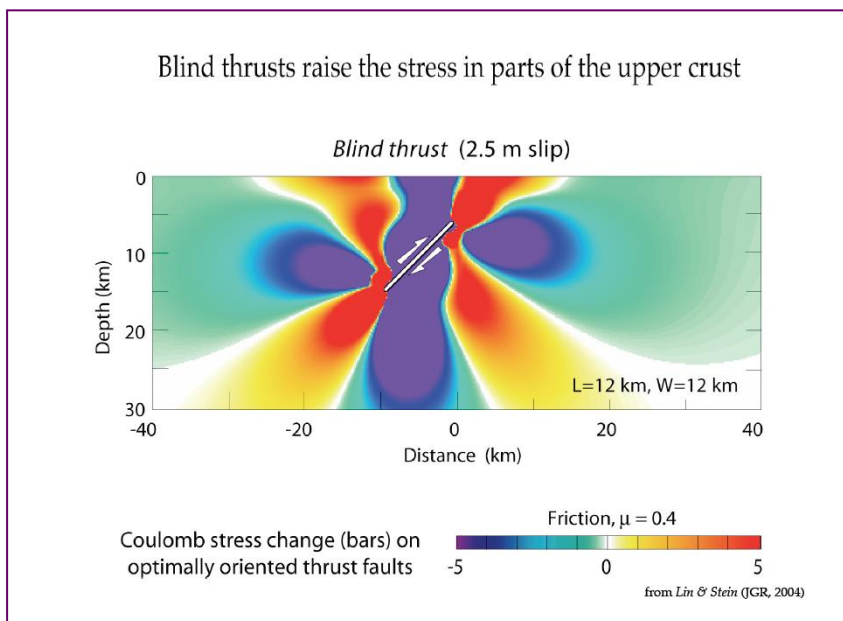
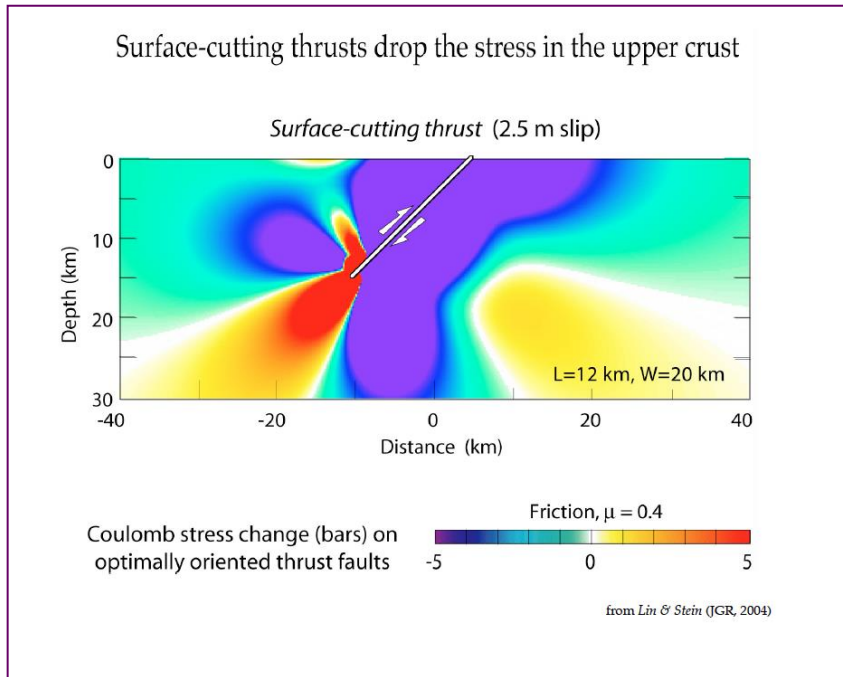


Figure B.50 Coulomb Stress changes around a surface cutting fault(top) and a blind thrust (bottom). The faults beneath the Po Basin are all Blind.

2. How do Earthquake faults fail?

Although it can appear that earthquakes are instantaneous releases of stored elastic energy they do in fact take a significant time to release their stored potential which can take some minutes in the case of giant earthquakes such as Sumatra 26 Dec 2004) as can be seen from the following table. (Table B.2)

Table B.2

Mw	Moment Mo	Length	Mean Slip	Area of slip	Duration
4	10^{15} N m	1000 m	2 cm	1 km ²	0.2 s
5	3.0×10^{16} Nm	3000 m	10 cm	9 km ²	0.4 s
6	1.1×10^{18} Nm	10 km	40 cm	100 km ²	5 s
7	3.5×10^{19} N m	80 km	1 m	1000 km ²	30 s
8	1.1×10^{21} Nm	300 km	6 m	6000 km ²	150 s
9	3.5×10^{22} Nm	800 km	20 m	6×10^4 km ²	300 s

A sequential set of 'patches' which are strong zones which have been preventing the fault from slipping, fail one after another often progressively outwards from an initial failure but sometimes returning close in as stress changes during the event. What had seemed to be a single giant event can be thought of as a consecutive assemblage of smaller events which simply happen very close together and their cumulative effect is catastrophic.

3. What is an aftershock?

It has been customary to divide earthquakes into:

- Foreshocks: i.e. occurring as precursor to a much larger ‘Mother’ event and probably on the fault surface which will eventually fully fail.
- Main Shock: The ‘Mother’ Event, with complete failure of the rupture surface.
- Aftershocks: i.e. progressively smaller events occurring on the same, or part of the same fault surface which failed in the mainshock.

The modified Omori-Utsu Law (which dates back to 1894!):

$$R(\tau) = K(c + \tau)^{-p}$$

is an attempt to describe the rate of decay (R) of aftershocks with the reciprocal of time (τ) with p being an exponent somewhere between 0.75 and 1.5 but conceptually something like unity.

Aftershock sequences are modelled by the Epidemic Type Aftershock Sequence (ETAS) model which assumes that all earthquakes are in general able to trigger subsequent aftershocks which can have even larger magnitudes than the ‘‘mother’’ earthquake (Ogata, 1988). In the ETAS model the earthquake rate, R_{ETAS} at a location x , and time t , is the sum of a constant background rate μ and the superposition of aftershock activity from preceding earthquakes, that is,

$$R_{ETAS} = \mu + \sum_{i:t_i < t_E} \frac{K_E 10^{\alpha(M_i - M_c)}}{(t_E - t_i + c)^p}$$

The seismicity rate R of a population of faults is inversely proportional to the state variable γ describing the creep velocities of the faults:

$$R(t) = r/\tau_r \gamma(t)$$

$$d\gamma = (dt - \gamma dCFS)/A\sigma$$

where r is the background seismicity rate, τ_r the tectonic loading rate, and A is a dimensionless fault constitutive parameter (Dieterich, 1994). Hence, the seismicity rate depends on the evolution of the Coulomb failure stress,

$$CFS = \tau + \mu\sigma$$

where as usual, τ is the shear stress on the assumed fault plane, σ is the effective normal stress (positive for extension), and μ is the friction coefficient. This model is able to explain an induced Omori-type occurrence of aftershocks in response to a single coseismic stress step (Dieterich, 1994).

4. Statistical properties of anthropogenic seismicity

Statistical analyses of induced seismicity reveal collective properties, which differ from those of natural seismicity (e.g. Lasocki, 2008; Weglarczyk and Laoscki, 2009; Lasocki and Orlecka-Sikora, 2013). The most predictable feature is non-stationarity; a time-dependence of induced seismic processes. An induced seismic process is partially controlled by technological operations, which vary on short-timescales resulting in time changes of the seismic process.

Natural earthquakes typically (but not always) follow the Gutenberg–Richter law which describes the relationship between the magnitude and total number of earthquakes in a region in a given time period.

$$N=10^{a-bM}$$

Where:

- N is the number of events greater or equal to M
- M is magnitude and a and b are constants

The b-value is a measure of the rate of increase in number of earthquakes with certain magnitudes and is often close to 1, i.e. each increase of 1 in magnitude produces a decrease in number of events by 10.

Variations of the activity rate and/or other parameters of the seismic process, e.g. temporal changes of Gutenberg-Richter b-value suggest a non-natural origin of a seismic series (Lasocki et al, 2013b). Induced seismicity should have properties, which are absent in natural seismicity: certain orderliness, internal correlations, and memory.

The magnitude distribution of induced seismicity often does not follow the Gutenberg-Richter law but is more complex and often multimodal. Out of six analyzed seismic series associated with: injection for geothermal energy production in Basel, Switzerland, injection for hydrocarbon recovery in Romashkino Oil Field in Russia, Açú dam reservoir in Rio Grande do Norte State in Brazil, Song Tranh 2 dam in Vietnam, Rudna copper-ore underground mine in Poland, Mponeng deep gold mine in South Africa; the hypothesis that their magnitude distributions follow the Gutenberg-Richter law has been rejected in every case with high to very high significance (Lasocki 2013a, Lasocki 2013b). The complexity of magnitude distribution becomes an important discriminator between induced and natural seismicity.

Even when significant deviations from the Gutenberg-Richter law for anthropogenic seismicity cases cannot be ascertained there are some subtleties such as described in **Figure B.51** from IEA Report 9/2013 and **Figure B.52** from the Basel study where there seems to be a clear relationship between reservoir permeability and the b value from induced seismicity recorded from there. Low permeabilities tend to be associated with high b values and high permeabilities with low b values, which is interpreted as stress is taken up in small perhaps tensile events in shales but greater fluid percolation distance in high permeability reservoirs may facilitate stimulation of more distance on existing structures.

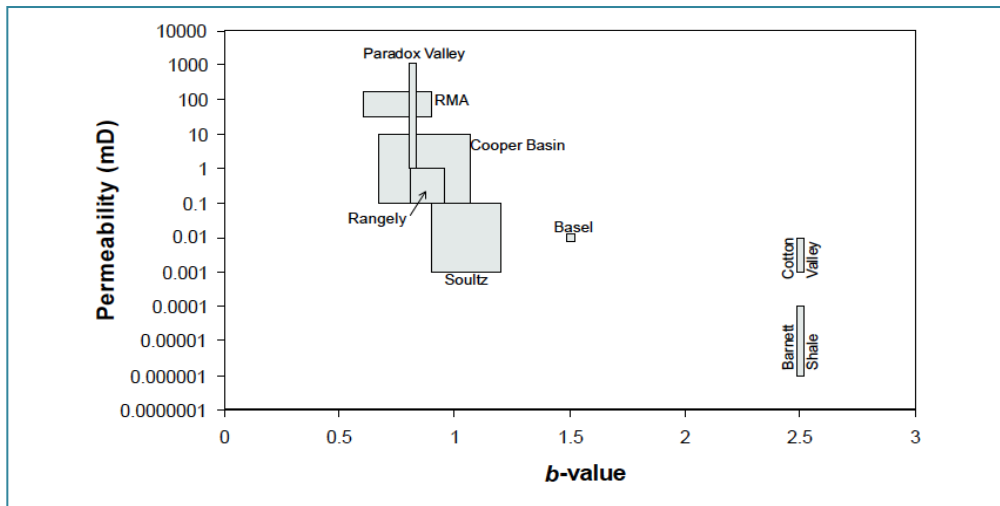


Figure B.51 Gutenberg-Richter b-values against permeability for a number of injection induced seismicity sites (from IEA9/2013)

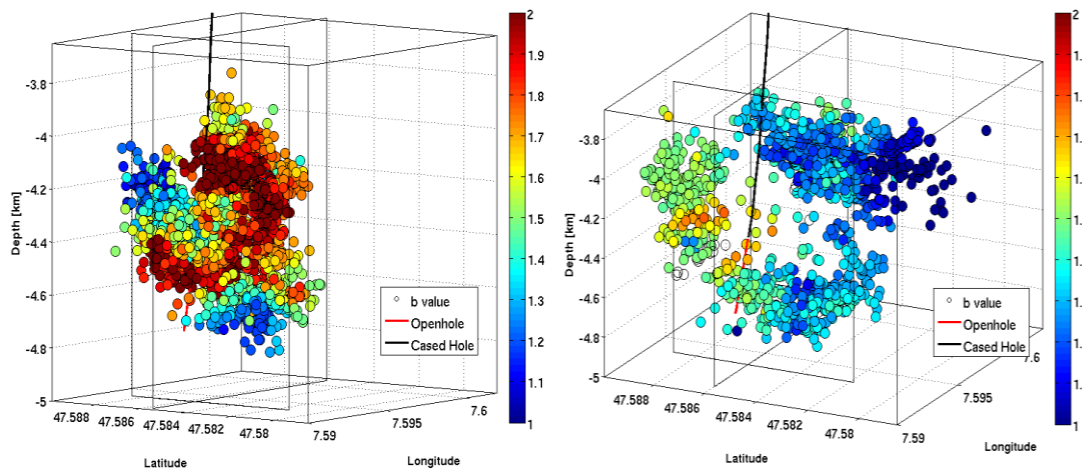


Figure B.52 Gutenberg-Richter b-values before injection (left) and after injection (right) at Basel after (Bachmann (2011))

A comparison of b-values for a range of European seismic event groupings has been generated by Gruenthal (2014) and is shown in **Table B.3**. The variation in b-values during the Basel swarm is shown in the visualization in **Figure B.52**, where it appears that values around 2 are seen during injection but these fall back to much lower values of around 1.1 to 1.2 in the post-injection period.

Table B.3 Comparison of b-values for a range of European seismic event, from Gruenthal (2014)

Source of seismicity	<i>b</i> -value with $\pm\sigma$
Geothermal projects	1.94(\pm 0.21)
Natural tectonic earthquakes Long-term data	1.25(\pm 0.01)
Natural tectonic earthquakes Short-term data	1.16(\pm 0.05)
Hydrocarbon exploitation	0.93(\pm 0.11)
Coal mining	1.59(\pm 0.05)
Copper mining	2.13(\pm 0.22)
Salt and potash mining	1.02(\pm 0.09)

5. Action at a distance: the effect of fluid injection

Murphy et (2013) describe a simulation of the effect of even a very limited injection over only 15 days to a pressure of only 170 bar on the criticality of a large fault situated outside the actual zone of injection which is a permeable reservoir but sandwiched between two impermeable layers at a depth of about 3 km (**Figure B.52** Gutenberg-Richter b-values **before injection (left) and** after injection (right) at Basel after (Bachmann (2011)and **Figure B.54**). This numerical study showed that active faults near injection sites, even when not in direct contact with the injected fluids, could be greatly affected by stress perturbations caused by their presence. Their simulated injection induces a M_w 6.7 event with a hypocentral depth at 8 to 10+ km. (**Figure B.55**) which is entirely controlled by the fault size and its previous tectonic loading and not the injected volume; the injection simply triggers the release of this stored energy.

Additionally the injection not only advances the next sequence of earthquakes affects their size and permanently alters the size and temporal occurrence of earthquakes but also temporarily shifts the fault to a state of subcriticality (ie stabler) but with continuous tectonic loading the fault returns to near self-organized criticality in about 200 yr.

Their results suggest that fluid injection can trigger earthquakes whose size is dependent on the size of the fault, NOT the injection and that these faults do not necessary need to be in the injection site.

Table. B.4 Parameters used in the Murphy et al (2013) models of fluid injection related seismicity

Strata	D_{xx} ($m^2 s^{-1}$)	D_{yy} ($m^2 s^{-1}$)	D_{zz} ($m^2 s^{-1}$)
Cap Layer 1	0.1	0.1	0.1
Reservoir	2.0	2.0	0.1
Cap Layer 2	0.1	0.1	0.1
Boundary	0.05	0.05	0.1

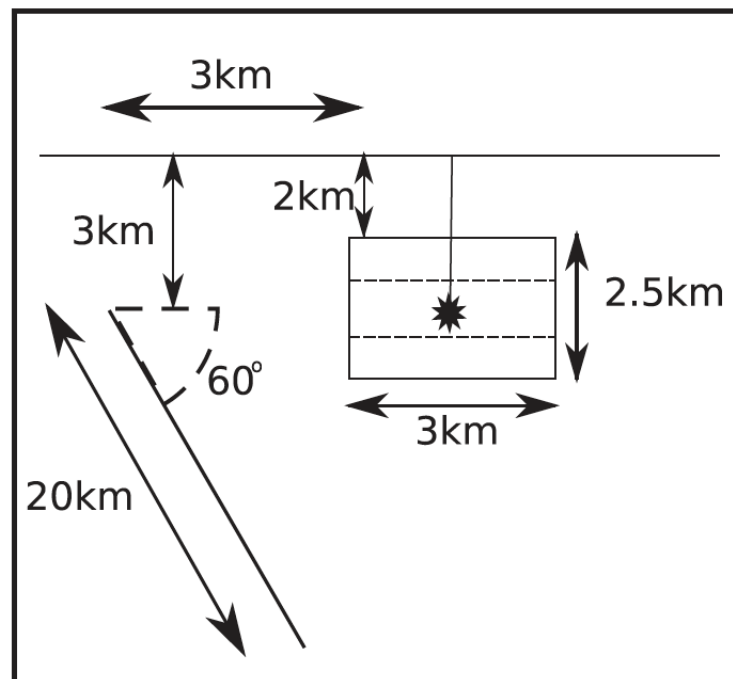


Figure B.53 Murphy et al (2013) schematic of the injection site relative to a fault. The injection occurs half way along the strike of the fault which is 40 km long at a depth of 3.3 km (denoted by the star) into a reservoir which extends from 3–4.5 km. The horizontal dashed lines are the boundary between the Reservoir layer and Cap Layers 1 and 2 (the diffusivities which are defined in Table 4

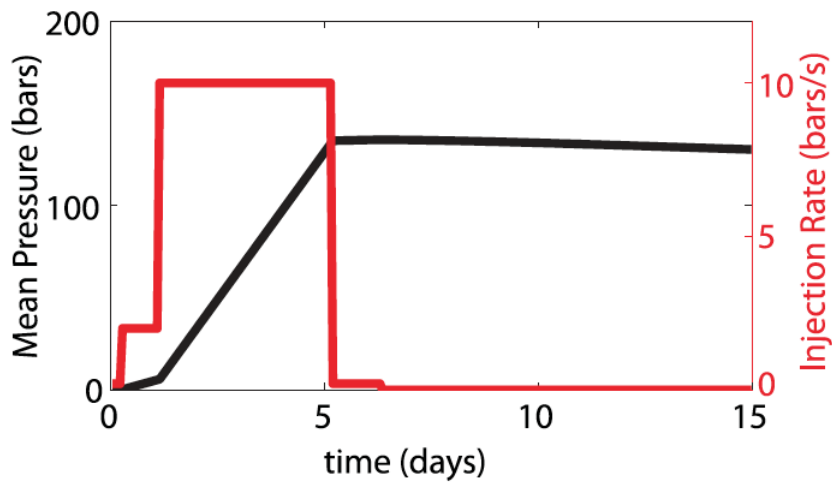


Figure B.54 Pressure injection history. Maximum injection rate (red line) is 10 Bar s⁻¹. Injection stops at 6.73 d. Mean pressure (black line) is for the whole simulation volume not just the reservoir

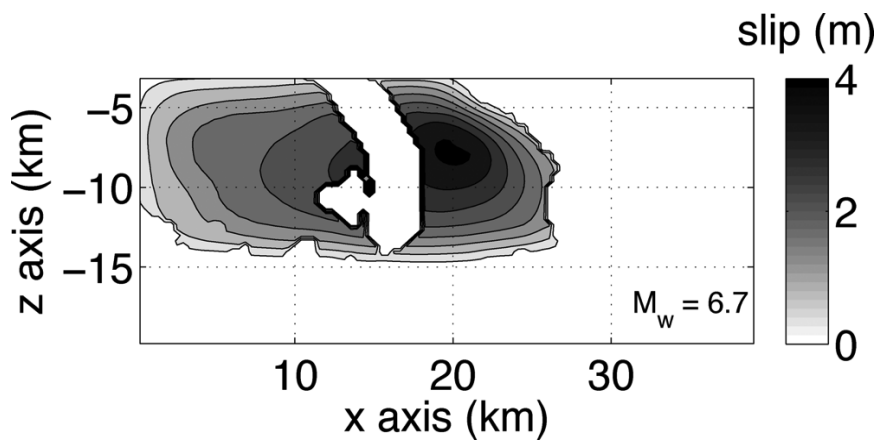


Figure B.55 Slip distribution for the induced Mw 6.7 event. Below 15 km the velocity strengthening section of the fault means no coseismic slip extends into this zone

E. CONCLUSIONS

- Extraction and/or injection of fluids in hydrocarbon fields can, in certain circumstances, induce or trigger seismic activity
- Several authoritative reports describe well-studied cases where extraction and/or injection of fluids in hydrocarbon or geothermal fields has been *associated* with the occurrence of earthquakes, of magnitudes even higher than 5. It is difficult, sometimes not possible, to use the word *proven* in these circumstances..
- The reported cases are only a small fraction of all of the existing cases of extraction and injection of fluids and are mostly related to the additional load imposed by very large reservoirs and to the injection of large volumes of fluid (usually waste water) into surrounding rocks and not into in the same reservoir during enhanced recovery or pressure maintenance. However, some cases do exist, where earthquakes have been associated with waste-water disposal within the same reservoir where oil and gas have been extracted.
- The induced, and specifically the triggered, seismic response to injections is complex and variable among cases and its correlation with technological parameters is far from being fully known.
- The magnitude of triggered earthquakes depends more on the dimensions of the fault and its strength, rather than the characteristics of the injection.
- Recent research on stress diffusion suggests that the activated fault may also be tens of km away from the injection/extraction location, some kilometres deeper than the reservoir and several years after activities commenced.
- The greater focal depths for some extraction-related earthquakes have been interpreted to be a direct reflection of the fact that extraction or injection of large volumes of fluids has the potential to induce crustal-scale deformation and seismicity.
- Many cases of earthquake activity have been recorded during the exploitation of geothermal energy. Most of them are related to projects for the development of Enhanced Geothermal Systems where induced fractures must be produced in impermeable igneous rocks to develop permeable pathways. Several cases are also related to traditional exploitation of geothermal energy. The induced earthquakes are generally of medium to low magnitude and no more than a few km away from the extraction or injection wells.

- Exhaustive examination of all the available literature shows that the discrimination between natural and triggered/induced earthquakes is a difficult problem and does not presently have a reliable, ready-to-use solution.

References

1. Adushkin V. V., Rodionov V. N., Turuntaev S., and Yudin A. E. (2000). Seismicity in the oil field. *Oil Field Review*, **12**: 2–17.
2. Ake J., Mahrer K., O’Connell D., and Block L. (2005). Deep-Injection and Closely Monitored Induced Seismicity at Paradox Valley, Colorado. *Bulletin of the Seismological Society of America*, **95**: 64–683.
3. Altmann, J., Müller T., Müller B., Tingay M. and Heidbach O. (2010). Poroelastic Contribution to The Reservoir Stress Path. *International Journal of Rock Mechanics and Mining Sciences*, **47**: 1104–1113.
4. Avouac J-P. (2012). Human-induced shaking. *Nature Geoscience* **5**: 763–764
5. Bachmann C. E., Wiemer S., Woessner J. and Hainzl S. (2011). Statistical analysis of the induced Basel 2006 earthquake sequence: introducing a probability-based monitoring approach for Enhanced Geothermal Systems. *Geophysical Journal International*, **186**: 793–807.
6. Bossu R., Grasso J. R., Plotnikova L. M., Nurtaev B., Frechet J., and Moisy M. (1996). Complexity of intracontinental seismic faultings: The Gazli, Uzbekistan, sequence. *Bulletin of the Seismological Society of America*, **86**: 959–971.
7. Brodsky E.E., Lajoie L.J. (2013). Anthropogenic Seismicity Rates and Operational Parameters at the Salton Sea Geothermal Field. *Science* 341, 543, doi: 10.1126/science.1239213
8. Bullen K. E., and Bolt B. A. (1985). An introduction to the theory of Seismology, ISBN-13: 978-0521283892.
9. Caloi P., De Panfis M., Di Filippo D., Marcelli L., Spadea M. C. (1956). Terremoti della Val Padana del 15-16 maggio 1951. *Annali Geofisica*, **9**: 63-1956.
10. Chanpura R., (2001). Fault reactivation as a result of reservoir depletion. PhD Thesis Georgia Institute of Technology, USA.
11. Chen Yong (2009). Did the reservoir impoundment trigger the Wenchuan earthquake? *Science in China Series D-Earth Science*, **52**: 431-433.
12. Cochran E.S., Sumy D.F., Keranen K.M., Abers G.A. and Savage H.M. (2012). Coulomb stress modeling of the 2011 M5.7 Oklahoma earthquake sequence. *American Geophysical Union 2012 Fall Meeting, San Francisco, California, 3–7 December 2012*, S53I–05.
13. Committee on Induced Seismicity Potential in Energy Technologies: Hitzman M.W. (Chair), Clarke D.D, Detournay E., Dieterich J.H., Dillon D.K., Green S.J, Habiger R.M., McGuire R.K., Mitchell J.K. Shemeta J.E., Smith J.L (Bill) (2013). Induced Seismicity Potential in Energy Technologies. National Academy of Sciences. *The National Academies Press Washington, D.C.*, pp. 248.
14. Dahm, T., Hainzl, S., Becker, D., Bisschoff, M., Cesca, S., Dost, B., Fritschen, R., Kuhn, D., Lasocki, S., Klose, C. D., Meier, T., Ohrnberger, M., Rivalta, E., Shapiro, S., Wegler, U. (2010). How to discriminate induced, triggered and natural seismicity. *Proceedings of the Workshop Induced seismicity: November 15 - 17, 2010, Hotel Hilton, Luxembourg, Grand-Duchy of Luxembourg, (Cahiers du Centre Européen de Géodynamique et de Séismologie ,30), Centre Européen de Géodynamique et de Séismologie*, 69-76.
15. Davies R., Foulgera G., Bindleya A., Styles P. (2013). Induced seismicity and hydraulic fracturing for the recovery of hydrocarbons. *Marine and Petroleum Geology*, **45**: 171–185.

16. Davis, S. D., and Frohlich C. (1993). Did (or will) fluid injection cause earthquakes? Criteria for a rational assessment. *Seismol. Res. Lett.*, **64**: 207–224.
17. de Pater C.J., Baisch S. (2011). Geomechanical Study of Bowland Shale Seismicity – Synthesis Report commissioned by Cuadrilla Resources Ltd. <http://www.cuadrillaresources.com/news/media-and-image-library/downloads/>
18. Dieterich J. (1994). A constitutive law for rate of earthquake production and its application to earthquake clustering. *J. Geophys. Res.*, **99**: 2601– 2618.
19. Durrheim, R.J. (2010). Mitigating the risk of rockbursts in the deep hard rock mines of South Africa: 100 years of research. In: *Extracting the Science: a century of mining research*, J. Brune (editor), Society for Mining, Metallurgy, and Exploration, Inc., pp. 156-171.
20. Ellsworth W.L. (2013). Injection-Induced Earthquakes. *Science* 341, doi: 10.1126/science.1225942
21. Evans K. F., Zappone A., Kraft T., Deichmann N. and Moia F. (2012). A survey of the induced seismic response to fluid injection in geothermal and CO2 reservoirs in Europe. *Geothermics*, **41**: 30-54.
22. Eyidoğan H., Nábělek J., Toksöz M.N. (1985). The Gazli, USSR, 19 March 1984 Earthquake: The mechanism and tectonic implications”. *Bull Seismol Soc Am*, **75**: 661-675.
23. Frohlich C., Ellsworth W., Brown W. A., Brunt M., Luetgert J. H., MacDonald T., and Walter S. (2014). The 17 May 2012 M4.8 earthquake near Timpson, east Texas: an event possibly triggered by fluid injection. *J. Geophys. Res. Solid Earth*, (in press), doi:10.1002/2013JB010755
24. Frohlich C., Hayward C., Stump B. and Potter E. (2011). The Dallas–Fort Worth Earthquake Sequence: October 2008 through May 2009. *Bulletin of the Seismological Society of America*, **101**: 327-340.
25. Gibowicz S.J. (2009). Seismicity induced by mining: recent research. *Advances in Geophysics*, **51**: 1-53.
26. Gibowicz, S.J., Lasocki, S. (2001). Seismicity induced by mining: Ten years later. *Advances in Geophysics*, **44**: 39-181.
27. González P.J., Tiampo K.F., Palano M., Cannavó F., Fernández J. (2012). The 2011 Lorca earthquake slip distribution controlled by groundwater crustal unloading. *Nature Geoscience*, **5**: 821–825, doi:10.1038/ngeo1610
28. Grasso J. R. and Wittlinger G. (1990). 10 years of seismic monitoring over a gas field area. *Bulletin of the Seismological Society of America*, **80**: 450–473.
29. Green C. A., Styles P., Baptie. B. J. (2012). Preese Hall Shale gas fracturing Review & recommendations For Induced seismic mitigation. *Report to UK Department of Energy and Climate Change*, 26pp.
30. Gruenthal G. (2013). Induced seismicity related to geothermal projects versus natural tectonic earthquakes and other types of induced seismic events in Central Europe. *Geothermics* 10.1016
31. Gupta H.K. (2002). A review of recent studies of triggered earthquakes by artificial water reservoirs with special emphasis on earthquakes in Koyna, India. *Earth-Science Reviews*, **58**: 279-310.
32. Hainzl S., Kraft T., Wassermann J., Igel H. and Schmedes E. (2006). Evidence for rainfall triggered earthquake activity. *Geophys. Res. Lett.*, **33**, L19303, doi: 10.1029/2006GL027642
33. Haring M., Ulich S., Ladner F., and B. Dyer (2008). Characterisation of the Basel 1 enhanced geothermal system. *Geothermics*, **37**: 469-495.

34. Healy, J. H., Rubey W. W., Griggs D. T., and Raleigh C. B. (1968). The Denver earthquakes. *Science*, **161**: 1301–1310.
35. Herrmann, R. B., Park, S. K., and Wang C. Y. (1981). The Denver earthquakes of 1967-1968. *Bull. Seism. Soc. Am.*, **71**: 731-745.
36. Holland, A. A. (2013). Earthquakes Triggered by Hydraulic Fracturing in South-Central Oklahoma. *Bull. Seismol. Soc. Am.*, **103**: 1784-1792.
37. Horton, S. (2012). Disposal of hydrofracking waste fluid by injection into subsurface aquifers triggers earthquake swarm in central Arkansas with potential for damaging earthquake. *Seism. Res. Lett.*, **83**: 250-260.
38. Hsieh, P. A., and J. S. Bredehoeft (1981). A reservoir analysis of the Denver earthquakes—a case study of induced seismicity, *J. Geophys. Res.* **86**, 903–920.
39. Kanamori H. and Brodsky E.E. (2001). The physics of earthquakes. *Physics Today* **54**: 34-40.
40. Keranen K.M., Savage H.M, Abers G.A., Cochran E.S. (2013). Potentially induced earthquakes in Oklahoma, USA: Links between wastewater injection and the 2011 Mw 5.7 earthquake sequence. *Geology*, **41**: 699-702.
41. Kim W.Y. (2013). Induced seismicity associated with fluid injection into a deep well in Youngstown, Ohio. *Journal of Geophysical Research: Solid Earth*. **118**: 3506–3518.
42. Lasocki S. (2013a). From hazard assessment to hazard management. The case of mining-induced seismicity. *Key-note lecture. Soc. Expl. Geophys. D&P Forum 'Integrated Geophysics for Unconventional Resources', Kraków, Poland 7-11 July 2013*
43. Lasocki S. (2013b). Induced seismicity. *EPOS workshop 'A Roadmap for Earth Science in Europe: The next generation of Geophysical Research Infrastructures'. 'Ettore Majorana' Foundation and Centre for Scientific Culture Erice, Sicily, Italy 26/08 – 4/09/2013*
44. Lasocki S., Dahle A., Dahm T., Dost B., Grasso J-R., Kraft T. and other Members of W10 “Infrastructure for Georesources, EPOS” (2013b). Science Plan. Conclusions from the discussion held during WG10:Infrastructure for Georesources Meeting in Kraków, Poland, 17-19.02.2013. *EPOS PP 2nd Regional Conference Bergen Norway, 25-26 February 2013.*
45. Lasocki S., Dahm T., Orlecka-Sikora B., Urban P., and other Members of W10 “Infrastructure for Georesources, EPOS” (2013a). The socio-economic impact of induced seismicity node of EPOS. Conclusions from the discussion held during WG10:Infrastructure for Georesources Meeting in Kraków, Poland, 17-19.02.2013. *EPOS PP 2nd Regional Conference Bergen Norway, 25-26 February 2013.*
46. Lasocki S., Orlecka-Sikora B. (2013) Key-note lecture. Nonstationarity, memory, interactions in mining-induced seismic process – a chance of predictability. Scientific Seminar of Observation and Monitoring of Geological and Geotechnical Risks, Precursory signs and prediction: between Myth and Scientific Reality. *INERIS, Nancy, France, 21.03.2013*
47. Lasocki, S. (2008). Some unique statistical properties of the seismic process in mines. *Proc. 1st Southern Hemisphere International Rock Mechanics Symposium SHIRMS 2008, Perth, 16-19 September 2008, (Potvin, Y., Carter, J., Dyskin, A., Jeffrey, R., eds.), Australian Centre for Geomechanics, pp. 667-678*

48. Lei X., Mas., Chen W., Pang C., Zeng J. , Jang B. (2013). A detailed view of the injection-induced seismicity in a natural gas reservoir in Zigong, southwester Sichuan Basin, China. *Journal of Geophysical Research: Solid Earth*, **118**: 1-16.
49. Lei X., Yu G., Ma S., Xueze W., Wang Q. (2008). Earthquakes induced by water injection at 3km depth within the Rongchang gas field, Chongqing, China. *Journal of Geophysical Research*. 113
50. Llenos A. L., and Michael A.J. (2013). Modeling Earthquake Rate Changes in Oklahoma and Arkansas: Possible Signatures of Induced Seismicity. *Bulletin of the Seismological Society of America*, **103**: 2850-2861.
51. Majer E.L., Baria, R., Stark, M., Oates, S., Bommer, J., Smith, B., and Asamuma, H. (2007). Induced seismicity associated with Enhanced Geothermal Systems. *Geothermics*, **36**: 185-222.
52. McGarr A. (1991). On a possible connection between three major earthquakes in California and oil production. *Bull Seismol Soc Am*, **81**: 948-970.
53. McGarr, A. (1976). Seismic Moments and Volume Changes. *Journal of Geophysical Research*, **81**: 1487-1494.
54. McGarr, A., Simpson, D. (1997). A broad look at induced and triggered seismicity. In: *Rockbursts and Seismicity in Mines (Gibowicz, S.J., Lasocki, S., eds.)*, Balkema, Rotterdam, pp. 385-396.
55. McGarr, A., Simpson, D., Seeber, L. (2002). Case histories of induced and triggered seismicity. In: *International Handbook of Earthquake and Engineering Seismology part A (Lee, W.H.K., Kanamori, H., Jennings, P.C., Kisslinger, C., eds.)*, Academic Press, London, pp. 647-661.
56. Meremonte, M.E., Lahr J. C., Frankel A. D., Dewey J. W., Crone A. J., Overturf D. E., Carver D. L., and Bice W. T. (2002). Investigation of an Earthquake Swarm near Trinidad, Colorado, August-October 2001, *USGS Open-File Report 02-0073*. <http://pubs.usgs.gov/of/2002/ofr-02-0073/ofr-02-0073.html>
57. Murphy S., O'Brien G.S., McCloskey J., Bean C.J., Nalbant S. (2013). Modelling fluid induced seismicity on a nearby active fault. *Geophys. J. Int.*, doi: 10.1093/gji/ggt174
58. Nicholson C. and Wesson R. L. (1990). Earthquake Hazard associated with Deep Well Injection, *USGS Report 1951*, 74pp.
59. Nicholson, C., Roeloffs E. and Wesson R. L. (1988). The northeastern Ohio earthquake of 31 January 1986: was it induced?. *Bull. Seism. Soc. Am.* **78**: 188-217.
60. Nicol, A., Carne R., Gerstenberger M., Christophersen A. (2011). Induced seismicity and its implications for CO2 storage risk. *Energy Procedia*, **4**: 3699-3706.
61. Ogata Y. (1998). Space-time point process models for earthquake occurrences. *Ann Inst Statist Math*, **50**: 379-402.
62. Ottemöller, L., Nielsen H. H., Atakan K., Braunmiller J. and Havskov J. (2005). The 7 May 2001 induced seismic event in the Ekofisk oil field, North Sea. *Journal of Geophysical Research*, 110, B10301.
63. Scholz C. (1990). Earthquakes as Chaos. *Nature*, **348**: 197-198
64. Seeber, L., Armbruster J., and Kim W. Y. (2004). A fluid-injectiontriggered earthquake sequence in Ashtabula, Ohio: Implications for seismogenesis in stable continental regions. *Bull. Seismol. Soc. Am.*, **94**: 76-87.

65. Segall, P. (1985). Stress and subsidence resulting from subsurface fluid withdrawal in the epicentral region of the 1983 Coalinga earthquake. *Journal of Geophysical Research*, **90**: 6801–6816.
66. Segall, P. (1989). Earthquakes triggered by fluid extraction. *Geology* **17**: 942-946.
67. Segall, P. (1992). Induced stresses due to fluid extraction from axisymmetric reservoirs. *Pure and Applied Geophysics*, **139**: 535–560.
68. Segall, P. and Yerkes R.F. (1990). Stress and fluid pressure changes associated with oil field operations: a critical assessment of effects in the focal region of the 1983 Coalinga earthquakes, In *The Coalinga, California Earthquake of May 2, 1983. U.S. Geological Survey Professional Paper, U.S. Geological Survey, 1990.*
69. Segall, P., Grasso J. R., and Mossop A., (1994). Poroelastic stressing and its effect near the Lacq gas field, southwestern France. *Journal of Geophysical Research*, **99**: 15423–15438.
70. Shapiro, S. A., and Dinske C. (2009). Scaling of seismicity induced by nonlinear fluid-rock interaction. *J. Geophys. Res.*, **114**.
71. Shemin Ge, Mian Liu, Ning Lu, Godt J.W., Gang Luo (2009). Did the Zipingpu Reservoir trigger the 2008 Wenchuan earthquake? *Geophysical Research Letters*, **36**, L20315, doi:10.1029/2009GL040349, 2009
72. Simpson D.W., Leith W. (1985). The 1976 and 1984 Gazli, USSR, earthquakes – were they induced? *Bull Seismol Soc Am*, **75**: 1465-1468.
73. Stein R. and Yeats R. S. (1989). Hidden Earthquakes. *Sci. Am.*, **260**: pp. 48-57.
74. Suckale J. (2009). Induced seismicity in hydrocarbon fields. *Advances in Geophysics*, **51**: 55-106.
75. Turuntaev S. (2012) Personal communication.
76. van der Elst N. J., Savage H. M., Keranen K. M., Abers G.A. (2013). Enhanced Remote Earthquake Triggering at Fluid-Injection Sites in the Midwestern United States. *Science*, **341**: 164-167.
77. Van Eck, T., Goutbeek F., Haak H. and Dost B. (2006). Seismic hazard due to small magnitude, shallow-source, induced earthquakes in The Netherlands. *Environmental Geology*, **87**: 105–121.
78. Węglarczyk, S., Lasocki, S. (2009). Studies of short and long memory in mining-induced seismic processes. *Acta Geophys.* **57**: 696-715.
79. Yerkes, R.F., and Castle, R.O. (1970). Surface deformation associated with oil and gas field operations in the United States. *Land subsidence: International Association of the Science of Hydrology, UNESCO Publication*, **89**: 55-66.
80. Zoback M. (2012). Managing the seismic risk posed by wastewater disposal. *Earth*, **57**: 38–43.
81. Zoback, M.D., and Harjes, H-P, 1997. Injection-induced earthquakes and crustal stress at 9km depth at the KTB deep drilling site, Germany. *J. Geophys. Res.*, **102(B8)**: 18477-18491
82. Zoback, M.L., M.D. Zoback, and 26 others (1989). Global patterns of tectonic stress. *Nature*, 341.6240291-298.

Appendix C. List of available data

1. Oil/Gas PRODUCTION, GAS STORAGE AND GEOTHERMAL DATA IN THE STUDY AREA (from MINISTRY OF ECONOMIC DEVELOPMENT, COMPANIES AND REGIONAL AUTHORITIES)

Data on Oil/Gas Production, Gas Storage and geothermal activities were provided straight by Ministry of Economic Development and, at the instance of the same Ministry, by Oil/Gas Production and Gas Storage Companies, by Emilia Romagna Region and Ferrara Province competent authorities.

General Data provided by Ministry

- HISTORICAL DRILLED WELLS MAPS AND DATA (depth, shutoff, current status) in the study area defined by ICHESE;
- MAP OF ACTIVE WELLS 2010-2012 IN THE AREA;
- CERTIFICATION OF ACTIVITY ABSENCE IN THE “RIVARA STORAGE” PROJECT AREA;
- “RIVARA STORAGE” DOCUMENTS OF PROCEDURE ADMINISTRATIVE;
- AGGREGATE PRODUCTION DATA from 2010 to 2012 (for Mirandola, Spilamberto, and Recovato);
- MAP AND GEOGRAPHICAL COORDINATES- STUDY AREA.

MIRANDOLA

ENI operated the Mirandola field until October 2010, from then PADANA (GAS PLUS GROUP) operates the field.

❖ BOREHOLES (WELLS)

- **.LAS AND .JPG FILES OF CAVONE WELLS** (1, 2, 3, 4, 5, 6, 7, 8, 9, 10, 11, 12, 13, 14, 15, 16, 17, 18, 19, 20, 20A, 21, 21A, 21B), CONCORDIA 1 WELL, SAN GIACOMO1 WELL;
- **.LAS OF SAN FELICE SUL PANARO 1 WELL, MIRANDOLA DI QUARANTOLI 28 WELL, BIGNARDI 1 WELL;**
 - **.JPG OF WELL LOG** OF MIRANDOLA DI QUARANTOLI 28 WELL, BIGNARDI 1 DIR BIS, CAMURANA 1, CAMURANA 2, CONCORDIA 1, MEDOLLA 1, RIVARA 1, RIVARA 2, SAN BIAGIO 1, SAN FELICE SUL PANARO 1, SAN GIACOMO, SPADA1;
 - **ACTIVE WELL NAME LIST by PADANA** (8 oil wells and 17 gas wells).

❖ PRODUCTION DATA

- **STATIC AND DYNAMIC STUDY REPORT OF FIELD (1986) by ENI;**
- **RESERVOIR STUDY (1994) by ENI;**
- **TOTAL MONTHLY VOLUME PRODUCTION FOR CAVONE FIELD FROM 05/05/1979 TO 30/10/2010 BY ENI;**
- **PRESSURE AND MONTHLY VOLUMES OF GAS/OIL PRODUCED BY EACH WELL (JUNE – OCTOBER 2010) by ENI;**
- **PRODUCTION CAPACITY** (production test on Cavone 2, 4, 7, 8, 9, 13, 17 wells and San Giacomo 1 well; Volumes measured at testing separator in the oil centre Cavone, years 2010 - 2012) **by ENI and by PADANA;**

- **PRESSURE BY EACH WELL (NOVEMBER 2010 – MAY 2012) by PADANA;**
- **MONTHLY PRODUCTION (GAS/OIL AND WATER) FOR EACH WELL (JAN 2010-DEC 2012) by PADANA;**
- **DAILY VOLUMES OF GAS/OIL PRODUCTION AND HEAD PRESSURE FOR EACH WELL (JAN 2012-MAY2012) by PADANA;**
- **DAILY HEAD AND CASING PRESSURE FOR EACH WELL (MAY 2012-JUN 2012), IN RELATION TO THE CHECKING OF WELLS CONDITIONS by PADANA;**
- **GEOCHEMICAL ANALYSIS OF TWO OIL SAMPLES by PADANA;**
- **SUMMARY OF ADDITIONAL DATA (Reservoir pressure behavior, Production history, wells location, Technical data of artificial lift, data sheet of injection pump);**
- **VOLUME AND PRESSURE DATA FOR THE DAILY PRODUCTION OF THE FIELD (OIL AND GAS) AND OF EACH INDIVIDUAL PRODUCTION WELL, FOR THE FOUR MONTHS PRECEDING THE MAY 2012 SEISMIC EVENTS. RELIABILITY OF PRODUCTION DATA FOR EACH INDIVIDUAL WELL by PADANA;**
- **REPORT ON THE PRODUCTION OF THE FIELD (OIL, GAS AND WATER), INDICATING THE REASONS BEHIND THE VARIATIONS IN PRODUCTION VALUES, IN PARTICULAR DURING THE PERIOD FROM NOVEMBER 2011 TO AUGUST 2012 by PADANA;**
- **REPORT ON THE HEAD PRESSURE OF CASINGS FROM 1 MAY 2012 TO 30 JUNE 2012 BY EACH WELL.**

❖ **INJECTION DATA**

- **MONTHLY VOLUME REINJECTION DATA FROM 05/05/1979 TO 30/10/2010 by ENI;**
- **RE-INJECTION TEST AND SBHP REPORTS OF CAVONE 14 ('85, '89, 2009) by ENI;**
- **MONTHLY VOLUMES OF INJECTED WATER IN CAVONE 14 FROM JULY 1985 TO MARCH 1999 by ENI;**
- **DAILY VOLUMES OF INJECTED WATER AND DYNAMIC PRESSURE FROM 1999 TO 2010 FOR CAVONE 14 by ENI;**
- **DAILY VOLUMES OF WATER INJECTED AND PRESSURE OF CAVONE 14 (NOVEMBER 2010 – MAY 2012) by PADANA;**
- **PRESSURE AND DAILY VOLUMES OF INJECTED WATER IN CAVONE 14 (JUNE– OCTOBER 2010) by ENI;**
- **MONTHLY WATER CHEMICAL ANALYSIS OF WATER INJECTED IN CAVONE 14 (2003-2007 and 2008)by ENI;**
- **COMPOSITION OF WATER INJECTED OF CAVONE 14 (2008) by ENI;**
- **MONTHLY CHEMICAL ANALYSIS OF THE RE-INJECTED WATER (2010-2012) - WELL CAVONE 14 by PADANA;**
- **MONTHLY VOLUMES OF WATER PRODUCED IN EACH WELL (JAN 2010-DEC 2012) by PADANA**
- **CHEMICAL ANALYSIS OF THE REINJECTED WATER (JULY-AUGUST 2013) by PADANA**
- **REPORT ON THE VOLUME OF WATER PRODUCED AND REINJECTED IN WELL CAVONE 14, WITH AN INDICATION OF THE CAPACITIES OF PUMPS AND STORAGE TANKS by PADANA;**

- **PRODUCED WATER REINJECTION DEPTH IN WELL CAVONE 14, WITH CORRESPONDING JUSTIFICATION by PADANA.**

❖ **SEISMIC PROFILES**

- **CROP LINES IN ITALY by ENI** (onshore-offshore);
 - **SEISMIC INTERPRETATION IMAGE** of the regional structure for Cavone field (selected seismic lines, SegY File) **by ENI.**

❖ **LOCAL SEISMIC NETWORK**

- **RECORDERS BY LOCAL SEISMIC NETWORK** (annual reports from 2010 to 2012, raw and elaborated seismic records, technical details and operative manual for the management of the network)**by ENI.**

❖ **OTHERS**

- **GPS DATA ANALYSIS** of Guastalla, Concordia sul Secchia and Boretto permanent stations **by ENI;**
- **DATA OF LEVELING** calculated in the survey of 2006 and 2008 near San Giacomo (MO) **by ENI.**

SPILAMBERTO

ENI operated the Spilamberto field until October 2010, from then PADANA (GAS PLUS GROUP) operates the field.

❖ **BOREHOLES (WELLS)**

- **.LAS AND .JPG FILES OF SPILAMBERTO WELLS** (from 1 to 36) **by ENI.**

❖ **PRODUCTION DATA**

- **RESERVOIR STUDY (1994)** by ENI
- **RESERVOIR STUDY (1999)** by PADANA;
- **YEARLY VOLUME PRODUCTION DATA FROM 01/11/1959 TO 31/12/2010** by ENI;
- **MONTHLY VOLUMES AND PRESSURE OF GAS PRODUCED BY EACH WELL (JUNE – OCTOBER 2010)** by ENI;
- **MONTHLY VOLUMES OF PRODUCED GAS AND PRESSURE OF EACH WELL (NOV 2010-MAY 2012)** by PADANA **GAS ANALYSIS BEFORE TREATMENT by PADANA;**
- **PRODUCTION CAPACITY** (San Martino 1c, 2; Spilamberto 7, 8, 10c, 10l, 16c, 16l, 17c, 17l, 19, 20c, 20l, 21, 23, 26, 29; Volumes measured at testing separator in the Spilamberto gas centre, years 2010-2012) **by PADANA.**

❖ **INJECTION DATA**

- **YEARLY VOLUME INJECTION DATA FROM 01/11/1959 TO 31/12/2010 by ENI;**
- **DAILY VOLUMES OF INJECTED WATER AND PRESSURE OF SPILAMBERTO 9 (JUNE– OCTOBER 2010) by ENI;**
- **DAILY VOLUMES OF INJECTED WATER AND PRESSURE OF SPILAMBERTO 9 (NOV 2010-MAY 2012) by PADANA;**

❖ **SEISMIC PROFILES**

- **SEISMIC INTERPRETATION IMAGE by ENI** (regional structure for Spilamberto field).

RECOVATO

❖ **BOREHOLES (WELLS)**

- **.LAS AND .JPG FILES OF RECOVATO WELLS** (Muzza1, Muzza2, Muzza3xdir, Castelfranco Emilia1, Castelfranco Emilia4, Nonantola1) **by ENI;**
- **DATA ON MUZZA 5 DIR WELL** (Drilling daily report from 10/09/2011 to 21/10/2011, profile at scale 1:1000, FMI Log, Density porosity Log) **by GASPLUS;**
- **ACTIVE WELLS NAME LIST by GASPLUS.**

❖ **PRODUCTION DATA**

- **RESERVOIR STUDY (2000) by ENI;**
- **YEARLY VOLUME PRODUCTION DATA 01/10/1996 TO 30/06/2001 by ENI;**
- **YEARLY VOLUME PRODUCTION DATA FROM 2001 TO 2009 by GASPLUS;**
- **PRODUCTION CAPACITY OF THE 4 WELLS by GASPLUS;**
- **PRESSURE AND DAILY VOLUMES OF INJECTED/EXTRACTED FLUIDS MOVED FOR EACH WELL FROM 01/06/2010 TO 31/05/2012).**

❖ **INJECTION DATA**

- **YEARLY VOLUME INJECTION DATA FROM 01/10/1996 TO 30/06/2001 by ENI;**
- **YEARLY VOLUME PRODUCTION DATA FROM 2001 TO 2009 by GASPLUS.**

MINERBIO NATURAL GAS STORAGE BY STOGIT

❖ BOREHOLES (WELLS)

- **ACTIVE WELLS NAME LIST** (51 storage wells and 8 monitoring wells);
- **DATA ON THE MINERBIO 85 DIR WELL** (2010) – Electrical logs, master log, profile at scale 1:1000, daily drilling report, drilling and completion program;

❖ STORAGE DATA

- **VOLUME MOVED FROM 2010 TO 2012 AND STATIC PRESSURE DAILY DATA FOR EACH WELL;**
- **DAILY INJECTION AND EXTRACTION TOTAL VOLUME FROM 2010 TO 2012;**
- **SUBSIDENCE MONITORING** (technologies and results);
- **DIFFERENTIAL SAR INTERFEROMETRY AND PERMANENT SCATTERERS TECHNIQUE;**
- **ANNUAL REPORT FOR UNMIG** – updates to December 2012 (reservoir study and state of plants).

❖ SEISMIC PROFILES

- **3D SEISMIC DATA** (swath summary, cartographical attachments, 2011 Acquisition Final Report).

❖ LOCAL SEISMIC NETWORK

- **RECORDERS BY LOCAL SEISMIC NETWORK** (raw and processed data from 2010 to 2012, annual report from 2010 to 2012).

FERRARA GEOTHERMAL FIELD DATA by EMILIA ROMAGNA REGION (ENI DATA)

❖ BOREHOLES (WELLS)

- **ACTIVE WELLS NAME LIST AND USE (PRODUCTION/INJECTION);**
- **.LAS FILES OF CASAGLIA 1 WELL , CASAGLIA 2 WELL;**
- **COMPOSITE LOG OF CASAGLIA 2 AND CASAGLIA 3 WELLS;**
- **WELLS COMPLETION PROFILES OF CASAGLIA 1, 2, 3 WITH OPEN STRATA FOR PRODUCTION AND INJECTION.**

❖ PRODUCTION DATA

- **“CASAGLIA 1 STRATIGRAPHIC REVIEW” - YEAR 1999;**
- **ANNUAL VOLUMES OF PRODUCED WATER FROM 1995 to 2012;**

- **DAILY VOLUMES OF PRODUCED WATER AND PRESSURE OF EACH WELL (JAN 2012-MAY 2012).**

❖ **INJECTION DATA**

- **ANNUAL VOLUMES OF REINJECTED WATER STARTING FROM 1995 TO 2012;**
- **DAILY VOLUMES OF PRODUCED WATER AND PRESSURE OF EACH WELL (JAN 2012-MAY 2012).**

❖ **LOCAL SEISMIC NETWORK**

- **“FERRARA” MICROSEISMIC MONITORING DATA (waveforms) with the technical setting of the network from 2010 to 2012**

FEASIBILITY STUDY OF RIVARA STORAGE PROJECT by INDEPENDENT

- **SUMMARY OF FEASIBILITY STUDY OF PROJECT RIVARA;**
- **TECHNICAL STUDIES CONDUCTED FOR RIVARA FEASIBILITY PROJECT** (introduction to the Rivara project; subsurface report, natural subsidence assessment report, report for EIA, physical model, analysis of seismic data before Emilia earthquake, physical data of the aquifer, description of microseismicity network project, seismic profiles, stress-strain state of reservoir simulation, paleogeographic and paleotectonic study, geochemical study);
- **TECHNICAL NORMS ON UNDERGROUND GAS STORAGE (UGS) IN AQUIFER;**
- **GEOMECHANICS PARAMETERS AND 3D RESERVOIR GEOMECHANICS STUDY.**

Appendix D. Available data (CD)

CD-ROM attached.

Appendix E. Earthquake location and focal parameters

Table E.1 Earthquake locations

PRESEQUENCE						
#Time (UTC)	Magnitude	Lat N	Long E	Depth	ErH	ErZ
2006-07-27 10:10:27.910	2.200	44.941	10.995	10.900	2.100	3.000
2006-12-26 23:42:44.070	2.500	44.799	10.653	10.000	1.700	2.500
2006-12-27 01:56:15.030	2.100	44.811	10.765	7.000	1.900	1.900
2007-05-09 08:18:51.960	1.900	44.832	10.411	7.500	2.100	2.300
2007-10-06 12:41:13.240	2.000	44.914	11.211	5.500	3.100	2.500
2008-03-11 19:17:30.870	2.200	44.824	10.822	5.400	2.500	2.000
2008-04-15 02:12:01.900	2.300	44.987	11.539	8.600	3.000	2.300
2008-06-03 09:31:15.830	2.100	44.839	10.546	9.300	2.800	2.000
2008-06-07 04:25:10.240	3.000	44.839	11.218	9.900	1.500	3.000
2008-07-15 02:33:45.100	1.900	44.507	10.985	9.500	3.000	2.800
2008-07-23 03:22:25.050	3.200	44.825	11.167	4.900	1.700	2.000
2008-07-24 02:07:06.120	2.500	44.793	11.200	3.900	1.900	2.000
2008-08-19 16:55:24.860	2.900	44.838	11.070	7.300	2.000	2.200
2008-12-19 09:07:03.110	2.500	44.992	11.223	4.000	2.500	2.000
2009-05-25 09:47:15.660	1.500	44.796	10.351	10.500	2.500	3.500
2009-08-05 07:49:18.890	2.000	44.745	11.719	10.300	2.000	2.500
2009-08-25 01:32:29.160	2.000	44.654	11.725	11.100	2.300	3.700
2009-11-16 22:21:37.860	3.000	44.867	11.386	3.500	1.500	2.100
2009-11-18 07:45:36.180	2.900	44.870	11.377	3.100	1.600	1.800
2009-12-10 12:20:18.370	2.600	45.008	10.769	3.300	2.000	2.100
2009-12-31 03:21:48.970	2.700	44.966	10.889	11.100	2.200	3.500
2009-12-31 03:29:56.130	2.600	44.922	10.922	7.000	2.000	2.800
2009-12-31 13:02:51.620	2.400	44.851	10.931	15.300	2.000	3.500
2010-01-14 04:34:36.710	2.500	44.802	11.502	15.300	3.300	3.400
2010-05-20 22:24:52.780	2.100	44.789	10.674	7.500	1.200	1.300
2010-05-24 02:14:36.170	1.700	44.782	10.653	9.900	2.000	1.900
2010-07-06 03:43:00.650	2.600	44.801	10.663	8.900	1.500	1.8
2010-07-26 07:13:52.100	2.300	44.973	11.362	3.500	1.500	1.2
2010-08-19 07:04:19.860	2.400	44.791	10.674	3.200	1.500	1.800
2011-06-01 01:13:33.560	2.100	44.785	10.666	6.000	2.000	2.000
2011-07-19 19:59:30.700	1.800	44.832	11.198	10.000	2.200	3.500
2011-07-23 20:37:16.050	1.900	44.762	10.673	5.800	2.000	2.300
2011-07-27 00:58:35.910	1.700	45.125	11.189	10.000	2.200	4.300
2011-07-27 01:23:24.330	2.200	45.032	11.228	7.600	1.500	2.500
2011-07-27 08:36:59.240	2.300	45.035	11.356	9.100	1.200	2.000
2011-09-17 18:16:54.360	2.400	44.783	10.765	15.200	2.500	3.300
2011-09-27 16:44:34.950	2.200	44.929	11.294	2.700	1.500	1.500
2011-10-30 21:04:55.740	2.200	44.639	10.974	10.000	2.000	3.000
2012-04-01 10:22:12.620	2.700	44.771	11.214	11.000	1.700	2.900
2012-05-18 19:40:18.000	2.900	44.955	11.734	10.000	5.000	5.000
2012-05-18 19:44:43.000	1.800	44.994	11.335	5.000	2.400	3.000

2012-05-19 17:09:35.000	2.500	44.939	11.268	10.000	1.200	3.000
2012-05-19 23:13:27.000	4.100	44.899	11.286	5.700	1.000	1.700
2012-05-19 23:42:54.000	2.200	44.938	11.281	3.300	1.500	1.500
SEQUENCE						
2012-05-20 02:03:52.000	5.900	44.885	11.253	5.300	1.300	1.000
2012-05-20 02:07:31.000	5.100	44.853	11.344	4.200	1.500	1.300
2012-05-20 02:11:46.000	4.300	44.832	11.357	7.800	1.400	1.900
2012-05-20 02:12:42.000	4.300	44.815	11.222	15.400	1.800	2.200
2012-05-20 02:21:53.000	4.100	44.832	11.235	4.500	1.500	2.000
2012-05-20 02:25:05.000	4.000	44.859	11.311	10.500	1.800	2.200
2012-05-20 02:35:37.000	4.000	44.816	11.468	15.300	2.100	2.500
2012-05-20 02:39:10.000	4.000	44.903	11.247	5.900	1.700	2.000
2012-05-20 03:02:50.000	4.900	44.857	11.136	6.700	1.500	2.000
2012-05-20 09:13:21.000	4.200	44.919	11.281	4.100	1.400	2.100
2012-05-20 13:18:02.000	5.100	44.826	11.464	4.800	1.200	0.900
2012-05-20 13:21:06.000	4.100	44.884	11.378	3.400	1.700	1.900
2012-05-20 17:37:14.000	4.500	44.876	11.382	3.200	1.700	1.600
2012-05-21 16:37:31.000	4.100	44.811	11.153	9.100	2.000	1.800
2012-05-23 21:41:18.000	4.300	44.852	11.263	6.200	1.000	1.700
2012-05-25 13:14:05.000	4.000	44.887	11.091	9.200	1.000	2.000
2012-05-27 18:18:45.000	4.000	44.882	11.158	4.700	1.500	1.700
2012-05-29 07:00:03.000	5.800	44.854	11.068	9.300	0.800	0.900
2012-05-29 07:07:21.000	4.000	44.854	10.992	9.700	1.200	1.500
2012-05-29 07:09:54.000	4.100	44.884	11.006	10.200	1.500	2.000
2012-05-29 08:25:51.000	4.500	44.825	10.733	6.200	2.500	2.300
2012-05-29 08:40:58.000	4.200	44.882	10.979	4.900	1.500	2.200
2012-05-29 09:30:21.000	4.200	44.888	11.011	4.200	1.300	1.600
2012-05-29 10:55:57.000	5.300	44.872	10.985	4.200	0.800	0.900
2012-05-29 11:00:02.000	4.900	44.873	10.950	9.500	1.500	1.700
2012-05-29 11:00:25.000	5.200	44.875	10.930	10.200	1.000	1.100
2012-05-29 11:07:05.000	4.000	44.876	11.076	15.000	1.300	1.900
2012-05-31 14:58:21.000	4.000	44.911	10.882	13.800	1.500	2.000
2012-05-31 19:04:04.000	4.200	44.891	10.980	11.500	1.500	2.000
2012-06-03 19:20:43.000	5.100	44.903	10.919	8.900	1.100	0.800
2012-06-12 01:48:36.000	4.300	44.915	10.919	12.700	1.100	1.800

Table E.2 Earthquake focal parameters

PRESEQUENCE							
#Time (UTC)	Magnitude	Strike	Erstrike	Dip	Erdip	Rake	Errake
2006-07-27 10:10:27.910	2.200	99	15	50	10	80	10
2006-12-26 23:42:44.070	2.500	120	13	48	10	110	12
2006-12-27 01:56:15.030	2.100	115	12	43	11	120	13
2007-05-09 08:18:51.960	1.900	100	10	40	10	95	10
2007-10-06 12:41:13.240	2.000	105	12	37	10	80	11
2008-03-11 19:17:30.870	2.200	110	13	40	10	115	10
2008-04-15 02:12:01.900	2.300	95	10	38	10	75	10
2008-06-03 09:31:15.830	2.100	115	12	45	10	100	10
2008-06-07 04:25:10.240	3.000	107	10	39	10	92	10
2008-07-15 02:33:45.100	1.900	100	10	40	10	85	10
2008-07-23 03:22:25.050	3.200	90	10	38	10	78	10
2008-07-24 02:07:06.120	2.500	85	10	43	10	120	10
2008-08-19 16:55:24.860	2.900	88	12	37	11	108	10
2008-12-19 09:07:03.110	2.500	90	10	33	10	100	10
2009-05-25 09:47:15.660	1.500	105	11	30	12	98	10
2009-08-05 07:49:18.890	2.000	109	10	40	11	78	10
2009-08-25 01:32:29.160	2.000	120	10	35	10	80	10
2009-11-16 22:21:37.860	3.000	105	10	38	10	83	10
2009-11-18 07:45:36.180	2.900	110	10	42	10	75	10
2009-12-10 12:20:18.370	2.600	120	12	46	12	110	10
2009-12-31 03:21:48.970	2.700	110	10	40	10	107	10
2009-12-31 03:29:56.130	2.600	105	10	36	10	98	10
2009-12-31 13:02:51.620	2.400	110	13	37	10	105	10
2010-01-14 04:34:36.710	2.500	85	5	48	8	120	10
2010-05-20 22:24:52.780	2.100	110	15	35	10	120	10
2010-05-24 02:14:36.170	1.700	115	13	33	10	105	10
2010-07-06 03:43:00.650	2.600	107	10	35	6	160	10
2010-07-26 07:13:52.100	2.300	105	12	40	10	120	10
2010-08-19 07:04:19.860	2.400	114	15	41	10	109	10
2011-06-01 01:13:33.560	2.100	120	8	32	7	143	10
2011-07-19 19:59:30.700	1.800	110	10	38	10	99	10
2011-07-23 20:37:16.050	1.900	112	10	34	10	115	10
2011-07-27 00:58:35.910	1.700	105	12	37	10	80	10
2011-07-27 01:23:24.330	2.200	100	10	32	10	85	10
2011-07-27 08:36:59.240	2.300	110	10	30	10	95	10
2011-09-17 18:16:54.360	2.400	118	10	32	10	120	10
2011-09-27 16:44:34.950	2.200	103	10	34	10	88	10
2011-10-30 21:04:55.740	2.200	98	12	47	10	80	10
2012-04-01 10:22:12.620	2.700	115	8	37	8	103	7
2012-05-18 19:40:18.000	2.900	102	6	44	6	134	8
2012-05-18 19:44:43.000	1.800	111	10	40	10	110	10
2012-05-19 17:09:35.000	2.500	99	6	41	5	96	6

2012-05-19 23:13:27.000	4.100	100	10	28	8	90	7
2012-05-19 23:42:54.000	2.200	97	10	35	7	99	5
SEQUENCE							
2012-05-20 02:03:52.000	5.900	99	12	38	6	85	11
2012-05-20 02:07:31.000	5.100	104	10	40	5	87	13
2012-05-20 02:11:46.000	4.300	92	8	40	6	89	10
2012-05-20 02:12:42.000	4.300	101	10	38	6	93	10
2012-05-20 02:21:53.000	4.100	95	10	39	8	105	10
2012-05-20 02:25:05.000	4.000	100	8	42	8	97	10
2012-05-20 02:35:37.000	4.000	98	8	40	8	110	10
2012-05-20 02:39:10.000	4.000	99	10	35	6	101	10
2012-05-20 03:02:50.000	4.900	96	8	30	8	90	10
2012-05-20 09:13:21.000	4.200	78	10	32	8	95	10
2012-05-20 13:18:02.000	5.100	114	12	33	6	97	9
2012-05-20 13:21:06.000	4.100	87	8	39	8	94	10
2012-05-20 17:37:14.000	4.500	75	8	40	6	100	10
2012-05-21 16:37:31.000	4.100	60	8	40	8	95	10
2012-05-23 21:41:18.000	4.300	95	8	39	8	85	10
2012-05-25 13:14:05.000	4.000	77	10	41	8	82	10
2012-05-27 18:18:45.000	4.000	130	10	87	7	170	10
2012-05-29 07:00:03.000	5.800	97	10	34	5	93	10
2012-05-29 07:07:21.000	4.000	91	10	44	8	97	10
2012-05-29 07:09:54.000	4.100	98	10	44	6	101	10
2012-05-29 08:25:51.000	4.500	100	8	46	8	91	10
2012-05-29 08:40:58.000	4.200	103	8	47	8	88	10
2012-05-29 09:30:21.000	4.200	93	8	45	6	99	10
2012-05-29 10:55:57.000	5.300	105	11	33	7	100	10
2012-05-29 11:00:02.000	4.900	75	8	41	8	106	10
2012-05-29 11:00:25.000	5.200	90	10	37	6	102	11
2012-05-29 11:07:05.000	4.000	97	8	44	7	100	10
2012-05-31 14:58:21.000	4.000	83	10	46	8	85	10
2012-05-31 19:04:04.000	4.200	89	8	48	6	95	10
2012-06-03 19:20:43.000	5.100	95	11	35	8	95	9
2012-06-12 01:48:36.000	4.300	82	8	45	8	78	10